Strike while the Iron is Hot – Optimal Monetary Policy under State-Dependent Pricing

Peter Karadi
European Central Bank and CEPR

Anton Nakov
European Central Bank and CEPR

Galo Nuño
Bank of Spain and CEPR

Ernesto Pastén
Central Bank of Chile

Dominik Thaler
European Central Bank

This version: February 3, 2025
First version: July 30, 2024
Latest version: Please click here

Abstract

We characterize optimal monetary policy under commitment in menu cost models. Their key feature is that frequency of price changes responds to shocks and monetary policy itself. In contrast, standard monetary policy analysis uses the Calvo (1983) assumption that frequency is invariant. In our setup, optimal monetary policy is non-linear by being more aggressive to control inflation as cost-push shocks are larger – a "strike while the iron is hot" policy. This is due to a sacrifice ratio decreasing in the size of shocks and the increasing incentives of the central bank tame the raise in frequency of price changes. In turn, the response of output is similar to the standard model. Additional results are that *divine coincidence* applies for productivity shocks, the optimal inflation trend is slightly positive, and time-inconsistency is weakened. Our results are particularly relevant for significant inflation surges as experienced worldwide post COVID.

JEL codes: E31, E32, E52

Keywords: State-dependent pricing, large shocks, nonlinear Phillips curve, optimal monetary policy

We are grateful to Guido Ascari, Vladimir Asryan, Andres Blanco, Davide Debortoli, Eduardo Engel, Aurélien Eyquem, Jordi Galí, Erwan Gautier, Mark Gertler, Mishel Ghassibe, Basil Halperin, Francesco Lippi, Albert Marcet, Alberto Martin, Virgiliu Midrigan, Giorgio Primiceri, Xavier Ragot, Morten Ravn, Tom Sargent, Edouard Schaal, Raphael Schoenle and Jaume Ventura, as well as to participants at various conferences and seminars for their comments and suggestions. The views expressed here are those of the authors only and do not necessarily represent those of the Bank of Spain, the Central Bank of Chile, the ECB, or the Eurosystem.

1. Introduction

What is the optimal design of monetary policy during an inflation surge? The traditional answer offered by the New Keynesian literature relies on a model of price setting, that of Calvo (1983), which disregards endogenous variation in the frequency of price changes: firms update prices randomly irrespective of the macroeconomic conditions.[1] In contrast, an emerging literature on state-dependent price-setting models highlights how firms endogenously decide when to adjust prices. The recent inflationary surge has provided empirical support to these models, as the frequency of price changes increased during the period of high inflation.[2] Normative aspects of these state-dependent models have received scant attention. To bridge this crucial gap, our paper characterizes optimal monetary policy under state-dependent price setting.

Our analysis arrives at a novel insight: in response to large cost-push shocks, the optimal monetary policy commits to quashing inflation and leaning against changes in the repricing frequency – a "strike while the iron is hot" policy. The reason is that the cost of the anti-inflationary policy in terms of output is smaller when the frequency of price changes increases in response to the shocks – as the price level becomes more flexible, the sacrifice ratio falls. Furthermore, as we show algebraically, optimal policy requires full inflation stabilization after total factor productivity shocks – a divine coincidence result after efficiency shocks, as in the canonical Calvo model.

Our baseline state-dependent price-setting model closely follows Golosov and Lucas (2007).[3] In the model, a representative household consumes a continuum of differentiated goods and supplies labor in a centralized, frictionless market. Each good is produced by a single firm with labor as the only input subject to aggregate productivity shocks, aggregate cost-push shocks, and idiosyncratic quality shocks.[4] Firms must incur a small, fixed, "menu cost" to adjust their prices. Thus, firms' pricing decisions are characterized by an (S, s) rule: when prices are within an endogenous band around the optimal reset price, firms keep them constant; otherwise, they pay the menu cost and update their price. The central bank sets the nominal interest rate.

The model economy is subject to three welfare distortions. The first two distortions are caused by markups deviating from the efficient (zero) markups – the first distortion is caused by the *average* markup; and the second by the *dispersion* of markups. The third distortion is the resource costs associated to price-adjustment. The average markup gap is conventional and is present both in our baseline model and in the canonical Calvo model.[5] It is driven by price rigidities, which drive average markups

[1] Woodford (2003); Galí (2008)

[2] For evidence, see Montag and Villar (2023); Cavallo et al. (2023); Blanco et al. (2024a)

[3] We show robustness using the CalvoPlus model of Nakamura and Steinsson (2010).

[4] We depart from the Golosov and Lucas (2007) model in this regard, which instead assumes idiosyncratic productivity shocks. We do so for ease of computation while its implications on our results are innocuous (see also Midrigan 2011; Alvarez et al. 2021).

[5] As is standard in optimal monetary policy analysis, we offset steady-state average markup distortion due to the market power with suitable subsidies. We reintroduce steady-state markup distortions only to analyze the impact of time-inconsistency.

persistently to suboptimal levels after changes in marginal costs, which are triggered by aggregate shocks. The distortion gives incentives to the policy maker to minimize variation in the average markup. The behavior of the second and third distortions is distinct in the two frameworks. In our framework, aggregate shocks can reduce markup dispersion on impact, as new adjusters are selected from those with the most misaligned markups; while aggregate shocks increase markup dispersion in the Calvo framework. Furthermore, resource costs of price changes become a relevant factor in our framework, while it is always zero in the Calvo framework, by construction. These distortions provide incentives to the policymaker to minimize markup distortions and the frequency of price changes.

We study the optimal design of monetary policy in the model. To this end, we propose a new algorithm to solve the nonlinear Ramsey problem under commitment. The algorithm relies on a projection method, so it is suitable to assess the impact of large aggregate shocks. In particular, it makes the planner's problem accurate and computationally feasible by approximating the value and distribution functions and solving the set of equilibrium conditions under perfect foresight over the sequence space. We calibrate the model parameters to match the frequency of the price changes in the U.S. before the inflation surge (Nakamura and Steinsson 2008), as well as a 20% frequency level accompanying a 10% inflation rate as experienced during the 2022-2023 inflation surge. We contrast the implications of our state-dependent model to those of a time-dependent Calvo model. [6]

We find that timeless monetary policy ((Woodford 2003)) should react more aggressively against inflation after large cost-push shocks when the frequency of price changes is endogenously high than either after small shocks or in a fixed-frequency Calvo setting – it is optimal to 'strike, while the iron is hot'. This establishes a key difference between our model and a standard Calvo model. Our calibration implies that this new policy prescriptions is relevant for the 2022-2023 inflation surge: optimal policy requires a more aggressive anti-inflationary stance already for inflation and frequency values observed during this period.

What explains the modified policy prescription? To gain intuition about the results, we find it useful to describe both the possibility frontier and welfare in terms of the output gap and the inflation gap, as is conventional in optimal monetary policy analysis under the Calvo price setting. The output gap measures the distance between output and its efficient level and is closely related to the average markup gap; the inflation gap measures the distance of inflation from its optimal steady-state level and is closely related to the markup dispersion and the resource costs of price changes. The possibility frontier maps out the available potential outcomes in terms of the inflation path and the output gap path after the aggregate cost-push shock. The welfare costs, in contrast, evaluate the outcomes in terms of welfare. The relationship between

[6] The Calvo model is recalibrated to generate the same price-flexibility as our baseline model for small shocks (Auclert et al. 2024). This recalibration compensates for the endogenous "selection" of large price changes, which raises substantially the flexibility of the aggregate price level.

inflation and output gap paths is nonlinear in our model: large shocks, which raise the frequency of price changes and, thereby, increase price flexibility, make inflation more sensitive to changes in the output gap. This makes the costs of reducing inflation in terms of output gap lower after large cost-push shocks – the sacrifice ratio declines with frequency. In contrast, this trade-off is linear and it is determined by the slope of the new Keynesian Phillips curve in the linearized Calvo model. The relative welfare costs of inflation versus output gap, in contrast, are essentially independent of the frequency of price changes in our baseline model, and are similar to the welfare costs in the Calvo framework. In fact, the household welfare costs are quite well approximated by a quadratic welfare function of output gap and inflation with a suitably chosen welfare weight.[7]

We find that the prescription for a stronger anti-inflationary stance after large cost-push shock is almost exclusively driven by the nonlinear trade-off between inflation and output gap. Intuitively, reducing inflation is cheaper after large shocks, when the frequency is higher and the price level is more flexible, than after small shocks or in the nonlinear Calvo framework where the relationship stays near linear. In contrast, variations in the relative importance of inflation versus output gap in welfare plays only a marginal role in the results due to the approximately quadratic welfare function, which implies a constant relative importance of inflation versus output gap.

We derive analytic results supporting this intuition in a simplified model. The simplification brings price-adjustment costs to zero in odd periods. The assumption improves the tractability of the model by turning the dynamic framework into a series of static ones, but keeps the key underlying channel qualitatively unaffected: the repricing rate responds endogenously to aggregate shocks.[8] Under this assumption, the trade-off between inflation and activity is described by a Phillips curve, and the relationship between inflation and the output gap under optimal Ramsey policy in the presence of cost-push shocks is described by a target rule, as in the Calvo framework. We characterize both the Phillips curve and the target rule and show that they are both *nonlinear* in the menu cost model, while they are near-linear in the Calvo model.

We also establish a series of additional results in the full model. First, we show that the model features a slightly positive Ramsey optimal steady-state inflation rate, at around 0.3%. This contrasts with the Calvo model, where optimal inflation is exactly zero. In our menu cost model, positive inflation reduces the frequency and thus helps firms to economize on costly price adjustments. In particular, it counterbalances the impact of too frequent price increases relative to price decreases, which is a consequence of the asymmetry of the profit function: firms dislike negative price misalignments when the demand for their product is high, relative to positive mis-

[7] This observation generalizes to large shocks the result of Woodford (2003), which shows that in the presence of small shocks, i.e. up to a second order in the neighborhood of an efficient steady state, that relevant welfare can be approximated by a quadratic function of output gap and inflation with relative welfare weights determined by structural parameters of the model (Woodford 2003).

[8] Furthermore, the model also assumes that the price-adjustment thresholds are predetermined. This assumption is unnecessary, but significantly simplifies the algebra.

alignments when the demand is low. Second, we also find that for small cost-push shocks, optimal policy "leans against the wind": the central bank temporarily drives output below its efficient level to contain the inflationary impact of a positive cost-push shock. This is very similar to the Calvo model, the reason, however, is different. In the Calvo model, the key distortion caused by inflation is the markup dispersion, while in our baseline model it is resource costs due to menu costs. Third, we show analytically that the optimal response to TFP shocks is characterized by the "divine coincidence" (Blanchard and Galí 2007). In other words, optimal policy stabilizes both inflation and the output gap. Finally, we show that the well-known time inconsistency problem of monetary policy is also present in our menu cost model, although it is attenuated relative to Calvo. In both models, when the steady state is inefficient, monetary policy has the incentive to stimulate output via an unexpectedly easy policy (Galí 2008). However, in the menu cost model, such a policy is less effective on output and more inflationary because the ensuing increase in the repricing rate raises the flexibility of the aggregate price level. The time-inconsistent motive to ease is thus considerably weaker.

Our results are robust to alternative parameterizations, and also hold in the "Calvo-Plus" model extension (Nakamura and Steinsson 2010). The latter framework assumes that firms face a free price adjustment possibility with some exogenous probability. This model can better match the fraction of small price changes in the data (see also Midrigan 2011; Alvarez et al. 2021), and achieve a realistic degree of monetary non-neutrality for small shocks. However, as we show, the optimal policy implications of the model stay very close to those in our baseline.

Related literature. Our paper builds on the seminal article by Golosov and Lucas (2007). They propose a menu cost model (Barro 1972; Sheshinski and Weiss 1977; Caballero and Engel 1993) that has become the backbone of a positive literature studying the relationship between monetary non-neutrality and the distribution of price changes at the micro level (Midrigan 2011; Costain and Nakov 2011; Alvarez et al. 2016), as well as the impact of large aggregate shocks on inflation and activity (Karadi and Reiff 2019; Alexandrov 2020; Auer et al. 2021). The model describes well firms' price-setting behavior in diverse environments with both low and high inflation (Nakamura and Steinsson 2008; Gagnon 2009; Alvarez et al. 2019). This price-setting framework provides a microfounded state-dependent alternative to the canonical time-dependent Calvo (1983) model, with widely different implications in terms of both the extent of monetary non-neutrality and price-flexibility as a response to large shocks. Indeed, most familiar price-setting models, such as the random-menu cost model of Dotsey et al. (1999); Alvarez et al. (2021), the Calvo-plus model of Nakamura and Steinsson (2010), the rational inattention model by Woodford (2009), or the control cost model by Costain and Nakov (2019), lie on a spectrum bracketed by these two polar cases. Normative results from the Golosov and Lucas (2007) model can provide qualitative insights that generalize to a wide class of price-setting frameworks.

To the best of our knowledge, our paper is the first to solve for optimal monetary

policy in this canonical menu cost model. Its main distinctive feature, relative to the textbook analysis based on Calvo (1983), such as in Woodford (2003) and Galí (2008), is a state-dependent relationship between inflation and the output gap, which has received new empirical support following the recent inflation surge (Benigno and Eggertsson 2023; Cerrato and Gitti 2023; Blanco et al. 2024a,b). Our conclusion prescribing aggressive anti-inflationary policy after large shocks is a direct consequence of this nonlinearity, which implies a favourable inflation-output trade-off that optimal policy should exploit.

Solving dynamic optimal policy in response to aggregate shocks in this framework complements previous research on optimal monetary policy, which has restricted attention to menu cost settings with a representative firm and small aggregate shocks (Nakov and Thomas 2014), sector-specific productivity shocks (Caratelli and Halperin 2023)[9] or to optimal *steady-state* inflation rate (Adam and Weber 2019; Blanco 2021; Nakov and Thomas 2014).

This paper proposes a new algorithm to solve Ramsey optimal policy in heterogeneous-agent models, building on González et al. (2024). The algorithm (i) makes the infinite-dimensional planner's problem finite-dimensional by approximating the infinite-dimensional value and distribution functions by piece-wise linear functions on a grid; (ii) accounts for the discrete price-adjustment choice using an endogenous grid; (iii) derives the FOCs of the planner's problem by symbolic differentiation; and (iv) solves the resulting set of equilibrium conditions nonlinearly under perfect foresight over the sequence space. Our approach complements other methods to solve for Ramsey policy in heterogeneous-agent models (Bhandari et al. 2021; Le Grand et al. 2022; Dávila and Schaab 2022; Nuño and Thomas 2022; Smirnov 2022).

2. Model

The baseline economy consists of a representative household consuming and supplying labor, monopolistic producers hit by aggregate and idiosyncratic shocks who must pay a fixed menu cost to update prices, and a central bank that sets monetary policy. We also present three auxiliary models meant for benchmarking and robustness: the textbook new-Keynesian model, a "non-linear Calvo model" and the "Calvoplus model".

2.1. Households

A representative household consumes C_t, supplies working hours N_t and saves in one-period, zero-net supply nominal bonds B_t. The household maximizes

$$\max_{C_t, N_t, B_t} \mathbb{E}_0 \sum_{t=0}^{\infty} \beta^t u(C_t, N_t), \tag{1}$$

[9] The former finds no significant difference between Calvo and an stylized menu cost model. The latter shows that in the face of sector-specific shocks optimal policy can be characterized as *nominal wage targeting*.

subject to

$$P_t C_t + Q_t B_t + T_t = B_{t-1} + W_t N_t + D_t, \tag{2}$$

where T_t are lump-sum taxes, W_t is the nominal wage, D_t are lump-sum dividends from firms, and Q_t is the price of the nominal bond. Aggregate consumption C_t is

$$C_t = \left\{ \int \left[A_t(j) C_t(j) \right]^{\frac{\epsilon-1}{\epsilon}} dj \right\}^{\frac{\epsilon}{\epsilon-1}}, \tag{3}$$

where $C_t(j)$ is the quantity purchased of product $j \in [0,1]$ and $A_t(j)$ is an idiosyncratic quality component of product j, which follows a random walk in logs with stochastic volatility σ_t:

$$\log A_t(j) = \log A_{t-1}(j) + \sigma_t \varepsilon_t(j), \tag{4}$$

ε_t is an i.i.d Gaussian innovation and σ_t is introduced to study the effect of price dispersion shocks.

The demand for product j is

$$C_t(j) = A_t(j)^{\epsilon-1} \left(\frac{P_t(j)}{P_t} \right)^{-\epsilon} C_t \tag{5}$$

and the aggregate price index is

$$P_t = \left[\int_0^1 \left(\frac{P_t(j)}{A_t(j)} \right)^{1-\epsilon} dj \right]^{\frac{1}{1-\epsilon}}. \tag{6}$$

We assume separable utility of the CRRA class, $u(C_t, N_t) = \frac{C_t^{1-\gamma}}{1-\gamma} - \upsilon N_t$. Thus, labor supply is given by the optimality condition:

$$w_t = \upsilon C_t^{\gamma}, \tag{7}$$

where $w_t = W_t / P_t$ is the real wage. The Euler equation is

$$1 = \mathbb{E}_t \left[\Lambda_{t,t+1} e^{i_t - \pi_{t+1}} \right], \tag{8}$$

where i_t is the nominal interest rate, and the the stochastic discount factor is

$$\Lambda_{t,t+1} \equiv \beta \frac{u'(C_{t+1})}{u'(C_t)}. \tag{9}$$

2.2. Monopolistic producers

Good $j \in [0,1]$ is produced by a single firm j according to

$$Y_t(j) = A_t \frac{N_t(j)}{A_t(j)}, \tag{10}$$

where $N_t(j)$ is labor hours, A_t is aggregate productivity and $A_t(j)$ is idiosyncratic quality. Firm j's nominal profit function is

$$\begin{aligned} D_t(j) =& P_t(j)Y_t(j) - (1-\tau_t)W_t N_t(j) \\ =& P_t(j)^{1-\epsilon} A_t(j)^{\epsilon-1} \left(\frac{1}{P_t}\right)^{-\epsilon} C_t - (1-\tau_t)\frac{W_t}{A_t} A_t(j)^{\epsilon} \left(\frac{P_t(j)}{P_t}\right)^{-\epsilon} C_t \end{aligned} \tag{11}$$

where $Y_t(j) = C_t(j)$ and τ_t is an employment subsidy financed by lump-sum taxes.

Critically, to change its price, firm j must incur in a fixed "menu cost" η defined in labor units. This is the source of endogenenity of price stickiness in the model.

To characterize firms' optimal pricing decisions, we rely on a change in variables that facilitates the analysis. Let define $p_t(j) \equiv \log\left(\frac{P_t(j)}{A_t(j)P_t}\right)$ as the quality-adjusted real price of good j and $x_t(j) \equiv p_t(j) - p_t^*(j)$ as the *log distance* between current and optimal quality-adjusted real price of good j, the "price gap". Casting the pricing problem in terms of price gaps has the computational advantage that it is the only firm-level state that pricing decisions depend upon. We postulate that firms' optimal pricing follows a (S_t, s_t) rule defined in $x_t(j)$ such that a firm j keeps its nominal price constant if $x_t(j) \in [s_t, S_t]$, raises it if $x_t(j) < s_t$ and cuts it if $x_t(j) > S_t$. When its price changes, $x_t(j) = 0$. Subindex t subsumes all aggregate states. Idiosyncratic quality shocks in (4) yield the realistic prediction that reset nominal prices $P_t^*(j)$ are heterogeneous across goods; however, $p_t^*(j)$ are all identical. Thus, from this point onward we drop subindex j to ease notation. If a firm keeps its nominal price constant, its price gap evolves according to

$$x_t = x_{t-1} + p_t - p_t^* + p_{t-1}^* = x_{t-1} - \sigma_t \varepsilon_t - \pi_t^* \tag{12}$$

where $\pi_t^* \equiv p_t^* - p_{t-1}^* + \pi_t$ is the inflation of the quality-adjusted real optimal reset price.

The optimality conditions for the pricing rule are

$$V_t(0) - \eta w_t = V_t(s_t), \tag{13}$$

$$V_t(0) - \eta w_t = V_t(S_t), \tag{14}$$

$$V_t'(0) = 0. \tag{15}$$

where, to simplify notation, firms' value function $V_t(\cdot)$ is expressed only in terms of

price gaps as all other states are aggregate and are subsumed by a time subindex:

$$
\begin{aligned}
V_t(x) &= \Pi(x, p_t^*, w_t, A_t) \\
&+ \mathbb{E}_t\left[\left(1-\lambda_{t+1}\left(x-\sigma_{t+1}\varepsilon_{t+1}-\pi_{t+1}^*\right)\right)\Lambda_{t,t+1}V_{t+1}(x-\sigma_{t+1}\varepsilon_{t+1}-\pi_{t+1}^*)\right] \\
&+ \mathbb{E}_t\left[\lambda_{t+1}\left(x-\sigma_{t+1}\varepsilon_{t+1}-\pi_{t+1}^*\right)\Lambda_{t,t+1}\left(V_{t+1}(0)-\eta w_{t+1}\right)\right] \qquad (16)
\end{aligned}
$$

and comprises the current period real profits $\Pi_t(\cdot)$ and the discounted continuation value evaluated when the price does not change at $t+1$ with probability $1-\lambda_{t+1}(\cdot)$, and when with probability $\lambda_{t+1}(\cdot)$ the firm sets a new price after paying the menu cost ηw_{t+1}. Firms' real profits in terms of price gaps are

$$
\Pi_t(x, p_t^*, w_t, A_t) \equiv \frac{D_t}{P_t} = C_t\left(\exp\left(x+p_t^*\right)\right)^{1-\epsilon} - C_t(1-\tau_t)\frac{w_t}{A_t}\left(\exp\left(x+p_t^*\right)\right)^{-\epsilon},
$$

and the price adjustment probability at period t is given by

$$
1-\lambda_t(x) = \mathbb{1}\{x \in [s, S]\}
$$

where $\mathbb{1}[\cdot]$ is the indicator function. Finally, Appendix A shows that $V_t'(0)$ can be expressed as the sum of the marginal effect of x on current profits and on the expected continuation value:

$$
\begin{aligned}
V_t'(0) = \Pi_t'(0) &+ \frac{\Lambda_{t,t+1}}{\sigma_{t+1}}\int_{s_{t+1}}^{S_{t+1}} V_{t+1}(x')\left.\frac{\partial\phi\left(\frac{x-x'-\pi_{t+1}^*}{\sigma_{t+1}}\right)}{\partial x}\right|_{x=0} dx' \\
&+ \frac{\Lambda_{t,t+1}}{\sigma_{t+1}}\left[\phi\left(\frac{-S_{t+1}-\pi_{t+1}^*}{\sigma_{t+1}}\right) - \phi\left(\frac{-s_{t+1}-\pi_{t+1}^*}{\sigma_{t+1}}\right)\right]\left(V_{t+1}(0)-\eta w_{t+1}\right).
\end{aligned}
$$

Given (12), x_{t+1} is Gaussian conditioning on x_t, π_{t+1}^* and σ_{t+1}, so $\phi(\cdot)$ denotes the standard normal density function.

2.3. Aggregation and equilibrium conditions

Firms' individual price-setting decisions give rise to an endogenous distribution price gaps, $g_t^c(x)$, which evolves according to

$$
g_t^c(x) = \frac{1}{\sigma_t}\int_{s_{t-1}}^{S_{t-1}} g_{t-1}^c(x_{-1})\phi\left(\frac{x_{-1}-x-\pi_t^*}{\sigma_t}\right)dx_{-1} + g_{t-1}^0\phi\left(\frac{-x-\pi_t^*}{\sigma_t}\right) \qquad (17)
$$

where the first term on its right-hand side describes the evolution of the density of price gaps of firms that do not change their nominal prices last period while the second term is the distribution of current price gaps of firms that did change last period. The frequency of price changes g_t^0 is

$$
g_t^0 = 1 - \int_{s_t}^{S_t} g_t^c(x)dx. \qquad (18)
$$

Thus, the aggregate price index satisfies

$$1 = \int_{S_t}^{S_t} e^{(x+p_t^*)(1-\epsilon)} g_t^c(x)\, dx + g_t^0 e^{(p_t^*)(1-\epsilon)} \tag{19}$$

where we have used that the quality-adjusted optimal real reset price p_t^* is the same for all price adjusters. In turn, the clearing condition for the labor market is given by

$$N_t = \frac{Y_t}{A_t}\left(\int_{S_t}^{S_t} e^{(x+p_t^*)(-\epsilon_t)} g_t^c(x)\, dx + g_t^0 e^{(p_t^*)(-\epsilon)}\right) + \eta g_t^0 \tag{20}$$

such that the total hours worked equals the total use of labor for the production of aggregate output (the first term on the right-hand side), where we have imposed the equilibrium condition $C_t = Y_t$ and the loss in aggregate output due to price dispersion (the term in parenthesis), and the total amount of working hours allocated to price adjustment (the second term).

2.4. Aggregate Shocks

The last piece we need to specify, besides monetary policy, is the stochastic process of aggregate shocks. The logarithm of aggregate productivity follows a first-order autoregressive process:

$$\log A_t = \rho_A \log A_{t-1} + \varepsilon_{A,t}, \tag{21}$$

where $\rho_A \in [0,1]$ and $\varepsilon_{A,t}$ is an aggregate productivity shock. The employment subsidy τ_t follows the autoregressive process

$$\tau_t - \tau = \rho_\tau(\tau_{t-1} - \tau) + \varepsilon_{\tau,t}, \tag{22}$$

where $\rho_\tau \in [0,1]$, τ is the steady-state employment subsidy, and $\varepsilon_{\tau,t}$ is interpreted as a cost-push shock. Next we introduce the autoregressive process for stochastic volatility of idiosyncratic quality of goods:

$$\sigma_t - \sigma = \rho_\sigma(\sigma_{t-1} - \sigma) + \varepsilon_{\sigma,t}, \tag{23}$$

where $\rho_\sigma \in [0,1]$, $\sigma > 0$ is the steady-state volatility, and $\varepsilon_{\sigma,t}$ is a *dispersion* shock.

2.5. Auxiliary models

We briefly present three alternative models we use in our analysis. Appendix X describes details.

Standard New-Keynesian model. This is a natural benchmark. Our baseline economy collapses to the textbook new Keynesian model when the idiosyncratic quality shocks are shut down, $\sigma_t = 0$, menu cost are $\eta = 0$ and the pricing friction is modelled *á la*

Calvo (1983), i.e., firms keep prices constant with probability α. Further, we perform a second-order approximation on welfare and a log-linear approximation of inflation dynamics, the "new-Keynesian Phillips curve."

Non-linear Calvo model. This model is also meant for benchmarking. It is identical to the baseline economy with $\sigma_t > 0$ but with pricing *á la* Calvo (1983).

Calvoplus model. We use this model for robustness of our main results. It is in a middle ground between the menu cost and the non-linear Calvo models: $\sigma_t > 0$ and the menu cost is stochastic, being η or zero with Poisson probability α and $1 - \alpha$. The additional parameter α allows to accommodate the share of small price changes in the data – a moment that a pure menu cost model fails to account for. Proposed by Nakamura and Steinsson (2010), it has been extensively studied for monetary non-neutrality due to its flexibility to embed several alternative models, for instance, Alvarez et al. (2016).

3. Optimal monetary policy problem and computational approach

We start our analysis by introducing the central bank's problem, presenting a new computational method to deal with the complexities associated with its high dimensionality, and specifying our baseline calibration for the United States. We consider the Ramsey problem, i.e., optimal monetary policy under commitment.

3.1. Ramsey problem

The central bank selects the path for all equilibrium variables subject to the competitive equilibrium conditions. Combining households' utility function in (1) and the clearing market conditions for final output $C_t = Y_t$ and for labor in (20), the problem of a benevolent central bank is

$$\max_{\substack{\{w_t, Y_t, V_t(\cdot), S_t, s_t,\\ p_t^*, \pi_t^*, g_t^c(\cdot), g_t^0\}_{t=0}^{\infty}}} \mathbb{E}_0 \sum_{t=0}^{\infty} \beta^t \left(\frac{Y_t^{1-\gamma}}{1-\gamma} - \upsilon \frac{Y_t}{A_t} \left(\int_{s_t}^{S_t} e^{-\epsilon\left(x+p_t^*\right)} g_t^c(x)\, dx + g_t^0 e^{-\epsilon p_t^*} \right) - \upsilon \eta g_t^0 \right)$$

subject to the labor supply in (7) relating the real wage w_t and output Y_t, firms' value function $V_t(\cdot)$ in (16), firms' optimal pricing $\{s_t, S_t, p_t^*\}$ in (13), (14) and (15), the definition for inflation of quality-adjusted real optimal reset price π_t^*, the distribution of price gaps $g_t^c(\cdot)$ in (17), the frequency of price changes g_t^0 in (18) and the aggregate price index in (19). Additional constraints are the stochastic processes for aggregate productivity A_t in (21), cost-push shocks τ_t in (22) and dispersion shocks σ_t in (23).

Several observations are due. First, we follow the approach in standard optimal monetary analysis (Woodford 2003; Galí 2008) of separating the Ramsey problem in

two: the equilibrium pinned down by a benevolent central bank and the implementation problem, i.e. the nominal interest rates path consistent with the equilibrium according to the household's Euler equation (8). There is a long literature discussing the determinants of the degree of monetary non-neutrality in menu cost models. This discussion affects implementation, which we abstract from, and instead concentrate on the equilibrium pinned down by optimal monetary policy.

Second, the central bank's objective and its constraints are fully non-linear which, with the exception of labor supply in (7), jointly characterize inflation dynamics. In turn, the objective and the constraint do not explicitly depend on inflation and output gap. In contrast, in the standard framework, welfare is quadratically approximated, the constraints boil down to a single equation characterizing the log-linearly approximated inflation dynamics, the new-Keynesian Phillips curve, and both objective and constrain are expressed in terms of inflation and output gap. In the exercises that come below, we cast the analysis in terms of inflation and output gap to make it comparable.

Finally, note that the constraints set for this problem is continuous and differentiable despite the individual firm's price policy function is not. This is so because each firm has zero mass, and thus the discontinuity in a single firm's behavior does not lead to a discontinuity in aggregates. Furthermore, $V_t(x)$ and $g_t^c(x)$ are continuously differentiable over the relevant range $[s_t, S_t]$.

3.2. Computational solution method

We propose a new algorithm similar to that in González et al. (2024) but in discrete time. The core idea is to represent the problem as a high-dimensional dynamic programming problem in which the Bellman equation and the law of motion of the price-gap distribution are constraints.

The solution of this Ramsey problem is involved because the value function $V_t(\cdot)$ and the distribution $g_t^c(\cdot)$ are infinite-dimensional variables. This poses a challenge as we need to compute the first-order conditions (FOCs) with respect to these infinite-dimensional variables.[10] Our algorithm first discretizes the planner's objective and constraints and then determines the FOCs, instead of first determining the FOCs for the planner's continuous space problem, and then discretizing them. Thus, we transform the original infinite-dimensional problem into a high-dimensional problem,

[10]There are a number of proposals in the literature to deal with this problem. Nuño and Thomas (2022), Smirnov (2022), and Dávila and Schaab (2022) deal with the full infinite-dimensional planner's problem in continuous time. This implies that the Kolmogorov forward (KF) and the Hamilton-Jacobi-Bellman (HJB) equations are constraints faced by the central bank. They derive the planner's FOCs using calculus of variations, thus expanding the original problem to also include the Lagrange multipliers, which in this case are also infinite-dimensional. These papers solve the resulting differential equation system using the upwind finite-difference method of Achdou et al. (2021). Bhandari et al. (2021) make the continuous cross-sectional distribution finite-dimensional by assuming that there are N agents instead of a continuum. They then derive standard FOCs for the planner. In order to cope with the large dimensionality of their problem, they employ a perturbation technique. Le Grand et al. (2022) employ the finite-memory algorithm proposed by Ragot (2019). It requires changing the original problem such that, after K periods, the state of each agent is reset. In this way the cross-sectional distribution becomes finite-dimensional.

in which the value function and the state density are replaced by large vectors with a dimensionality equal to the number of grid points used to approximate the individual state space. This approximation needs to be smooth and accurate enough to capture the higher-order effects of policy.

An additional computational challenge is that a simple discrete-state approximation may fail, as equilibrium conditions include discrete choices. Therefore, we approximate the distribution and value function not by discrete functions on a predetermined grid, but by *piece-wise linear* functions over an *endogenous* grid. The endogenous grid is selected to always include the two boundaries of the inaction region $[s_t, S_t]$ and price gap $x_t = 0$. Furthermore, we explicitly take the mass point at 0 into account in the distribution. Integrals to compute expectations are evaluated algebraically, conditional on those piecewise linear functions.

Appendix E presents the details of the computational solution method. The Bellman equation can thus be approximated over a grid of price gaps x as

$$\mathbf{V}_t = ''_t + [\mathbf{A}_t \mathbf{V}_{t+1} - \mathbf{b_{t+1}} \eta w_{t+1}]$$

where $\mathbf{V}_t$ and $\mathbf{b}_t$ are vectors with the value function and the expected adjustment probability evaluated at different grid points, respectively, and $\mathbf{A}_t$ is a matrix that captures the idiosyncratic transitions due to firm-level quality shocks and aggregate inflation. Similarly, the law of motion of the density for $x \neq 0$ is

$$\mathbf{g_t^c} = \mathbf{F}_t \mathbf{g_{t-1}^c} + \mathbf{f}_t g_{t-1}^0.$$

where $\mathbf{g_t^c}$ and $\mathbf{f}_t$ are vectors representing the probability distribution function and the scaled and shifted normal distribution, respectively, $\mathbf{F}_t$ is a matrix that captures the evolution of the price distribution due to firm-level quality shocks and aggregate inflation, and

$$g_t^0 = 1 - \mathbf{e}_t^\top \mathbf{g_t^c}.$$

is the mass point at $x_t = 0$ where $\mathbf{e}_t$ is a vector of weights corresponding to the trapezoid rule. The labor market clearing condition and the aggregate price index can be written in a similar form. Once we have the discretized version of the problem, we find the planner's FOCs by symbolic differentiation. This delivers a large-dimensional system of difference equations, as we have Lagrange multipliers associated with each grid point of the value function or the probability function.

Next, we find the Ramsey steady state. To do so, we construct a nonlinear multi-dimensional function mapping inflation to the rest of the steady-state equilibrium variables. We then combine this function with the planner's FOCs. As the system is linear in Lagrange multipliers, the solution boils down to finding the zero of a non-linear function of the initial variable (inflation) using the Newton method. Finally, to compute the dynamics of the Ramsey problem, we solve the system of difference equations non-linearly in the sequence space also using the Newton method.

The symbolic differentiation and the two applications of the Newton method can be automated using several available software packages, in our case, Dynare (Adjemian et al. 2023). The approach is compatible with the nonlinear sequence-space Jacobian toolboxes. This algorithm can be employed to compute optimal policies in a large class of heterogeneous-agent models. Compared to other algorithms, it stands out as easy to implement. González et al. (2024) show that this algorithm delivers the same results as computing the FOCs by hand using calculus of variations and then discretizing the model. Our algorithm runs in a few minutes on a normal laptop.

3.3. Baseline calibration

Table 1 presents our baseline calibration. The discount factor is $0.96^{1/12}$, the elasticity of substitution across products is $\epsilon = 7$, so the frictionless net markup is 1/6. Utility of consumption is log, $\gamma = 1$, as in Midrigan (2011), and the weight of leisure in utility is $\upsilon = 1$, so $w_t = Y_t$. The menu cost is $\eta = 3.59\%$ and the steady-state standard deviation of idiosyncratic quality shocks is $\sigma = 2.36\%$. This way the model yields in steady state the 8.7% of average frequency of price changes and the 8.5% of average absolute size of non-zero price changes estimated for the U.S. (Nakamura and Steinsson 2008).[11] Finally, the persistence of shocks is taken from Smets and Wouters (2007), once transformed from quarterly to monthly frequency: $\rho_A = 0.95^{1/3}$ for aggregate productivity shocks and $\rho_\tau = 0.9^{1/3}$ for employment subsidy shocks (interpreted as cost-push shocks). The persistence of dispersion shocks on idiosyncratic quality shocks is $0.75^{1/3}$.

β	ϵ	γ	υ	η	σ	ρ_A	ρ_τ	ρ_σ
$0.96^{1/12}$	7	1	1	0.036	0.024	$0.95^{1/3}$	$0.90^{1/3}$	$0.75^{1/3}$

TABLE 1. Parameter values

4. Strike while the iron is hot

We postpone the steady-state analysis to focus on our main result: the non-linearity of optimal monetary policy for cost-push shocks.[12] This section relies on numerical simulations to present the nature of this non-linearity, its intuition, its dependence on key parameters and moments of the empirical distribution of price changes, and its robustness in the Calvoplus model.

Our main focus is on the systematic monetary policy response to shocks. We therefore analyze *timeless* optimal monetary policy (Woodford 2003; Galí 2008). This corresponds to the optimal monetary policy starting from the Ramsey steady state when a shock hits the economy and all of the Lagrange multipliers are initialized at their steady-state values.

[11] The calibration is conducted at the optimal steady state inflation rate to be introduced below.

[12] We defer to Section 6 for an analysis of the steady state of the optimal Ramsey problem.

4.1. Non-linear optimal monetary response to cost-push shocks

Figure 1 compares impulse-response functions implied by optimal monetary policy in the menu cost model to a large cost-push shock, a rescaled small shock and a large shock in the non-linear Calvo model.[13] In all of them, inflation increases (panel a) and output gap drops (panel b), i.e., the standard prescription of "leaning against the wind" in the new-Keynesian model holds.[14]

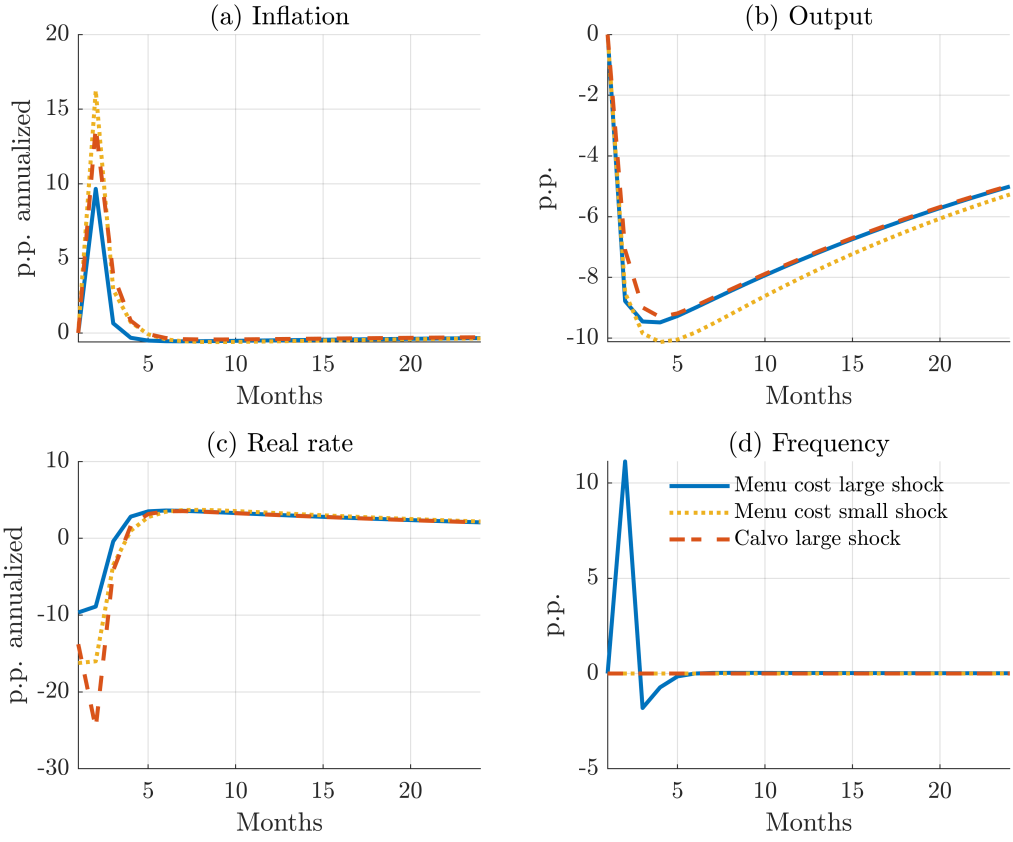


FIGURE 1. Impulse responses to a large cost-push shock in the Calvo model, and to a large and a small cost-push shock in the menu cost model under the optimal monetary policy.

Note: all displayed variables except frequency are linearly scaled in the small shock according to the ratio between the large and small shocks.

The main difference in the responses is that, in the menu cost model, optimal monetary policy is non-linear. To see this non-linearity, we compare responses to the large shock and the rescaled small shock: The former yields a significant response of frequency of price changes (in this example, above 20%, solid blue line in panel c of Figure 1), while the latter keeps frequency almost constant (yellow dotted line).

[13] To produce the small shock, we divide the size of the large shock by 100 and then multiply responses by 100.

[14] One feature that somewhat simplifies the analysis is that, for cost-push shocks, output equals the output gap as this type of shock yields no variation of efficient output. Thus, in this section, we indistinctively refer to output and output gap.

The response of inflation is much milder for the large shock (solid blue line, panel b) than for the rescaled small shock (yellow dotted line, panel b), which is closer to the non-linear Calvo model (red dashed line, panel b). The tighter monetary policy in the menu cost model after a large shock leads to a somewhat more adverse output-gap response (panel a). For small shocks, the policy in the two models approximately coincides (not shown).

Figure 2 draws the optimal impact response of inflation and output gap to a range of cost-push shock sizes. For the menu cost model, the response of inflation has an inverted-S shape (solid blue, panel a) which contrasts with its quasi-linearity in the non-linear Calvo model (dashed red, panel a). When shocks are small, the optimal response of inflation in both models is quasi-linear and with the same slope. As shocks are larger, optimal monetary policy is more aggressive to control inflation in the menu cost model: The central bank "strikes while the iron is hot". In turn, this does not imply a stronger response of output (solid blue line compared to dashed red line in panel b).

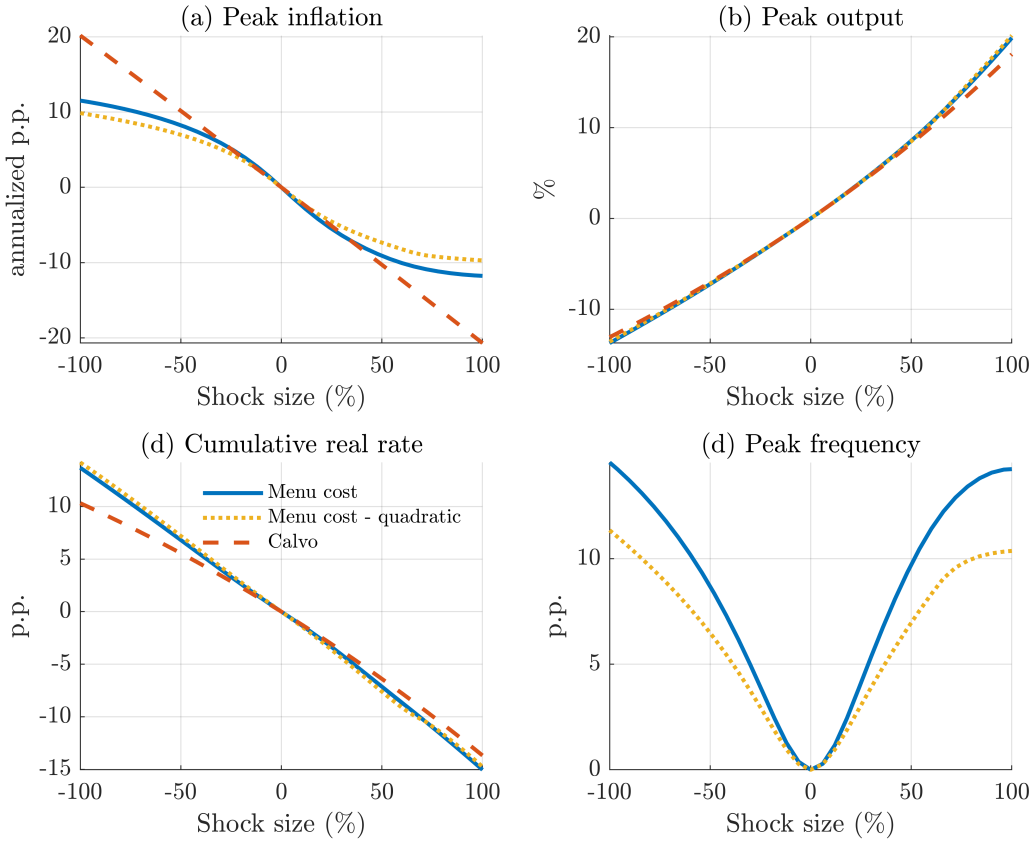


FIGURE 2. Optimal response to a cost-push shock for different shock magnitudes. DROP FROM THIS FIGURE THE QUADRATIC MENU COST. DROP PANELs C and D. CHANGE LEYEND TO "NON-LINEAR CALVO".

Note: The figure displays the difference in the value of inflation, output gap, and repricing frequency between the period after the shock arrival and the value in the deterministic steady state. The real interest rate is evaluated over the entire life of the shock.

In addition, Figure 2 shows some sign-dependence, as the optimal policy response depends on shocks sign. This is due to asymmetries in firms' profit function, a feature we come back when we study the optimal long-run inflation in Section Y.

4.2. Inspecting the mechanism

We now explain the intuition for the non-linear optimal monetary policy. In short, it hinges on the endogeneity of price stickiness in menu cost models. This endogeneity affects both the central bank's objective and inflation dynamics implicitly characterized in the set of constraints of the Ramsey problem. Thus, it potentially affects the "standard" trade-offs involved in monetary policy as well new elements in these trade-offs may appear.

4.2.1. A textbook benchmark

To frame the analysis, we use the textbook new-Keynesian model. When the menu cost friction is replaced by Calvo pricing and there are no idiosyncratic quality shocks, Appendix X shows that the linear-quadratic approximation of the Ramsey problem is

$$\max_{\{\pi_t, \tilde{y}_t\}_{t=0}^{\infty}} \quad -\mathbb{E}_0 \sum_{t=0}^{\infty} \beta^t \left(\frac{\epsilon}{\kappa} \pi_t^2 + \tilde{y}_t^2 \right) \text{ subject to } \pi_t = \kappa \tilde{y}_t + \beta \mathbb{E}_{t+1} \pi_{t+1} + \tau_t \tag{24}$$

where inflation dynamics is characterized by a single equation, the new-Keynesian Phillips curve, which enters as constraint in every period t, π_t and $\tilde{y}_t$ are log-linear deviations from steady state of inflation and output gap, and τ_t is a cost-push shock.[15] This problem solves

$$\pi_t = -\frac{1}{\epsilon} (\tilde{y}_t - \tilde{y}_{t-1}) \tag{25}$$

such that optimal monetary policy "leans against the wind" by tolerating temporary deviations of inflation to accommodate the response of the output gap to the cost-push shock. The "optimal rule" in (25) is log-linear and depends only on the elasticity of substitution across varieties ϵ and not on compound parameter $\kappa \equiv (1-\beta)(1-\beta\alpha)/\alpha$ where $1-\alpha$ is the frequency of price changes and β is the discount factor.

To see why, the Ramsey objective in (24) is the welfare loss due to the pricing friction depending on inflation and output gap, respectively capturing the effect of inefficient price dispersion and average markup fluctuations. Inefficient price dispersion depends on ϵ/κ: If prices are fully flexible, $\alpha = 0$, $\kappa \to \infty$, so there is no inefficient price dispersion for any level of inflation. Thus, ϵ/κ affects the relative weight of inflation

[15] Strictly speaking, the Ramsey objective depends on the log-linear deviation of inflation from optimal long-run inflation π_{ss}, which in this benchmark model is $\pi_{ss} = 0$. Section Y shows that optimal long-run inflation is slightly positive in our menu cost model. To make them comparable, we express inflation in log-linear deviation from optimal long-run inflation and simply refer to it as inflation. In addition, we implicitly assume that the steady-state subsidy τ is set to achieve efficient output in steady state.

and output gap in the central bank's objective. In turn, $1/\kappa$ enters in the constraint governing the effect on output of monetary policy taming inflation given expected inflation, the "sacrifice ratio". When solving for optimal monetary policy, these two effects cancel out: if prices are more flexible, the sacrifice ratio and the weight of inflation relative output gap in the Ramsey objective decrease in the same proportion.

With this benchmark in mind, "strike while the iron is hot", i.e., the non-linear optimal monetary policy in Figures 1 and 2, may have two complement sources. First, the "standard" trade-offs may be different in menu cost models if there is not a one-to-one mapping between the sacrifice ratio and the weight of inflation relative to inflation in the central bank's objective. Second, the endogeneity of nominal price stickiness in menu cost models may give raise to new elements in this trade-offs. In the following we independently explore these two potential sources.

4.2.2. A non-linear sacrifice ratio

We start by showing that the sacrifice ratio is non-linear in the menu cost model. To do so, we must abstract from optimal policy. Thus, for this purpose alone, we assume that monetary policy follows a Taylor rule

$$i_t = \phi_\pi \pi_t + \phi_y \tilde{y}_{t+1} + \varepsilon_t \tag{26}$$

IS THIS TAYLOR RULE RIGHT? where $\phi_\pi = 1.5$ and $\phi_y = 0.5/12$ as in Taylor (1993) and ε_t is an i.i.d. monetary shock. We then produce Figures 3 and 4. Figure 3 shows, in panel (a), the relationship between the impact response of inflation π_t and the cumulative discounted sum of output gaps responses, $\sum_{j=0}^{\infty} \beta^j \mathbb{E}_t \tilde{y}_{t+j}$, in our menu cost model (solid blue line) and in the new-Keynesian Phillips curve (dashed red line) for a range of monetary policy shocks sizes.[16] In the latter, the slope of this relationship is κ, the inverse of the sacrifice ratio. The dashed red line has by construction the same slope than the solid blue line for small shocks. We follow Auclert et al. (2024) who show that a menu cost model approximately yields the same Phillips curve for small shocks than a Calvo model calibrated to a counterfactual high frequency of price changes to mimic the "selection effect".[17] The main observation is that, for large shocks, this relation becomes steeper and eventually even bends backwards in the menu cost model (blue line in panel a).

To provide intuition, panel (b) in Figure 3 depicts the relationship between impact responses of inflation and frequency of price changes in the menu cost model for the same range of monetary shocks than panel (a). For small shocks, the frequency of price

[16] Impulse responses are computed non-linearly under perfect foresight. For small shocks, our approach is equivalent to the first-order approximation to the stochastic problem, as discussed by Boppart et al. (2018). For large shocks, its interpretation is similar to that in Cavallo et al. (2023): an unexpected once-and-for-all large shock starting from the deterministic steady state.

[17] This selection effect (Golosov and Lucas 2007) refers to price changes being in average larger in menu cost models than in the Calvo model, so the former yields less nominal price stickiness once both are calibrated to match the frequency of price changes.

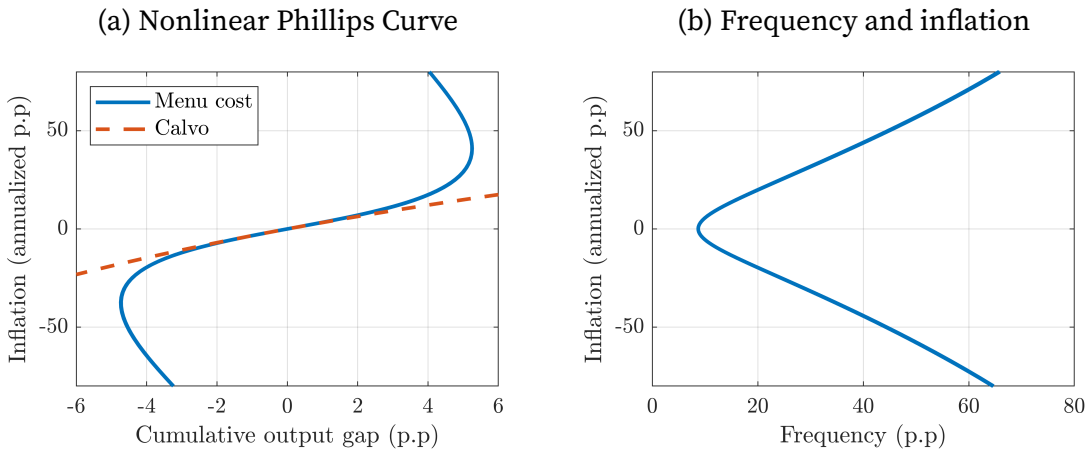


FIGURE 3. Inflation-output trade-offs in the menu cost and Calvo models. CHANGE RED LINE TO TEXTBOOK CALVO AND CHANGE LEGEND"

Note: The figure is produced by computing the impulse responses to monetary policy shocks of different magnitudes assuming a Taylor rule. The solid blue line is the baseline menu cost model and the dashed red line is the recalibrated Calvo model.

changes remains close to its steady-state, 8.7% in our calibration. As shocks are larger, the response of both inflation and frequency rise. This makes the responsiveness of the cumulative output gap to decrease in panel (a). At frequencies over 40%, the inflation-output gap relationship is backward bending. At this level, monetary policy reaches its maximum real effects and any further monetary easing raises inflation with smaller output effects. However, such a case is fairly extreme. For the rest of the analysis we restrict our attention to shocks not as large as to go beyond this point.

Quantitatively, the slope of the solid blue line in panel (a) of Figure 3 doubles when frequency reaches 20%, a magnitude documented during the post-COVID inflation surge (Montag and Villar 2023). Thus, while in a low-frequency and low-inflation environment, the sacrifice ratio is high, it becomes much lower once frequency and inflation increases.[18] Besides, responses are asymmetric in the sign of shocks, although it is quantitatively small. This is due to the shape of firms' profit function.

THIS PART HAS TO BE ADJUSTED AFTER FIG 4 IS CHANGED TO BE THE SAME AS FIG 3 BUT FOR COST-PUSH SHOCKS => Figure 4 shows similar analysis for cost-push shocks τ_t. the responses of inflation (panel a), output gap (panel b), frequency of price changes (panel c) and interest rates (panel d) to cost-push shocks of different magnitudes under a Taylor rule. The shock is a persistent decline in employment subsidy τ_t. Inflation and frequency are evaluatedon impact, output gap is evaluated at its peak response (5-6 months after impact) and the real interest rate gap is the cumulated. The figure displays both the menu cost model (solid blue line) and the (recalibrated) Calvo model (dashed red line).

In Figure 4, the nonlinearity is quantitatively small when the shock is small enough to yield a response of frequency below 10 p.p. In this region, the Calvo model behaves

[18] Blanco et al. (2024b) also discuss how the sacrifice ratio changes with the level of inflation.

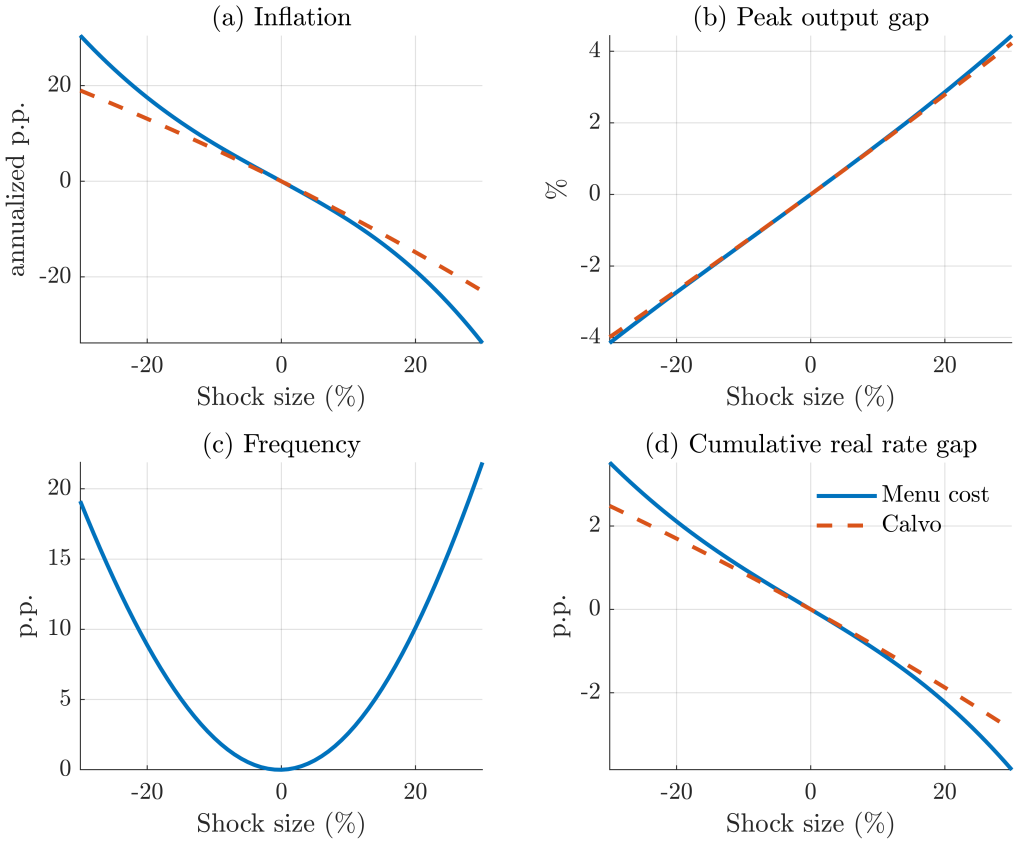


FIGURE 4. Response to a cost-push shock for different shock magnitudes. ADJUST FIG 4 TO BE THE SAME AS FIG 3 BUT FOR COST-PUSH SHOCKS

Note: The figure displays the difference in the value of inflation and the frequency of price changes between the period of the shock arrival and the value in the deterministic steady state. The output gap is evaluated at the peak of the impact relative to the deterministic steady state. Panel (d) shows the difference of the real interest rate from steady state, cumulated from $t = 1$ to $t = \infty$.

similarly.[19] For larger cost-push shocks, the menu cost model yields a larger response of inflation (panel a). As the frequency approaches 20% (up 11 p.p. from the steady state of 8.7%), the response of inflation in the menu cost model is significantly larger than in the Calvo model. The intuition again hinges on the increase in the frequency of price changes as a result of the shock, which makes the price level endogenously more flexible. As the Taylor rule is the same for both models, the interest rate responds more in the menu cost model (panel d). This leads to a marginally amplified response of the output gap in the menu cost model (panel b).

4.2.3. The central bank's objective

We now explore whether the different Ramsey objective in the menu cost model presented in Section 3.1 from the quadratic benchmark in (24) is behind the non-linear

[19] Figure A4 in Appendix D.3 shows how the full impulse responses to a small cost-push shock are similar to those of the recalibrated Calvo model.

"strike while the iron is hot" optimal monetary policy. In short, it is not as the objective in (24) is a good approximation of the Ramsey objective in the menu cost model. This implies that "strike while the iron is hot" is mostly driven by the endogeneity of price stickiness. To see the distinction, note that (25) also holds for a problem analogous to (24) where κ is a non-linear function of the cost-push shock τ_t. However, it does not hold if κ is function of monetary policy. <-NOt clear or Wrong It does not hold either if the weight of inflation relative to output gap in the central bank's objective does not scale with $1/\kappa$. It is this latter possibility what we explore here and leave the implications of the endogeneity of price stickiness for Section 4.2.4.

To start, panel (a) of Figure 5 depicts the relationship between optimal impact responses of inflation and output to a range of cost-push shocks for several alternative models. Impact responses conveniently map cumulative responses and abstract from lagged output, so the inflation-output relationship for the textbook benchmark (dotted yellow line) has direct interpretation as the "optimal rule" in (25) with slope $-1/\epsilon$. This rule contrasts with the inverted-S shaped inflation-output relationship in the menu cost model (solid blue line), a corollary of the "strike while the iron is hot" optimal monetary policy. Its slope is exactly $-1/\epsilon$ when shocks are small, i.e., when the frequency of price changes remains close to its steady state level. However, for larger shocks, its slope increasingly flattens as frequency responds.

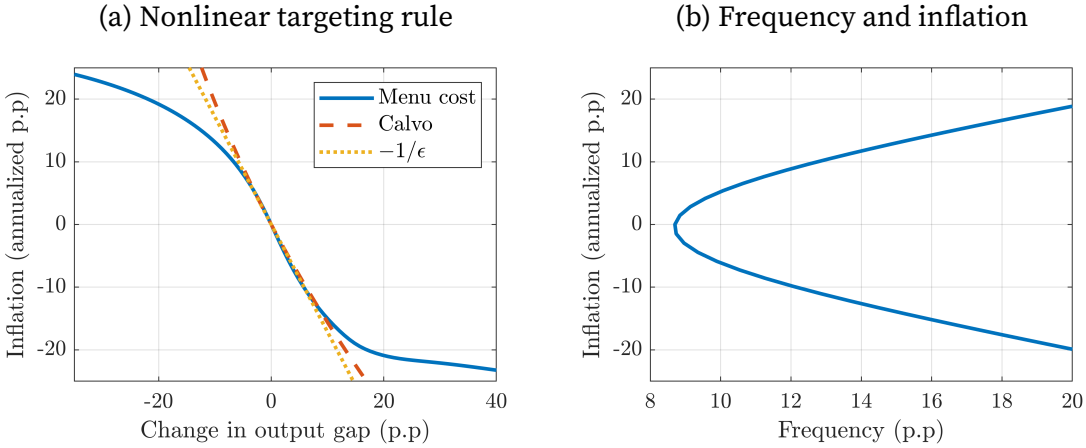


FIGURE 5. Optimal target rule. CHANGE LEGENDS: DASHED RED LINE IS "NON-LINEAR CALVO", DOTTED YELLOW LINE IS "TEXTBOOK" OR "LQ BENCHMARK". ALSO, ADD DOTTED BLUE LINE WITH "MENU COST-QUADRATIC" IN BOTH PANELS

Note: Panel (a) shows the relationship between annualized inflation and the change in output gap on impact as a function of a series of cost-push shocks under the optimal policy (blue solid line); and contrasts it to the optimal target rule in the Calvo model (dashed red line) and in the linearized Calvo model (dotted yellow line). Panel (b) shows the frequency at each inflation level.

To gauge the implications of a fully non-linear instead of a quadratic central bank's objective, panel (a) of Figure 5 draws the optimal impact inflation-output relationship in the non-linear Calvo model (dashed red line). Its slope is $-1/\epsilon$ for small shocks and quite close for large shocks. We thus conclude that a fully non-linear objective is *per*

se not a quantitatively important source of the inverted-S shaped optimal monetary policy.Not just the objective also the constraint is nonlinear. So the conclusion from this is that the fully nonlinear Calvo model doesnt give rise to S shaped policy However, it can be once interacted with other departures of the optimal monetary problem in the menu cost model versus the textbook benchmark in (24). Last sentence makes no sense

To explore this possibility, the dotted blue line in panel (a) of Figure 5 draws the optimal impact inflation-output relationship in our menu cost model where the central bank's objective is as in (24). To do this, we compute the sacrifice ratio as a function of cost-push shocks by.... and interpret it as $1/\kappa$ in the quadratic objective. EXPLAIN THIS <-What? We use the same (constant) weight as in Calvo dIt exhibits the same "strike while the iron is hot" property than in the fully non-linear menu cost model. We thus conclude that it is the new trade-offs for monetary policy involved in the endogeneity of nominal price stickiness in menu cost models and not a modification of its "standard" trade-offs due to non-linearity of the sacrifice ratio or the central bank's objective. FINISH THIS PARAGRAPH ONCE I UNDERSTAND WELL THE NATURE OF THE EXERCISE IN FIGURE 2.

Welfare decomposition. It is well known that, in menu cost models, firms' gap between actual and desired price is bound by the size of the menu cost while it can be arbitrary large in the Calvo model. Thus, how could both models have similar Ramsey objectives? We answer this question using an analytical decomposition of the welfare loss $W_0 - W_0^e$ due to the pricing friction:

$$(27)\quad W_0 - W_0^e = \sum_{t=0}^{\infty} \beta^t \left(\underbrace{-\log(1-\tau_t) - \overline{\mu}_t - \left(\frac{1}{e^{\overline{\mu}_t}(1-\tau_t)} - 1 \right)}_{\text{Average markup gap}} \right.$$
$$\left. \underbrace{-\left(\frac{1}{e^{\overline{\mu}_t}(1-\tau_t)} (\zeta_t^{\mu-\overline{\mu}} - 1) \right)}_{\text{Price dispersion}} \underbrace{-\eta g_t^0}_{\text{Menu costs}} \right).$$

REVISE INDEXES IN μ which is derived in Appendix B.2 and has three components. First, fluctuations in firms' markups $\mu_t(i) = p_t(i) - mc_t(i)$ create *misallocation* while markups remain constant absent of pricing frictions.[20] Misallocation can be decomposed into the "average markup gap" caused by time variation in average markups $\overline{\mu}_t$ and "price dispersion" caused by cross-sectional markup dispersion, $\zeta_t^{\mu_t(i)-\overline{\mu}_t}$. The average markup gap thus describes *aggregate* over- or under-consumption, while the price dispersion gap refers to the inefficient *relative* consumption of different goods. The

[20] The steady-state employment subsidy τ is set to offset the inefficiency of steady-state markups.

third component accounts for labor being inefficiently allocated to price adjustment (*menu costs*).

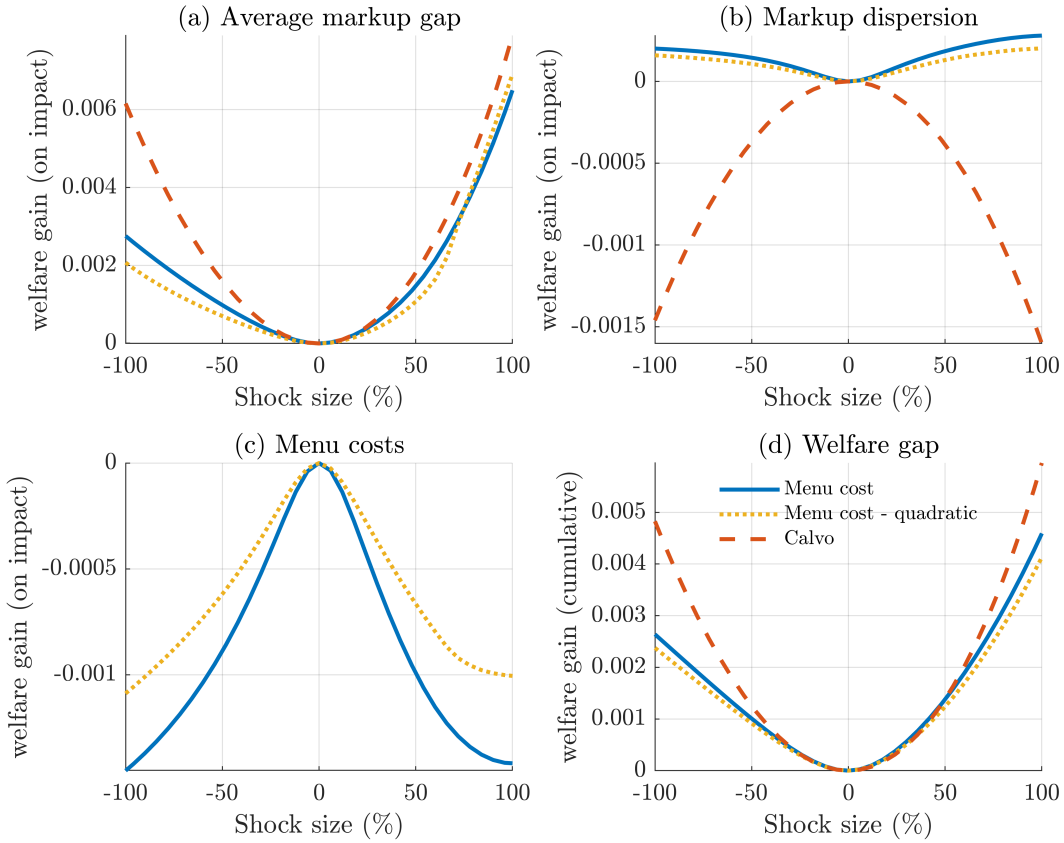


FIGURE 6. Welfare decomposition of a cost-push shock for different shock magnitudes. BE CONSISTENT IN WITH THE COLORS OF LINES FROM FIGURE 5

Note: The figure displays the difference in the different components of the welfare gap in equation (27). Panels a, b, c report impact effects, panel d reports the cumulative discounted welfare gap.

Figure 6 displays the welfare gap (panel d) and its components caused by the average markup gap (panel a), price dispersion (panel b) and menu costs (panel c) for a range of cost-push shocks for the menu cost model (solid blue line), the menu cost model with the quadratic central bank's objective (dotted yellow line) and the textbook new-Keynesian model in (24) (dashed red line).

Panel (d) of Figure 6 shows that, for the baseline calibration, the full Ramsey's objective is well approximated by a quadratic objective when the pricing friction is either due to menu costs or the Calvo assumption. Calvo Quaddratic is not shown The decomposition of welfare shows why. All three models yield similar average markups gap component (panel a). Instead, the price dispersion component is convex on the size of cost-push shocks in the Calvo model (dashed red line in panel b) while it is mild decreasing in the two menu cost models. This is due to the selection effect: Firms' with large price gaps are more likely to adjust prices after a cost-push shock. Instead, in the two versions of the menu cost model, panel (c) shows that the welfare cost of price

adjustment (menu) costs is increasing in the size of cost-push shocks. This is because the price adjustment component is larger than the price dispersion component and thus the former quantitatively dominates. Peter, the new figure doesnt fit the text

4.2.4. Endogeneity of price stickiness

This is the core reason behind the non-linear "strike while the iron is hot" optimal monetary policy in the menu cost model. Endogeneity of price stickiness yields new trade-offs for monetary policy, such that it does not only "lean against the wind", as the standard prescription, but also "lean against frequency of price changes", especially for large cost-push shocks. To do so, it is optimal to be more aggressive against inflation than in our two benchmarks where price stickiness is invariant to monetary policy, the new-Keynesian model and the non-linear Calvo model.

For illustration, we use a simplified version of our menu cost model where the Ramsey problem can be conveniently cast as an objective function depending on inflation and output,[21] and a single constraint characterizing inflation dynamics. Thus, it preserves the structure of the textbook benchmark in (24). Specifically, we assume that households and firms fully discount the future, $\beta = 0$, so the Ramsey problem is effectively static and takes the form:

(28)
$$\max_{\{\pi_t, Y_t\}} \frac{Y_t^{1-\gamma}}{1-\gamma} - \upsilon \left(\frac{\varepsilon(1-\tau_t)}{\varepsilon-1}\right)^{-\varepsilon} Y_t^{1-\varepsilon} \left[\int_{s(Y_t,\tau_t)}^{S(Y_t,\tau_t)} e^{-\varepsilon x} g^c(x;\pi_t)dx + \left(1 - \int_{s(Y_t,\tau_t)}^{S(Y_t,\tau_t)} g^c(x;\pi_t)dx\right)\right] - \upsilon\eta\left(1 - \int_{s(Y_t,\tau_t)}^{S(Y_t,\tau_t)} g^c(x;\pi_t)dx\right).$$

subject to

$$1 = \left(\frac{\varepsilon(1-\tau_t)Y_t}{\varepsilon-1}\right)^{1-\varepsilon} \left[\int_{s(Y_t,\tau_t)}^{S(Y_t,\tau_t)} e^{(1-\varepsilon)x} g^c(x;\pi_t)dx + \left(1 - \int_{s(Y_t,\tau_t)}^{S(Y_t,\tau_t)} g^c(x;\pi_t)dx\right)\right]$$

where first term in the objective is households' utility for consumption once $C_t = Y_t$ is imposed and all the rest is disutility of hours worked. Hours worked is affected by how much the cost-push shock τ_t offsets market power (first term in parenthesis), the cross sectional distribution of prices (terms in square brackets), including prices that do not change (first integral) and those which change (second integral), and the inefficient use of labor to pay for the menu cost (term in the second line). The constraint is given by the aggregate quality-adjusted price index which has the same components. Appendix X presents the details of derivation of this expression. Note that the cost-push shock τ_t enters here in the same way than in the full Ramsey problem in Section 3.1, although there it is implicit in the optimal quality-adjusted real reset price p_t^*. Cost-push shocks also affect real wages and thus the effective size of menu costs which in turn affect the

[21] Recall that for cost-push shocks efficient output remains constant.

boundaries of the inaction band (s_t, S_t).

For comparison, the Ramsey problem in the non-linear Calvo model for $\beta = 0$ is

$$\max_{\{\pi_t, Y_t\}} \frac{Y_t^{1-\gamma}}{1-\gamma} - \upsilon \left(\frac{\varepsilon(1-\tau_t)}{\varepsilon - 1} \right)^{-\varepsilon} Y_t^{1-\varepsilon} \left[\alpha \int_{-\infty}^{\infty} e^{-\varepsilon x} g^c(x; \pi_t) dx + (1-\alpha) \right] \tag{29}$$

subject to

$$1 = \left(\frac{\varepsilon(1-\tau_t) Y_t}{\varepsilon - 1} \right)^{1-\varepsilon} \left[\alpha \int_{-\infty}^{\infty} e^{(1-\varepsilon)x} g^c(x; \pi_t) dx + (1-\alpha) \right]$$

which follows the same logic than (28) once we consider that, instead of firms deciding when to pay for the menu cost, a share $1 - \alpha$ of firms is randomly selected to change its price for free. The additional trade-offs for monetary policy arising from the endogeneity of nominal price stickiness in the menu cost model can be seen by inspecting the differences between the Ramsey problems in (28) and (29). As monetary policy affects both inflation and output, we start by describing the effect of them on price stickiness, i.e., on the mass of price adjusters (also equivalent to the frequency of price changes). With that intuition at hand, we describe the additional trade-offs for monetary policy in the menu cost model versus the non-linear Calvo model.

First, the distribution of price gaps $g^c(\cdot)$ in (28) depends on inflation. If, *ceteris paribus*, inflation is higher, firms are more willing to increase their prices, so $g^c(\cdot)$ shifts downward. More firms hit the lower bound of the inaction band s_t, so the mass of positive (negative) price changes increases (decreases). Inflation also affects $g^c(\cdot)$ in (29), but as firms randomly adjust, this implies only an intensive margin effect, the average size of price changes increase, which is also in (28). In the menu cost model, if the exogenous inflation raise is small, the mass of price adjusters remains close its steady-state level, but it increases as the inflation is larger.

Second, the boundaries of the inaction band (s_t, S_t) in (28) depend on output. If, *ceteris paribus*, output is higher, the mass of adjusters responds through two opposing mechanisms. The real wage is higher via a contraction in labor supply, so the menu cost effectively increases. This calls for wider inaction band, i.e., assuming an invariant distribution $g^c(\cdot)$, lower mass of price adjusters, both positive and negative. However, higher output also means that firms face higher demand, so the effect on profits of deviations from optimal prices scales up. This in turn calls for narrower inaction band and thus larger mass of price adjusters. As the former mechanism dominates the latter in our quantitative exercises, for the sake of the argument, let assume that an exogenous increase in output yields lower mass of price adjusters.

The effect of inflation and output on price stickiness poses new monetary policy trade-offs. As standard, monetary policy decides how much of a cost-push shock must be absorbed by inflation and output. If the cost-push shock is large, the mass of price adjusters increase. If monetary policy tame the response of inflation, it can thus tame the response of price adjusters and thus decrease the welfare effect of inflation, as shown in Section 4.2.3. But by doing so, it increases the sacrifice ratio, as shown

in Section 4.2.2. In turn, as the standard monetary policy trade-off points out, the constraint implies that lower inflation response to the cost-push shock means that output must fall by more. This implies that inaction bands widens, which further decrease the mass of price adjusters. Overall, these two effects reinforce each other on making optimal for central banks to respond strongly respond to the inflation surge. If cost-push shocks are small, then the mass of adjusters do not respond, and thus optimal monetary policy is similar than way than in the new-Keynesian model or in the non-linear Calvo model for large cost-push shocks.

[INSERT NEW FIGURE HERE]

REVISE THIS WHOLE PARAGRAPH ONCE WE GET THE FIGURE This intuition is confirmed in our quantitative exercises. Panel (a) of Figure X draws the relationship between optimal impact responses of inflation and output for the baseline calibration in the full menu cost model assuming that the inaction band (s_t, S_t) is invariant. This way, we shut down one of the channels monetary policy affects price stickiness. The inflation-ouput relationship when the (s_t, S_t) is invariant is in the middle ground between its inverted-S shape in the full menu cost model (solid blue line) and its quasi-linearity in the non-linear Calvo model (dashed red line).

I DO NOT KNOW WHAT TO DO WITH THIS PARAGRAPHThe IS curve (**??**) implies that the output gap is equal to the negative sum of all future deviations of the real interest rate from its efficient level (which is unaffected by cost push shocks and equal to the steady state real rate). Interpreting the real interest rate gap as the current "policy stance", this intertemporal sum is a summary measure of the policy stance to which the central bank commits for the future. Substituting the output gap by this intertemporal policy stance and inverting the axis (see Figure A8 in the Appendix), allows a convenient re-interpretation of the target rule highlighting the "strike while the iron is hot" nature of optimal policy: When inflation is high, the central bank sets the nominal rate so as to achieve an over-proportional increase in the real rate. In other words, when firms adjust prices more frequently, the policy stance is more reactive to inflation.

4.3. Robustness and sensitivity analysis

We now show the robustness of the non-linear "strike while the iron is hot" optimal monetary policy. In particular, we explore alternative parameter choices and an extension of the Golosov and Lucas (2007) model, the CalvoPlus model (Nakamura and Steinsson 2008).

Calvoplus model. This is a variation of the canonical menu cost model where firms may adjust prices by paying the menu cost, as standard, or when they have an opportunity to adjust prices for free, which has a Poisson probability, as in Calvo (1983). This setup has become a popular model as it allows to match additional moments of the distribution of price changes (Nakamura and Steinsson 2010) and, under simplifying

assumptions, is solvable in closed form for the response of aggregate variables to a once-and-for-all money supply shock (Alvarez et al. 2011; Alvarez and Lippi 2014). At the macro level, its key prediction is that selection is decreasing in the probability of free price adjustment, so monetary policy has stronger real effects, which are more in line with time-series evidence. In the context of our analysis, the probability of free price adjustments affects the nonlinearity of the Phillips curve, which raises concerns that it may potentially influence monetary policy prescriptions. However, we show that this is not the case. This result validates our choice of using the canonical Golosov-Lucas model as the workhorse setup.

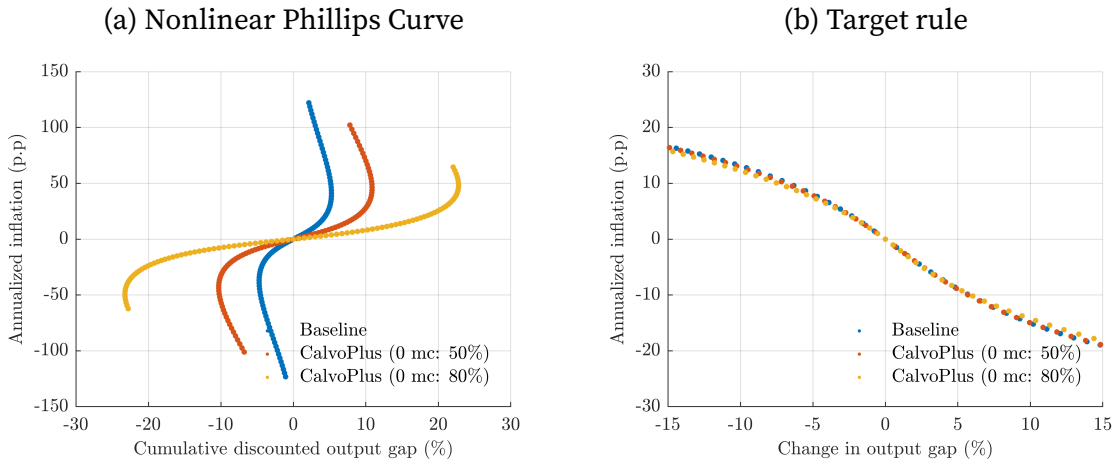


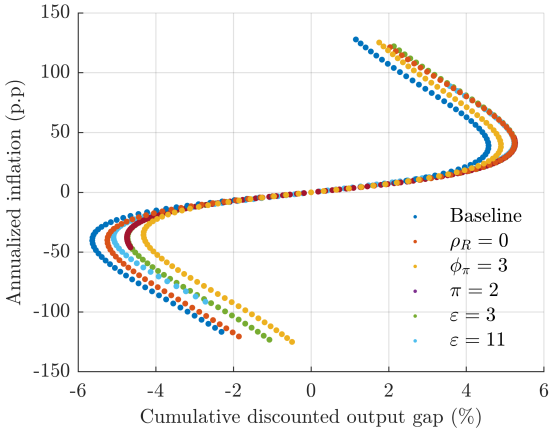
FIGURE 7. Nonlinearity of the Phillips curve and the target rule in the CalvoPlus model
Note: The figures recreate the nonlinear Phillips curve (a) and the target rule (b) for the baseline menu cost model and the CalvoPlus model with two parametrizations: (i) the probability of zero menu cost is 50% and (ii) it is 80%.

Appendix F presents the CalvoPlus setup. We calibrate it such that (i) half and (ii) 80% of the steady-state frequency of price changes is due to free price adjustments. We recalibrate the menu cost η and the dispersion of idiosyncratic shocks σ parameters to match the empirical frequency and absolute size of price changes in U.S. data.

Results are presented in Figure 7. Panel (a) shows that the CalvoPlus model can substantially reduce the slope of Phillips curve after small shocks, improving the realism of the framework (Nakamura and Steinsson 2010). At the same time, the CalvoPlus framework still implies a highly nonlinear Phillips curve, with a slope that increases even faster than the baseline for similar increases in the inflation rate. The main result of this exercise is that, in spite of the differences among models in the shape of the Phillips curve, panel (b) in Figure 7 shows that the CalvoPlus model has almost identical optimal target rule than the baseline menu cost model. The reason is that, for small shocks, both models behave similar to Calvo, so the optimal monetary policy rule depends only on $1/\epsilon$ – which is the same in both models. For large shocks, the CalvoPlus model behaves similarly to the menu cost model as most of the price changes triggered by the shock are due to firms paying the menu cost.

Alternative parametrization.. Panel (a) of Figure 8 shows the robustness of the non-linear Phillips curve. The figure reports the relationship between the impact effect of annualized inflation and the cumulative discounted output gap for different i.i.d. monetary policy shocks of varying sizes as Figure 3. It reports how the relationship changes for varying Taylor rule parameters: no smoothing ($\rho_R = 0$), more aggressive anti-inflationary stance ($\phi_\pi = 3$), 2 percent inflation target ($\pi^* = 2\%$). Additionally, it shows the relationship for varying the elasticity of substitution parameter $\epsilon = 3, 11$[22]. The figure shows that the relationship is not structural in the sense that it is not independent of the policy rule, but it is quantitatively robust in the sense that modifying the Taylor rule parameters and the elasticity of substitution parameters modify the figure only slightly. It's qualitative features concerning size-dependence and asymmetry described in Section D.1 stay unchanged.

(a) Nonlinear Phillips Curve



(b) Target rule

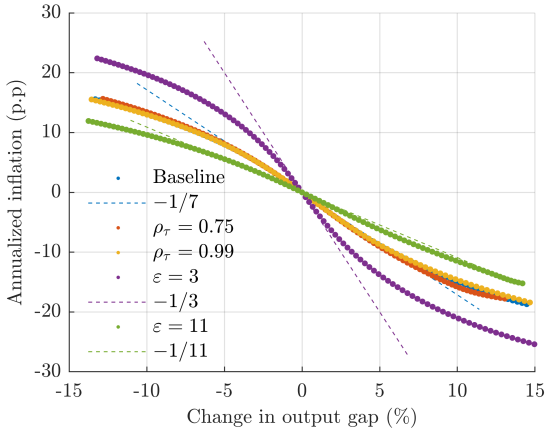


FIGURE 8. Non-linearity of the Phillips curve and the target rule for alternative parameters

Note: The figures recreate the nonlinear Phillips curve (a) and the target rule (b) for alternative parameter values. The Phillips curve shows robustness to alternative Taylor rule coefficients: no smoothing ($\rho_R = 0$), more aggressive anti-inflationary stance ($\phi_\pi = 3$), 2 percent inflation target ($\pi^* = 2\%$). And both show robustness to alternative elasticity of substitution parameters $\epsilon = 3, 11$.

Panel (b) of Figure 8 contrasts the relationship between annualized impact inflation and the change in the output gap on impact under Ramsey optimal policy in the baseline with alternatives with varying degree of persistence of the cost-push shock ($\rho_\tau = 0.75, 0.99$); with alternative values of the elasticity of substitution parameter ($\epsilon = 3, 11$). It also shows straight lines with slope $-1/\epsilon$ for $\epsilon = 3, 7, 11$. The figure shows that (i) the target rule is influenced by the persistence of the underlying shock, but the variation is quantitatively small. Furthermore, (ii) the elasticity of substitution plays a key role in determining the slope of the target rule just as in the Calvo model. Lastly, (iii) the qualitative features of the nonlinearity are robust: it is optimal to strike-while-

[22] We recalibrate the menu cost and the idiosyncratic quality shock volatility such that the frequency and the size of price changes stay constant across calibrations

the-iron-is-hot for a wide range of parameter values.

5. The inflation surge

[I BELIEVE THAT HAVING A SECTION WITH COST-PUSH SHOCKS AND DISPERSION SHOCKS THAT SPEAK TO THE INFLATION SURGE WILL ADD LOTS OF VALUE TO THE PAPER. WE HAVE SPACE: THE CURRENT DRAFT IS ONLY 32 PAGES LONG IN THE CURRENT FONT AND FORMAT STYLE.] I disagree. 32 is already longer than what most journals accept. Let's write another paper with more realistic price setting frictions including dispersion shocks.

6. Optimal monetary policy: results

We now proceed to investigate additional results: optimal long-run inflation, optimal monetary policy to an aggregate productivity shock, and time-inconsistency of the Ramsey optimal monetary policy (commitment).

6.1. The steady state under the optimal policy

The solution of the Ramsey planner's problem has a steady state featuring a slightly positive inflation of 0.25%.[23] This is different from the standard New Keynesian model with Calvo pricing (Galí 2008), where the optimal inflation in the Ramsey steady state is zero. The value of inflation in the Ramsey steady state in the menu cost model is very close to the value of steady-state inflation that maximizes steady-state welfare, which in turn is also very close to the value of inflation that minimizes the frequency of price adjustments.

What explains the positive optimal inflation? The key is the asymmetry of the profit function (**??**). For a firm, a negative price gap is more undesirable than a positive price gap of the same size because a negative price gap $-x$ leads to much larger sales at a markup loss of $-x$, while the positive price gap x leads to only somewhat smaller sales at a markup gain of x. This implies that the (S, s) band is asymmetric: the lower threshold s_t is closer to the optimal price than the upper one S_t (see Figure 9). Thus, in the zero inflation steady state, there is more mass of firms close to the lower threshold of the inaction band than to the upper threshold. As a result, there are more upward than downward price adjustments. Small positive inflation raises the optimal reset price p^* and shifts the (S, s) band leftwards and thus reduces the number of upward price movements by more than it increases the number of downward price movements. The frequency of price adjustments decreases and, with it, the distortions caused by menu costs. Quantitatively, this effect is small but not negligible.

[23] In our numerical exploration, we have only found a single steady state.

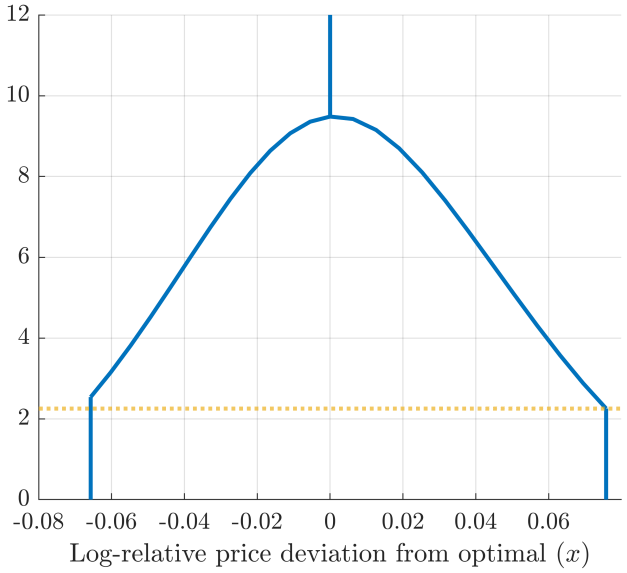


FIGURE 9. Steady-state price-gap density.

Note: The figure displays the steady-state price-gap density $g(x)$ with zero inflation. The dashed yellow line indicates the mass of firms at the upper threshold of the (S, s) band.

6.2. Timeless optimal monetary response to TFP shocks

Next, we consider TFP shocks, which affect the efficient allocation. In the standard New Keynesian model with Calvo prices, the response to such shocks is characterized by strict price stability: the central bank steers real interest rates to replicate the path of natural interest rates, which leads to inflation and the output gap remaining at zero. This is commonly known as the "*divine coincidence*" (Blanchard and Galí 2007).

A version of the divine coincidence also holds in our economy. As we have shown in Section 6.1, the Ramsey plan features a positive level of trend inflation in the long run. In response to a TFP shock, optimal timeless commitment policy keeps inflation at its steady-state level. We prove this formally in Appendix C. As inflation remains constant, the frequency of repricing also stays constant. In other words, the optimal policy offsets the dynamic impact of the efficient shocks in a form of "dynamic divine coincidence".

The conclusion is that strict targeting of the optimal steady-state inflation rate simultaneously minimizes inefficient output fluctuations and the costs of nominal rigidities. Notice that the shape of the Phillips curve plays no role in this result and thus the prescription is the same for small and large shocks.

6.3. Time-0 problem

We now turn to investigating the time inconsistency of optimal policy. To assess its magnitude, we solve the optimal policy problem, starting from the price distribution in the Ramsey steady state, assuming that the central bank faces no previous pre-

commitment. In this case, the Lagrange multipliers associated with forward-looking equations are initially set to zero. This problem is often referred to as the "time-0 problem" (Woodford 2003).

The solid blue lines in Figure 10 show the time path under the optimal policy. The labor subsidy is set to zero in this exercise, which, therefore, ceases to offset any markup distortions caused by the firms' market power. The optimal policy is time-inconsistent: without pre-commitment, the central bank engineers a temporary expansion. Thereby, it raises welfare by bringing output closer to its efficient level at a cost of elevated pricing distortions arising from the higher inflation.

The dashed red line on Figure 10 shows the equivalent time-0 response in the Calvo model. The figure shows that the incentive to surprise is substantially weaker in the menu cost model: both the inflation and output gap increases are smaller relative to the Calvo model. The reason is that the price level becomes more flexible in the state dependent model: the unexpected easing causes a sizable inflation spike, which causes an increase in the frequency of price changes. As a result, the output gap increases by less than it would under exogenous frequency. That is, the output boost from a given amount of inflation is lower than under Calvo. Since, as we saw before, the planners objective function isn't significantly different than under Calvo, the social planner thus eases less aggressively.

There is a countervailing force that raises the time inconsistency in our baseline model relative to the Calvo model. Namely, the markup distortions are higher, as discussed below, and a labor subsidy of $\tau = 1/\epsilon$ is insufficient to bring the distortions caused by the average markup to zero, as it is the case in the Calvo model. A time-0 optimal policy, therefore, stays time inconsistent even with a $\tau = 1/\epsilon$ labor subsidy (not shown). The optimal policy easing in this scenario, however, is two orders of magnitude smaller than those under no labor subsidy. Therefore, this channel is too weak to counteract the opposite effect caused by the more flexible price level detailed above.

A corollary to the negligibility of the time inconsistency with an appropriate labor subsidy is that the analysis in the previous sections, where we adopted a timeless perspective, would go through without any quantitatively relevant changes also if we adopted a time-0 perspective.

7. Conclusion

This paper characterizes the Ramsey optimal monetary policy problem in a canonical a menu cost model. We find that in the presence of large cost-push shocks, optimal monetary policy should commit to quelling inflation aggressively. Along the trajectory of optimal commitment, the central bank utilizes the reduction in the sacrifice ratio, leading to lower inflation at a cost of a slightly more marked decline in output. Optimal policy thus *strikes while the iron is hot*. This policy prescription diverges markedly from that of the standard New Keynesian model with exogenous timing of price adjustment,

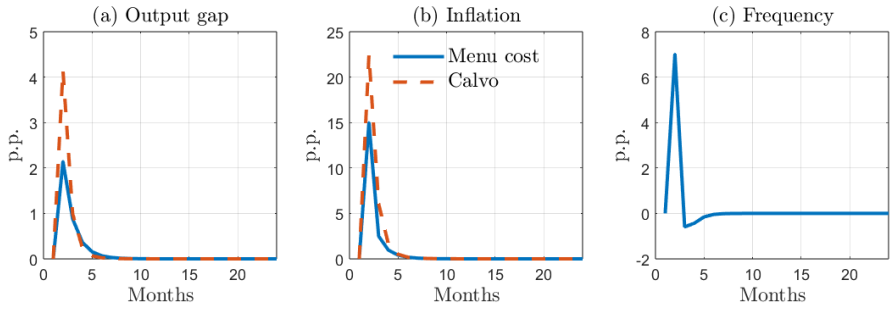


FIGURE 10. Time inconsistency of the optimal policy.

Note: The figure compares the time-0 optimal policies in the menu cost model and in the Calvo model.

which fails to capture such nonlinear dynamics. When confronted with TFP shocks, our findings indicate that the optimal policy in the menu cost model involves a commitment to full price stability, akin to the standard Calvo model.

In sum, our research underscores the importance of an aggressive anti-inflationary policy by the central bank in the face of large shocks. By committing to policies that curb inflation and stabilize the repricing frequency, the central bank can deliver a more favorable macroeconomic outcome. Our analysis is confined to the case of nominal price rigidities in the seminal fixed menu cost price setting model; we leave for future research the interaction with wage rigidities and assessment of optimal policy in more complex and realistic price-setting frameworks.

References

Achdou, Yves, Jiequn Han, Jean-Michel Lasry, Pierre-Louis Lions, and Benjamin Moll (2021) "Income and wealth distribution in macroeconomics: A continuous-time approach," *The Review of Economic Studies*, Vol. 89, pp. 45–86.

Adam, Klaus and Henning Weber (2019) "Optimal Trend Inflation," *American Economic Review*, Vol. 109, pp. 702–737.

Adjemian, Stéphane, Houtan Bastani, Michel Juillard, Frédéric Karamé, Ferhat Mihoubi, Willi Mutschler, Johannes Pfeifer, Marco Ratto, Sébastien Villemot, and Normann Rion (2023) "Dynare: Reference Manual Version 5," working papers, HAL.

Alexandrov, Andrey (2020) "The Effects of Trend Inflation on Aggregate Dynamics and Monetary Stabilization," CRC TR 224 Discussion Paper Series, University of Bonn and University of Mannheim, Germany.

Alvarez, Fernando, Martin Beraja, Martín Gonzalez-Rozada, and Pablo Andrés Neumeyer (2019) "From Hyperinflation to Stable Prices: Argentina's Evidence on Menu Cost Models," *The Quarterly Journal of Economics*, Vol. 134, pp. 451–505.

Alvarez, Fernando E, Francesco Lippi, and Luigi Paciello (2011) "Optimal Price Setting with Observation and Menu Costs," *The Quarterly Journal of Economics*, Vol. 126, pp. 1909–1960.

Alvarez, Fernando, Hervé Le Bihan, and Francesco Lippi (2016) "The Real Effects of Monetary Shocks in Sticky Price Models: A Sufficient Statistic Approach," *American Economic Review*, Vol. 106, pp. 2817–51.

Alvarez, Fernando and Francesco Lippi (2014) "Price Setting with Menu Cost for Multiproduct Firms," *Econometrica*, Vol. 82, pp. 89–135.

Alvarez, Fernando, Francesco Lippi, and Aleksei Oskolkov (2021) "The Macroeconomics of Sticky Prices with Generalized Hazard Functions*," *The Quarterly Journal of Economics*, Vol. 137, pp. 989–1038.

Auclert, Adrien, Rodolfo Rigato, Matthew Rognlie, and Ludwig Straub (2024) "New Pricing Models, Same Old Phillips Curves?" *The Quarterly Journal of Economics*, Vol. 139, pp. 121–186.

Auer, Raphael, Ariel Burstein, and Sarah M Lein (2021) "Exchange Rates and Prices: Evidence from the 2015 Swiss Franc Appreciation," *American Economic Review*, Vol. 111, pp. 652–686.

Barro, Robert J. (1972) "A Theory of Monopolistic Price Adjustment," *Review of Economic Studies*, Vol. 39, pp. 17–26.

Benigno, Pierpaolo and Gauti Eggertsson (2023) "It's Baaack: The Surge in Inflation in the 2020s and the Return of the Non-Linear Phillips Curve," NBER Working Papers 31197, National Bureau of Economic Research, Inc.

Berger, David and Joseph Vavra (2019) "Shocks versus Responsiveness: What Drives Time-Varying Dispersion?" *Journal of Political Economy*, Vol. 127, pp. 2104–2142.

Bhandari, Anmol, David Evans, Mikhail Golosov, and Thomas J Sargent (2021) "Inequality, Business Cycles, and Monetary-Fiscal Policy," *Econometrica*, Vol. 89, pp. 2559–2599.

Blanchard, Olivier and Jordi Galí (2007) "The Macroeconomic Effects of Oil Price Shocks: Why Are the 2000s so Different from the 1970s?" in *International Dimensions of Monetary Policy*: National Bureau of Economic Research, Inc, pp. 373–421.

Blanco, Andrés (2021) "Optimal Inflation Target in an Economy with Menu Costs and a Zero Lower Bound," *American Economic Journal: Macroeconomics*, Vol. 13, pp. 108–141.

Blanco, Andrés, Corina Boar, Callum J Jones, and Virgiliu Midrigan (2024a) "Nonlinear Inflation Dynamics in Menu Cost Economies," NBER Working Papers 32094, National Bureau of Economic Research.

Blanco, Andrés, Corina Boar, Callum J. Jones, and Virgiliu Midrigan (2024b) "The Inflation Accelerator," NBER Working Papers 32531, National Bureau of Economic Research, Inc.

Boppart, Timo, Per Krusell, and Kurt Mitman (2018) "Exploiting MIT shocks in heterogeneous-agent economies: the impulse response as a numerical derivative," *Journal of Economic Dynamics and Control*, Vol. 89, pp. 68–92.

Caballero, Ricardo and Eduardo Engel (1993) "Heterogeneity and Output Fluctuations in a Dynamic Menu-Cost Economy," *The Review of Economic Studies*, Vol. 60, pp. 95–119.

Calvo, Guillermo A. (1983) "Staggered Prices in a Utility-Maximizing Framework," *Journal of Monetary Economics*, Vol. 12, pp. 383 – 398.

Caratelli, Daniele and Basil Halperin (2023) "Optimal monetary policy under menu costs," unpublished manuscript.

Cavallo, Alberto, Francesco Lippi, and Ken Miyahara (2023) "Large Shocks Travel Fast," NBER Working Papers 31659, National Bureau of Economic Research, Inc.

Cerrato, Andrea and Giulia Gitti (2023) "Inflation Since COVID: Demand or Supply," unpublished manuscript.

Costain, James and Anton Nakov (2011) "Distributional Dynamics under Smoothly State-Dependent Pricing," *Journal of Monetary Economics*, Vol. 58, pp. 646 – 665.

——— (2019) "Logit Price Dynamics," *Journal of Money, Credit and Banking*, Vol. 51, pp. 43–78.

Dávila, Eduardo and Andreas Schaab (2022) "Optimal Monetary Policy with Heterogeneous Agents: A Timeless Ramsey Approach," *Working Paper*.

Dotsey, Michael, Robert G. King, and Alexander L. Wolman (1999) "State-Dependent Pricing and the General Equilibrium Dynamics of Money and Output," *The Quarterly Journal of Economics*, Vol. 114, pp. 655–690.

Gagnon, Etienne (2009) "Price Setting during Low and High Inflation: Evidence from Mexico," *The Quarterly Journal of Economics*, Vol. 124, pp. 1221–1263.

Galí, Jordi (2008) *Monetary Policy, Inflation, and the Business Cycle: An Introduction to the New Keynesian Framework*: Princeton University Press.

Golosov, Mikhail and Robert E. Lucas (2007) "Menu Costs and Phillips Curves," *Journal of Political Economy*, Vol. 115, pp. 171–199.

González, Beatriz, Galo Nuño, Dominik Thaler, and Silvia Albrizio (2024) "Firm Heterogeneity, Capital Misallocation and Optimal Monetary Policy," Working Paper Series 2890, European Central Bank.

Karadi, Peter and Adam Reiff (2019) "Menu Costs, Aggregate Fluctuations, and Large Shocks," *American Economic Journal: Macroeconomics*, Vol. 11, pp. 111–146.

Le Grand, Francois, Alais Martin-Baillon, and Xavier Ragot (2022) "Should monetary policy care about redistribution? Optimal monetary and fiscal policy with heterogeneous agents,"Technical report, Paris School of Economics.

Midrigan, Virgiliu (2011) "Menu Costs, Multiproduct Firms, and Aggregate Fluctuations," *Econometrica*, Vol. 79, pp. 1139–1180.

Montag, Hugh and Daniel Villar (2023) "Price-Setting During the Covid Era," *FEDS Notes*.

Nakamura, Emi and Jón Steinsson (2008) "Five Facts about Prices: A Reevaluation of Menu Cost Models," *The Quarterly Journal of Economics*, Vol. 123, pp. 1415–1464.

——— (2010) "Monetary Non-neutrality in a Multisector Menu Cost Model," *The Quarterly Journal of Economics*, Vol. 125, pp. 961–1013.

Nakov, Anton and Carlos Thomas (2014) "Optimal Monetary Policy with State-Dependent Pricing," *International Journal of Central Banking*, Vol. 36.

Nuño, Galo and Carlos Thomas (2022) "Optimal Redistributive Inflation," *Annals of Economics*

and Statistics, pp. 3–63.

Ragot, Xavier (2019) "Managing Inequality over the Business Cycles: Optimal Policies with Heterogeneous Agents and Aggregate Shocks," 2019 Meeting Papers 1090, Society for Economic Dynamics.

Sheshinski, Eytan and Yoram Weiss (1977) "Inflation and Costs of Price Adjustment," *Review of Economic Studies*, Vol. 44, pp. 287–303.

Smets, Frank and Rafael Wouters (2007) "Shocks and Frictions in US Business Cycles: A Bayesian DSGE Approach," *The American Economic Review*, Vol. 97, pp. 586–606.

Smirnov, Danila (2022) "Optimal Monetary Policy in HANK," Unpublished manuscript, Universitat Pompeu Fabra.

Taylor, John B (1993) "Discretion versus Policy Rules in Practice," in *Carnegie-Rochester Conference Series on Public Policy*, Vol. 39, pp. 195–214, Elsevier.

Vavra, Joseph (2014) "Inflation Dynamics and Time-Varying Volatility: New Evidence and an Ss Interpretation," *The Quarterly Journal of Economics*, Vol. 129, pp. 215–258.

Woodford, Michael (2003) *Interest and Prices: Foundations of a Theory of Monetary Policy*: Princeton University Press.

——— (2009) "Information-Constrained State-Dependent Pricing," *Journal of Monetary Economics*, Vol. 56, pp. S100–S124.

ONLINE APPENDIX

Appendix A. Optimality condition of the reset price

If the value function is convex, the optimal reset price is fully characterized by the system of first-order conditions in Section **??**.[24] This appendix presents the derivation of $V_t'(0)$. To start, we reproduce here the value function presented in equation (16):

$$\begin{aligned} V_t(x) &= \Pi(x, p_t^*, w_t, A_t) \\ &\quad + \mathbb{E}_t\left[\left(1-\lambda_{t+1}\left(x-\sigma_{t+1}\varepsilon_{t+1}-\pi_{t+1}^*\right)\right)\Lambda_{t,t+1}V_{t+1}(x-\sigma_{t+1}\varepsilon_{t+1}-\pi_{t+1}^*)\right] \\ &\quad + \mathbb{E}_t\left[\lambda_{t+1}\left(x-\sigma_{t+1}\varepsilon_{t+1}-\pi_{t+1}^*\right)\Lambda_{t,t+1}\left(V_{t+1}(0)-\eta w_{t+1}\right)\right]. \end{aligned}$$

Since the only source of uncertainty is the idiosyncratic shocks, $V_t(x)$ becomes

$$\begin{aligned} V_t(x) &= \Pi(x, p_t^*, w_t, A_t) \\ &\quad + \Lambda_{t,t+1}\int\left[\left(1-\lambda_{t+1}\left(x-\sigma_{t+1}\varepsilon-\pi_{t+1}^*\right)\right)V_{t+1}(x-\sigma_{t+1}\varepsilon-\pi_{t+1}^*)\phi(\varepsilon)\right]d\varepsilon \\ &\quad + \Lambda_{t,t+1}\left(V_{t+1}(0)-\eta w_{t+1}\right)\int\left[\lambda_{t+1}\left(x-\sigma_{t+1}\varepsilon-\pi_{t+1}^*\right)\phi(\varepsilon)\right]d\varepsilon, \end{aligned}$$

where $\phi(\cdot)$ denotes the standard normal p.d.f. The term $x-\sigma_{t+1}\varepsilon-\pi_{t+1}^*$ is the state of the firm at $t+1$, conditional on the state x at t and the realization $\varepsilon_{t+1}=\varepsilon$ of the shock at $t+1$. Denoting the state at $t+1$ as $x' \equiv x-\sigma_{t+1}\varepsilon-\pi_{t+1}^*$, such that $\varepsilon \equiv \frac{x-x'-\pi_{t+1}^*}{\sigma_{t+1}}$, and applying the corresponding change of variable to the integral yields

$$\begin{aligned} V_t(x) &= \Pi(x, p_t^*, w_t, A_t) + \frac{\Lambda_{t,t+1}}{\sigma_{t+1}}\int\left[\left(1-\lambda_{t+1}\left(x'\right)\right)V_{t+1}(x')\phi\left(\frac{x-x'-\pi_{t+1}^*}{\sigma_{t+1}}\right)\right]dx' \\ &\quad + \left(V_{t+1}(0)-\eta w_{t+1}\right)\frac{\Lambda_{t,t+1}}{\sigma_{t+1}}\int\left[\lambda_{t+1}\left(x'\right)\phi\left(\frac{x-x'-\pi_{t+1}^*}{\sigma_{t+1}}\right)\right]dx'. \end{aligned}$$

The probability of updating a price λ_{t+1} given any state of nature is either 0 in the "inaction region" or 1 otherwise. Defining the inaction region as the (s_t, S_t) band, we restrict the first integral in the latter expression. We also replace the second integral, which is the probability mass of updating the price, by 1 minus the probability mass of not updating the price. Thus:

$$\begin{aligned} V_t(x) &= \Pi(x, p_t^*, w_t, A_t) + \frac{\Lambda_{t,t+1}}{\sigma_{t+1}}\int_{s_{t+1}}^{S_{t+1}}\left[V_{t+1}(x')\phi\left(\frac{x-x'-\pi_{t+1}^*}{\sigma_{t+1}}\right)\right]dx' \\ &\quad + \Lambda_{t,t+1}\left(V_{t+1}(0)-\eta w_{t+1}\right)\left\{1-\frac{1}{\sigma_{t+1}}\int_{s_{t+1}}^{S_{t+1}}\phi\left(\frac{x-x'-\pi_{t+1}^*}{\sigma_{t+1}}\right)dx'\right\} \\ &= \Pi_t(x) + \frac{\Lambda_{t,t+1}}{\sigma_{t+1}}\int_{s_{t+1}}^{S_{t+1}}\left[V_{t+1}(x')\phi\left(\frac{x-x'-\pi_{t+1}^*}{\sigma_{t+1}}\right)\right]dx' \\ &\quad + \Lambda_{t,t+1}\left(V_{t+1}(0)-\eta w_{t+1}\right)\left\{1-\left[\Phi\left(\frac{x-s_{t+1}-\pi_{t+1}^*}{\sigma_{t+1}}\right)-\Phi\left(\frac{x-S_{t+1}-\pi_{t+1}^*}{\sigma_{t+1}}\right)\right]\right\} \end{aligned}$$

[24] We verify convexity ex post.

where $\Phi(\cdot)$ denotes the standard normal c.d.f. and, to simplify notation, we suppress the dependence of Π on aggregate variables.

Finally, taking the derivative of $V_t(x)$ with respect to x and reformulating, we get $V_t'(x)$:

$$\begin{aligned} V_t'(x) &= \Pi_t'(x) + \frac{\Lambda_{t,t+1}}{\sigma_{t+1}} \frac{\partial \int_{s_{t+1}}^{S_{t+1}} V_{t+1}(x')\phi\left(\frac{x-x'-\pi^*_{t+1}}{\sigma_{t+1}}\right)dx'}{\partial x} \\ &\quad + \frac{\Lambda_{t,t+1}}{\sigma_{t+1}}\left(\phi\left(\frac{x-S_{t+1}-\pi^*_{t+1}}{\sigma_{t+1}}\right) - \phi\left(\frac{x-s_{t+1}-\pi^*_{t+1}}{\sigma_{t+1}}\right)\right)(V_{t+1}(0) - \kappa w_{t+1}) \\ &= \Pi_t'(x) + \frac{\Lambda_{t,t+1}}{\sigma_{t+1}} \int_{s_{t+1}}^{S_{t+1}} V_{t+1}(x') \frac{\partial \phi\left(\frac{x-x'-\pi^*_{t+1}}{\sigma_{t+1}}\right)}{\partial x} dx' \\ &\quad + \frac{\Lambda_{t,t+1}}{\sigma_{t+1}}\left(\phi\left(\frac{x-S_{t+1}-\pi^*_{t+1}}{\sigma_{t+1}}\right) - \phi\left(\frac{x-s_{t+1}-\pi^*_{t+1}}{\sigma_{t+1}}\right)\right)(V_{t+1}(0) - \kappa w_{t+1}) \end{aligned}$$

which must be evaluated at $x = 0$.

Appendix B. Efficiency and welfare analysis

B.1. Efficient and natural level of output

This appendix derives efficient output, efficient real interest rate, and natural output.

Efficient output. We obtain it as the solution to a social planning problem. The problem maximizes household welfare in equation (1) subject to (i) the aggregate consumption equation (3), (ii) aggregate labor supply in ($N_t = \int_i N_t(j)$) and (iii) product-level production functions in (10) with respect to product-level consumption and labor ($C_t(j), N_t(j), j \in [0,1], t = 0, 1, 2, \ldots$).

After some algebra, the optimization problem simplifies to

$$\max_{N_t(j)} \mathbb{E}_0 \sum_{t=0}^{\infty} \beta^t \frac{\left[A_t\left(\int N_t(j)^{\frac{\epsilon-1}{\epsilon}} di\right)^{\frac{\epsilon}{\epsilon-1}}\right]^{1-\gamma}}{1-\gamma} - \upsilon \int N_t(j) di,$$

subject to $\int N_t(j) di = N_t$. The solution implies that the efficient output fluctuates with aggregate productivity but is independent of demand shocks as well as of cost-push shocks. In particular, the efficient level of output is

$$Y_t^e = C_t^e = A_t N_t^e = \upsilon^{-1/\gamma} A_t^{1/\gamma}. \tag{A1}$$

For our parametrization, $\upsilon = 1$ and $\gamma = 1$, we thus have that

$$\begin{aligned} N_t^e &= 1, \\ C_t^e &= A_t. \end{aligned} \tag{A2}$$

The efficient labor supply is equal across products and the efficient product-level consumption varies across products j inversely proportional to the product-level quality, in particular

$$\begin{aligned} N_t^e(j) =& N_t^e \\ C_t^e(j) =& \frac{A_t N_t^e}{A_t(j)}. \end{aligned}$$

Efficient real interest rate. It is implicitly defined by the Euler equation after substituting in efficient consumption:

$$r_t^e = -\log\beta - \gamma(1-\rho_A)\log A_t$$

Natural output. It is defined as the counterfactual output with flexible prices. Under flexible prices, firms maximize their real profit function (**??**) in each period t by choosing

$$\frac{P_t^n(j)}{A_t(j)P_t^n} = \frac{\epsilon}{\epsilon-1}(1-\tau_t)\frac{w_t^n}{A_t}.$$

The expression implies that the quality-adjusted relative price is homogeneous across products j. Together with the definition of the price-level in equation (6) in the main text, this implies that the natural level of the quality-adjusted log relative price is zero ($p_t(j) = 0$). Or equivalently, the natural level of relative price is equal to the quality: $P_t^n(j)/P_t^n = A_t(j)$. The product-level demand function and the unit quality-adjusted relative price implies that product-level natural consumption is inversely proportional to the quality of product j:

$$C_t^n(j) = \frac{1}{A_t(j)}C_t^n.$$

Furthermore, the natural real wage, output and labor are given by the following closed-form expressions:

$$\begin{aligned} w_t^n =& A_t \frac{\epsilon-1}{\epsilon}\frac{1}{1-\tau_t}, \\ Y_t^n =& C_t^n = \left(\frac{w_t^n}{\upsilon}\right)^{1/\gamma}, \\ N_t^n =& \frac{Y_t^n}{A_t}. \end{aligned}$$

Notably, the productivity shock affects the natural and the efficient output similarly, but the cost-push (labor-tax) shocks only affect the natural level of output.

B.2. Welfare decomposition

This appendix derives the welfare decomposition presented in equation (27) in the main text. We start by obtaining expressions that are used at the end for the welfare

decomposition.

Markups. The real marginal cost of firm j is

$$MC_t(j) = \frac{\partial\left((1-\tau_t)w_t N_t(j)\right)}{\partial Y_t(j)} = \frac{(1-\tau_t)w_t A_t(j)}{A_t},$$

where we have used that $N_t(j) = A_t(j)Y_t(j)/A_t$.

The (log-) markup $\mu_t(j)$ is the (log-) difference between the relative price and the real marginal cost:

$$\text{(A3)}\quad \mu_t(j) = \log\frac{P_t(j)}{P_t} - \log\frac{(1-\tau_t)w_t A_t(j)}{A_t} = \log\frac{P_t(j)}{A_t(j)P_t} - \log\frac{(1-\tau_t)w_t}{A_t} = p_t(j) - mc_t,$$

where $p_t(j)$ is the quality-adjusted relative price and

$$mc_t \equiv \log\left(MC_t(j)/A_t(j)\right) = \log\left((1-\tau_t)w_t/A_t\right) = \log(1-\tau_t) - \log A_t + \log\upsilon + \gamma\log Y_t,$$

is the 'aggregate component' of the marginal cost. Notice that we have employed eq. (7).

Aggregate markup and output. The aggregate (log-) markup $\overline{\mu}_t$ is

$$\overline{\mu}_t = \log\left(\int e^{\mu_t(j)(1-\epsilon)}dj\right)^{\frac{1}{1-\epsilon}} = \log\left(\int \frac{e^{p_t(j)(1-\epsilon)}}{e^{mc_t(1-\epsilon)}}dj\right)^{\frac{1}{1-\epsilon}} = \log\frac{1}{e^{mc_t}}\left(\int e^{p_t(j)(1-\epsilon)}dj\right)^{\frac{1}{1-\epsilon}} = -mc_t,$$

where we used the observation that the average quality-adjusted relative price is one (eq. **??**). Therefore

$$\text{(A4)}\qquad \overline{\mu}_t = -\log(1-\tau_t) + \log A_t - \log\upsilon - \gamma\log Y_t$$

or equivalently

$$\text{(A5)}\qquad e^{\overline{\mu}_t} = \frac{A_t}{\upsilon(1-\tau_t)Y_t^{\gamma}}$$

expressing the tight relationship between average markup and the output.

Taking into account eq. (A1), the efficient output gap can be expressed

$$\text{(A6)}\qquad \log Y_t - \log Y_t^e = \frac{1}{\gamma}\left(-\log(1-\tau_t) - \overline{\mu}_t\right),$$

which is proportional to the negative average markup.

Markup dispersion. The dispersion of the quality-adjusted relative prices (ζ_t^p) is

$$\zeta_t^p = \int e^{p_t(j)(-\epsilon)}g(p_t(j))dj = \int e^{(\mu_t(j)+mc_t)(-\epsilon)}g(\mu_t(j)+mc_t)dj = \int e^{(\mu_t(j)-\overline{\mu}_t)(-\epsilon)}g(\mu_t(j)-\overline{\mu}_t)dj \equiv \zeta_t^{\mu-\overline{\mu}}$$

where $\zeta_t^{\mu-\overline{\mu}}$ is the dispersion of the demeaned markups which equals price dispersion.

Welfare. Finally, consider the case with $\gamma = 1$. We can express the difference between welfare (W_t) from the welfare in the efficient equilibrium (W_t^e) subject to ashock in period 0 as

$$
\begin{aligned}
W_0 - W_0^e = \sum_{t=0}^{\infty} \beta^t \left(U_t - U_t^e\right) &= \sum_{t=0}^{\infty} \beta^t \left((\log C_t - N_t) - (\log C_t^e - N_t^e)\right) \\
&= \sum_{t=0}^{\infty} \beta^t \left((\log Y_t - N_t) - (\log Y_t^e - 1)\right) \\
&= \sum_{t=0}^{\infty} \beta^t \left(-\log(1-\tau_t) - \overline{\mu}_t - \frac{C_t}{A_t} \int e^{p(-\epsilon)} g_t(p)\, dp - \eta g_t^0 + 1\right) \\
&= \sum_{t=0}^{\infty} \beta^t \left(-\log(1-\tau_t) - \overline{\mu}_t - \left(\frac{1}{e^{\overline{\mu}_t}(1-\tau_t)} \zeta_t^{\mu-\overline{\mu}} - 1\right) - \eta g_t^0\right) \\
&= \sum_{t=0}^{\infty} \beta^t \left(-\log(1-\tau_t) - \overline{\mu}_t - \left(\frac{1}{e^{\overline{\mu}_t}(1-\tau_t)} - 1\right) - \left(\frac{1}{e^{\overline{\mu}_t}(1-\tau_t)} (\zeta_t^{\mu-\overline{\mu}} - 1)\right) - \eta g_t^0\right)
\end{aligned}
$$

where U_t^e is the utility in the efficient equilibrium and where we have used (A2) and $C_t = Y_t$ in line 1 and (A6) and (**??**) in line 2 and (A5) and $C_t = Y_t$ and $\gamma = 1$ in line 3. The final expression decomposes welfare into terms related to average markup, markup dispersion, and adjustment costs.

Appendix C. Response to TFP shocks

This appendix proves that, in response to a TFP shock, optimal timeless commitment policy keeps inflation at its steady-state level $\pi_t = \pi$.

The planner's problem is:

$$\max_{\substack{\{g_t^c(\cdot), g_t^0, V_t(\cdot), C_t,\\ w_t, p_t^*, s_t, S_t, \pi_t^*\}_{t=0}^{\infty}}} \mathbb{E}_0 \sum_{t=0}^{\infty} \beta^t \left(\log C_t - \upsilon L_t\right)$$

subject to

$$\begin{aligned}
w_t &= \upsilon C_t, \\
L_t &= \frac{C_t}{A_t}\left(\int e^{\left(x+p_t^*\right)(-\epsilon_t)} g_t^c\left(p\right) dx + g_t^0 e^{\left(p_t^*\right)(-\epsilon)}\right) - \upsilon\eta g_t^0 \\
V_t(x) &= \Pi(x, p_t^*, w_t, A_t) + \frac{\Lambda_{t,t+1}}{\sigma_{t+1}} \int_{s_t}^{S_t} \left[V_{t+1}(x')\phi\left(\frac{\left(x-x'\right)-\pi_{t+1}^*}{\sigma_{t+1}}\right)\right] dx' + \\
&\quad \Lambda_{t,t+1}\left(1 - \frac{1}{\sigma_{t+1}}\int_{s_t}^{S_t}\left[\phi\left(\frac{\left(x-x'\right)-\pi_{t+1}^*}{\sigma_{t+1}}\right)\right] dx'\right)\left[\left(V_{t+1}\left(0\right) - \eta w_{t+1}\right)\right], \\
V_t\left(s_t\right) &= V_t\left(0\right) - \eta w_t, \\
V_t\left(S_t\right) &= V_t\left(0\right) - \eta w_t, \\
0 &= \Pi_t'(0) + \frac{\Lambda_{t,t+1}}{\sigma_{t+1}} \int_{s_{t+1}}^{S_{t+1}} V_{t+1}(x') \left.\frac{\partial\phi\left(\frac{x-x'-\pi_{t+1}^*}{\sigma_{t+1}}\right)}{\partial x}\right|_{x=0} dx' \\
&\quad + \Lambda_{t,t+1}\left(\phi\left(\frac{-S_{t+1}-\pi_{t+1}^*}{\sigma_{t+1}}\right) - \phi\left(\frac{-s_{t+1}-\pi_{t+1}^*}{\sigma_{t+1}}\right)\right)\left(V_{t+1}(0) - \eta w_{t+1}\right). \\
g_t^c(x) &= \frac{1}{\sigma_t}\int_{s_{t-1}}^{S_{t-1}} g_{t-1}^c(x_{-1})\phi\left(\frac{x_{-1}-x-\pi_t^*}{\sigma_t}\right) dx_{-1} + g_{t-1}^0\phi\left(\frac{-x-\pi_t^*}{\sigma_t}\right), \\
g_t^0 &= 1 - \int_{s_t}^{S_t} g_t^c(x) dx, \\
1 &= \int e^{\left(x+p_t^*\right)(1-\epsilon)} g_t^c\left(x\right) dx + g_t^0 e^{\left(p_t^*\right)(1-\epsilon)}.
\end{aligned}$$

We now transform it in a convenient fashion. First, normalize the constraints involving $V_t(x)$ by A_t and substitute for the wage $w_t = \upsilon C_t$ and the discount factor $\Lambda_{t,t+1} = \beta\frac{C_t}{C_{t+1}}$. With this, the constrains involving $V_t(x)$ become:

$$\begin{aligned}
\frac{V_t(x)}{A_t} &= \frac{C_t}{A_t}\left(\exp\left(x_t + p_t^*\right)\right)^{1-\epsilon} - \frac{C_t}{A_t}(1-\tau_t)\upsilon\frac{C_t}{A_t}\left(\exp\left(x_t + p_t^*\right)\right)^{-\epsilon} \\
&\quad + \beta\frac{A_{t+1}}{A_t}\frac{C_t}{C_{t+1}}\frac{1}{\sigma_{t+1}}\int_{s_{t+1}}^{S_{t+1}}\left[\frac{V_{t+1}(x')}{A_{t+1}}\phi\left(\frac{\left(x-x'\right)-\pi_{t+1}^*}{\sigma_{t+1}}\right)\right] dx' \\
&\quad + \frac{A_{t+1}}{A_t}\beta\frac{C_t}{C_{t+1}}\left(1 - \frac{1}{\sigma_{t+1}}\int_{s_{t+1}}^{S_{t+1}}\left[\phi\left(\frac{\left(x-x'\right)-\pi_{t+1}^*}{\sigma_{t+1}}\right)\right] dx'\right)\left[\left(\frac{V_{t+1}\left(0\right)}{A_{t+1}} - \eta\upsilon\frac{C_{t+1}}{A_{t+1}}\right)\right],
\end{aligned}$$

$$
\begin{aligned}
\frac{V_t(s_t)}{A_t} &= \frac{V_t(0)}{A_t} - \eta\upsilon\frac{C_t}{A_t}, \\
\frac{V_t(S_t)}{A_t} &= \frac{V_t(0)}{A_t} - \eta\upsilon\frac{C_t}{A_t}, \\
0 &= (1-\epsilon)\frac{C_t}{A_t}\left(\exp\left(x_t + p_t^*\right)\right)^{1-\epsilon} + \epsilon\frac{C_t}{A_t}(1-\tau_t)\upsilon\frac{C_t}{A_t}\left(\exp\left(x_t + p_t^*\right)\right)^{-\epsilon} \\
&\quad + \frac{1}{\sigma_{t+1}}\beta\frac{A_{t+1}}{A_t}\frac{C_t}{C_{t+1}}\int_{s_{t+1}}^{S_{t+1}}\frac{V_{t+1}(x')}{A_{t+1}}\left.\frac{\partial\phi\left(\frac{x-x'-\pi_{t+1}^*}{\sigma_{t+1}}\right)}{\partial x}\right|_{x=0} dx' \\
&\quad + \beta\frac{A_{t+1}}{A_t}\frac{C_t}{C_{t+1}}\left(\phi\left(\frac{-S_{t+1}-\pi_{t+1}^*}{\sigma_{t+1}}\right) - \phi\left(\frac{-s_{t+1}-\pi_{t+1}^*}{\sigma_{t+1}}\right)\right)\left(\frac{V_{t+1}(0)}{A_{t+1}} - \eta\upsilon\frac{C_{t+1}}{A_{t+1}}\right).
\end{aligned}
$$

Second, define $\frac{V_t(x)}{A_t} \equiv \hat{V}_t(x)$, so that these constrains become

$$
\begin{aligned}
\hat{V}_t(x) &= \frac{C_t}{A_t}\left(\exp\left(x_t + p_t^*\right)\right)^{1-\epsilon} - \frac{C_t}{A_t}(1-\tau_t)\upsilon\frac{C_t}{A_t}\left(\exp\left(x_t + p_t^*\right)\right)^{-\epsilon} \\
&\quad + \beta\frac{C_t}{A_t}\frac{A_{t+1}}{C_{t+1}}\frac{1}{\sigma_{t+1}}\int_{s_{t+1}}^{S_{t+1}}\left[\hat{V}_{t+1}(x')\phi\left(\frac{\left(x-x'\right)-\pi_{t+1}^*}{\sigma_{t+1}}\right)\right]dx' \\
&\quad + \beta\frac{C_t}{A_t}\frac{A_{t+1}}{C_{t+1}}\left(1 - \frac{1}{\sigma_{t+1}}\int_{s_{t+1}}^{S_{t+1}}\left[\phi\left(\frac{\left(x-x'\right)-\pi_{t+1}^*}{\sigma_{t+1}}\right)\right]dx'\right)\left[\left(\hat{V}_{t+1}(0) - \eta\upsilon\frac{C_{t+1}}{A_{t+1}}\right)\right], \\
\hat{V}_t(s_t) &= \hat{V}_t(0) - \eta\upsilon\frac{C_t}{A_t}, \\
\hat{V}_t(S_t) &= \hat{V}_t(0) - \eta\upsilon\frac{C_t}{A_t}, \\
0 = \hat{V}_t'(0) &= (1-\epsilon)\frac{C_t}{A_t}\left(\exp\left(x_t + p_t^*\right)\right)^{1-\epsilon} + \epsilon\frac{C_t}{A_t}(1-\tau_t)\upsilon\frac{C_t}{A_t}\left(\exp\left(x_t + p_t^*\right)\right)^{-\epsilon} \\
&\quad + \frac{1}{\sigma_{t+1}}\beta\frac{C_t}{A_t}\frac{A_{t+1}}{C_{t+1}}\int_{s_{t+1}}^{S_{t+1}}\hat{V}_{t+1}(x')\left.\frac{\partial\phi\left(\frac{x-x'-\pi_{t+1}^*}{\sigma_{t+1}}\right)}{\partial x}\right|_{x=0} dx' \\
&\quad + \beta\frac{C_t}{A_t}\frac{A_{t+1}}{C_{t+1}}\left(\phi\left(\frac{-S_{t+1}-\pi_{t+1}^*}{\sigma_{t+1}}\right) - \phi\left(\frac{-s_{t+1}-\pi_{t+1}^*}{\sigma_{t+1}}\right)\right)\left(\hat{V}(0) - \eta\upsilon\frac{C_{t+1}}{A_{t+1}}\right).
\end{aligned}
$$

Finally, define $\hat{C}_t = \frac{C_t}{A_t}$. The planner's problem becomes

$$
\max_{\substack{\left\{g_t^c(\cdot), g_t^0, \hat{V}_t(\cdot), \hat{C}_t, \\ w_t, p_t^*, s_t, S_t, \pi_t^*, L_t\right\}_{t=0}^{\infty}}} \mathbb{E}_0\sum_{t=0}^{\infty}\beta^t\left(\log\left(\hat{C}\right) + \log\left(A_t\right) - \upsilon L_t\right)
$$

$$
\begin{aligned}
\hat{V}_t(x) &= \hat{C}_t\left(\exp\left(x_t + p_t^*\right)\right)^{1-\epsilon} - \hat{C}_t(1-\tau_t)\upsilon\hat{C}_t\left(\exp\left(x_t + p_t^*\right)\right)^{-\epsilon} \\
&\quad + \beta\hat{C}_t\hat{C}_{t+1}^{-1}\frac{1}{\sigma_{t+1}}\int_{s_{t+1}}^{S_{t+1}}\left[\hat{V}_{t+1}(x')\phi\left(\frac{\left(x-x'\right)-\pi_{t+1}^*}{\sigma_{t+1}}\right)\right]dx'
\end{aligned}
$$

$$
\begin{aligned}
&+\beta\hat{C}_t\hat{C}_{t+1}^{-1}\left(1-\frac{1}{\sigma_{t+1}}\int_{s_{t+1}}^{S_{t+1}}\left[\phi\left(\frac{\left(x-x'\right)-\pi_{t+1}^{*}}{\sigma_{t+1}}\right)\right]dx'\right)\left[\left(\hat{V}_{t+1}(0)-\eta\upsilon\hat{C}_{t+1}\right)\right],\\
\hat{V}_t\left(s_t\right) &= \hat{V}_t\left(0\right)-\eta\upsilon\hat{C}_t,\\
\hat{V}_t\left(S_t\right) &= \hat{V}_t\left(0\right)-\eta\upsilon\hat{C}_t,\\
0=\hat{V}_t'\left(0\right) &= (1-\epsilon)\hat{C}_t\left(\exp\left(x_t+p_t^{*}\right)\right)^{1-\epsilon}+\epsilon\hat{C}_t(1-\tau_t)\upsilon\hat{C}_t\left(\exp\left(x_t+p_t^{*}\right)\right)^{-\epsilon}\\
&\quad+\frac{1}{\sigma_{t+1}}\beta\hat{C}_t\hat{C}_{t+1}^{-1}\int_{s_{t+1}}^{S_{t+1}}\hat{V}_{t+1}(x')\left.\frac{\partial\phi\left(\frac{x-x'-\pi_{t+1}^{*}}{\sigma_{t+1}}\right)}{\partial x}\right|_{x=0}dx'\\
&\quad+\beta\hat{C}_t\hat{C}_{t+1}^{-1}\left(\phi\left(\frac{-S_{t+1}-\pi_{t+1}^{*}}{\sigma_{t+1}}\right)-\phi\left(\frac{-s_{t+1}-\pi_{t+1}^{*}}{\sigma_{t+1}}\right)\right)\left(\hat{V}(0)-\eta\upsilon\hat{C}_{t+1}\right).\\
L_t &= \hat{C}_t\left(\int e^{\left(x+p_t^{*}\right)(-\epsilon_t)}g_t^{c}\left(p\right)dx+g_t^{0}e^{\left(p_t^{*}\right)(-\epsilon)}\right)\\
g_t^{c}(x) &= \frac{1}{\sigma_t}\int_{s_{t-1}}^{S_{t-1}}g_{t-1}^{c}(x_{-1})\phi\left(\frac{x_{-1}-x-\pi_t^{*}}{\sigma_t}\right)dx_{-1}+g_{t-1}^{0}\phi\left(\frac{-x-\pi_t^{*}}{\sigma_t}\right),\\
g_t^{0} &= 1-\int_{s_t}^{S_t}g_t^{c}(x)dx,\\
1 &= \int e^{\left(x+p_t^{*}\right)(1-\epsilon)}g_t^{c}\left(x\right)dx+g_t^{0}e^{\left(p_t^{*}\right)(1-\epsilon)}.
\end{aligned}
$$

which do not depend on A_t. Therefore, the redefined Ramsey policy does not respond to TFP shocks. Going back to the original variables definition, this implies that under optimal policy $C_t \propto A_t$ and $V_t(x) \propto A_t$ while all other variables remain constant at their steady-state values. Thus, inflation π_t also remains constant at its steady-state value.

Appendix D. Additional figures

D.1. Slope of the nonlinear New Keynesian Phillips curve

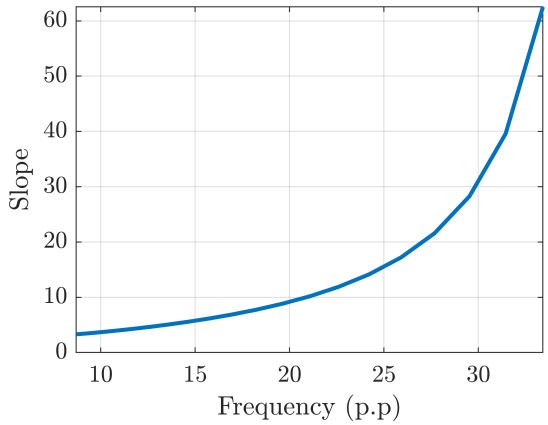


FIGURE A1. Slope of the nonlinear New Keynesian Phillips curve in the Golosov-Lucas model. *Note*: The figure is produced by computing the impulse responses to monetary policy shocks of different magnitudes and signs and then computing the slope.

D.2. Nonlinear New Keynesian Phillips curve

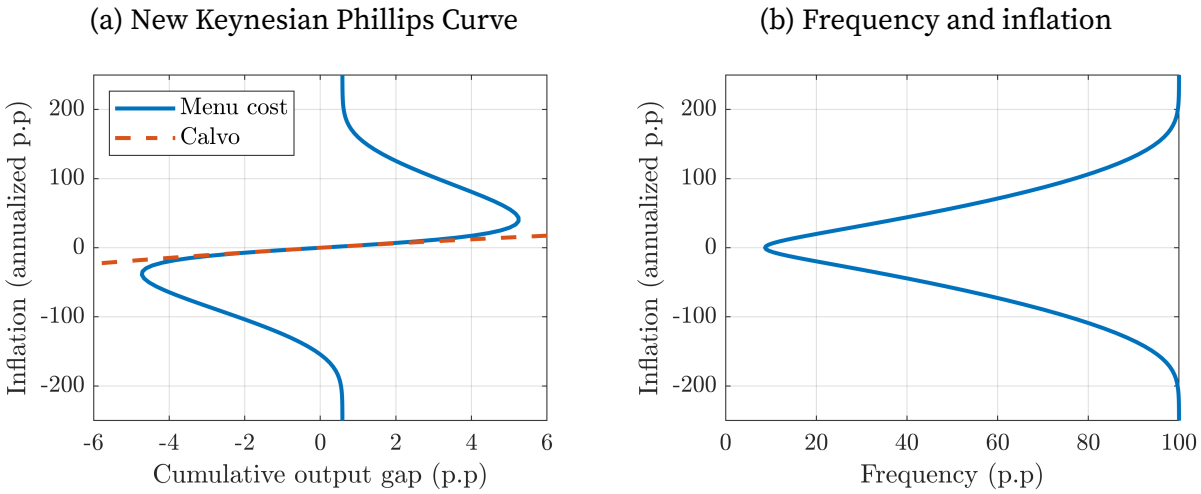


FIGURE A2. Inflation-output trade-offs in the menu cost model.
Note: The figure is produced by computing the impulse responses to monetary policy shocks of different magnitudes and signs.

D.3. Impulse responses under a Taylor rule

Cost-push shocks. The solid green lines on the first row of Figure A3 show the responses to a large cost-push shock. The shock is implemented as a persistent decline in the firms' employment subsidy τ_t. The shock size is calibrated to generate a 20% frequency on impact (a frequency increase of 20% – 8.7% = 11.3%, see panel d), a magnitude that has been documented during the 2022-2023 inflation surge (Montag and Villar 2023). The exercise assumes that monetary policy follows an inertial Taylor rule (eq. **??**). The shock captures some realistic features of the recent inflation surge. First, it generates a large increase in inflation (panel b), characterized by an initial temporary spike followed by a period of persistent inflation. Second, the shock causes a mild downturn as the output gap decreases (panel a).

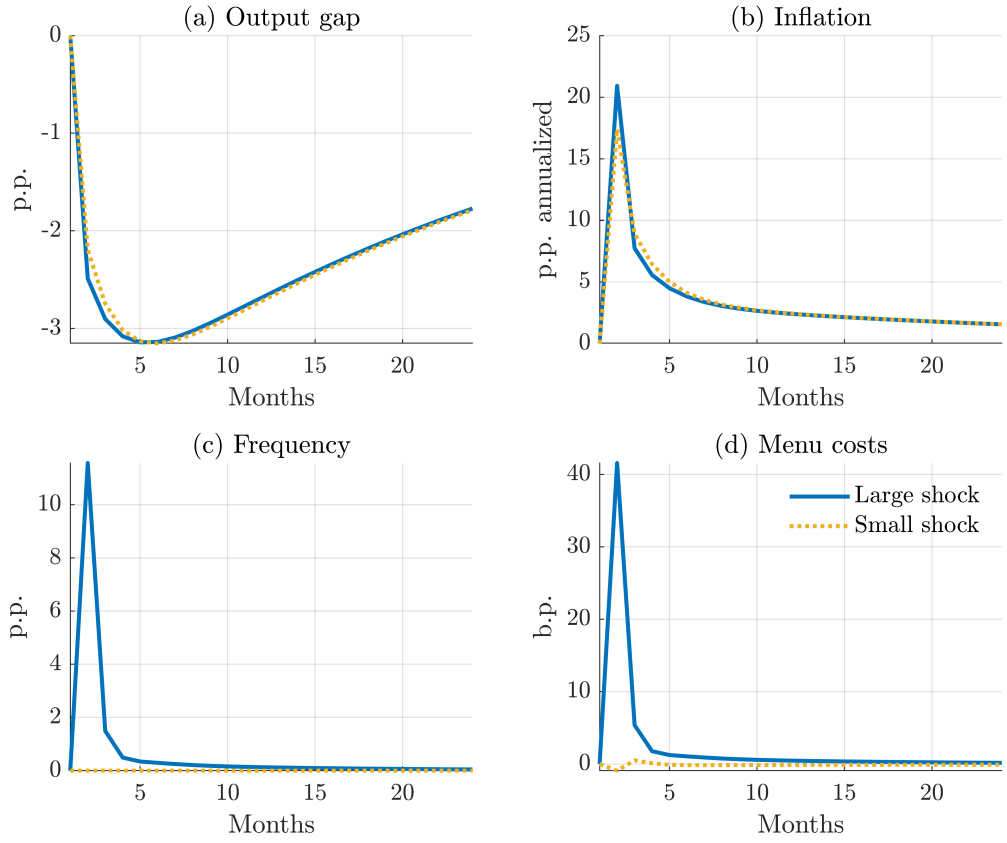


FIGURE A3. Impulse responses to a large and a small cost-push shock in the menu cost model. *Note*: all displayed variables except frequency are linearly scaled in the small shock according to the ratio between the large and small shocks.

In contrast, the black dashed lines show the responses to a *small* cost-push shock, scaled up linearly to the size of the large shock. The small shock is a 25 basis point decrease in the annualized employment subsidy. The difference between the figures illustrates the nonlinearity of the model. The inflation response is roughly 25% larger after the large shock than after the linearly scaled small shock. The key reason behind

this is the sizable difference between the frequency responses: while the frequency jumps after the large shock, it stays almost unchanged in response to the small shock.[25]

Comparison with the Calvo model. We compare the results above, for the small shock re-scaled, with the standard Calvo model in Figure A4. We consider two calibrations for the Calvo parameter. The dotted-dashed green line corresponds to a calibration in which the frequency of price adjustment, which in Calvo is constant, matches the frequency of price adjustments of 8.7% in the Golosov-Lucas model. In this case, the response of both inflation and output gap is much attenuated compared to the menu cost model (solid gray line).

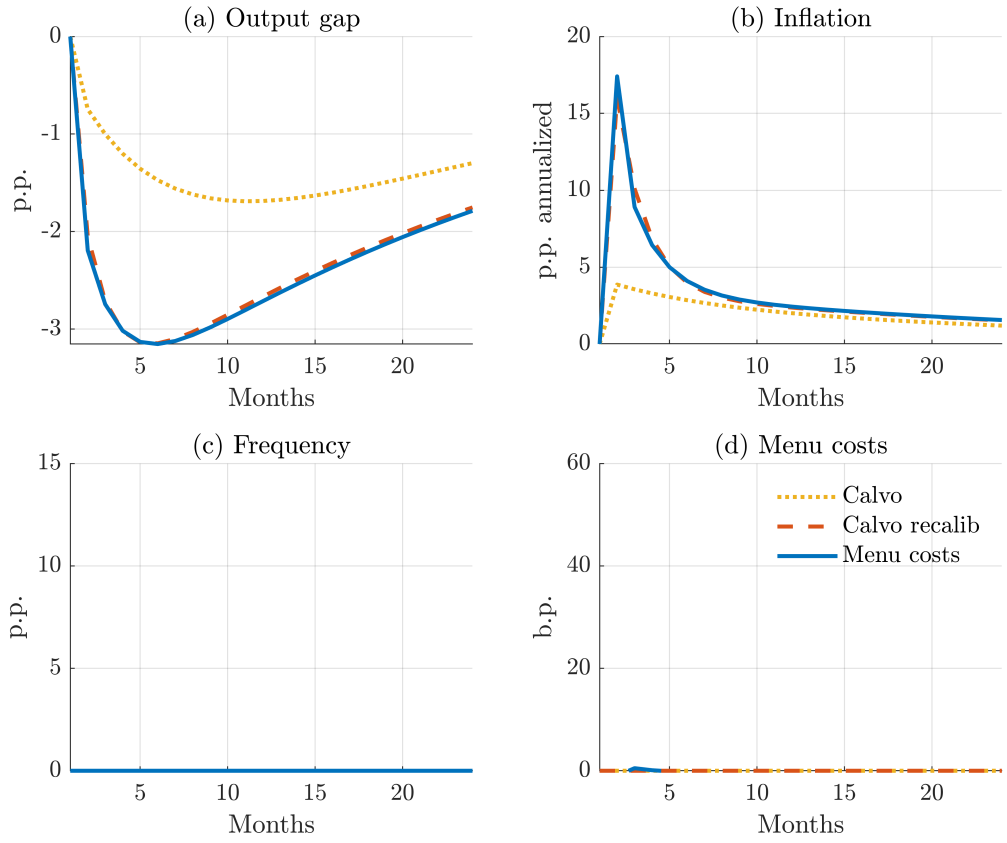


FIGURE A4. Impulse responses to a small cost-push shock in the menu cost and in the Calvo model. *Note*: all displayed variables except frequency are linearly-scaled in the small shock according to the ratio between the large and small shocks. The Calvo recalibrated model replicates the slope of the Phillips curve

The dashed blue line in Figure A4 shows the recalibrated Calvo model. The Calvo parameter in that case is set to to match the slope of the Phillips curve in the Golosov-Lucas model (discussed below). The recalibrated Calvo model approximately replicates the dynamics of the Golosov-Lucas model in response to small shocks. The fact that

[25]The larger initial inflation bout in the case of large shocks is then compensated by a lower inflation path, relative to the small shock counterfactual, from month 3 onwards, and both paths coincide after 9 months.

the Golosov-Lucas model can be locally approximated for small inflation levels by a re-calibrated Calvo model with a large frequency was studied by Auclert et al. (2024).

Price dispersion shocks. Figure A5 shows the impulse responses to a shock to the volatility of the idiosyncratic quality shocks (σ_t). The shock raises the dispersion of optimal reset prices and generates a persistent increase in the frequency of price changes (Vavra 2014). The observed increase in the dispersion of price changes during the recent inflation surge (Montag and Villar 2023) indicates the presence of a similar idiosyncratic dispersion shock either parallel or as a result of the aggregate shocks (Berger and Vavra 2019). The size of the large shock is calibrated to generate a 11.3% increase in frequency, which coincides with the peak of the cost-push shock. Notably, the shock is inflationary. This is primarily due to the asymmetry of the value function: firms with too low quality-adjusted prices face high demand, so they are relatively more motivated to *increase* their prices than firms with too high quality-adjusted prices are motivated to *decrease* theirs due to their low demand. The output gap declines primarily as a result of the high price distortions. The differences relative to the linearly scaled small volatility shock (black dashed lines) reveal a sizable nonlinearity of the model with respect to this shock. Nonetheless, notice how the impact of the shock on inflation and output is one order of magnitude lower than that of the cost-push shock presented in Figure A3.

TFP and monetary policy shocks. Figures A6 and A7 show analogous impulse responses to a TFP and monetary policy shocks, respectively. These shocks are calibrated to replicate the 11.3% increase in frequency. The model again displays significant nonlinearities in both cases, as the inflation surge is larger, and the output gap surge is smaller, in the case of a large shock.

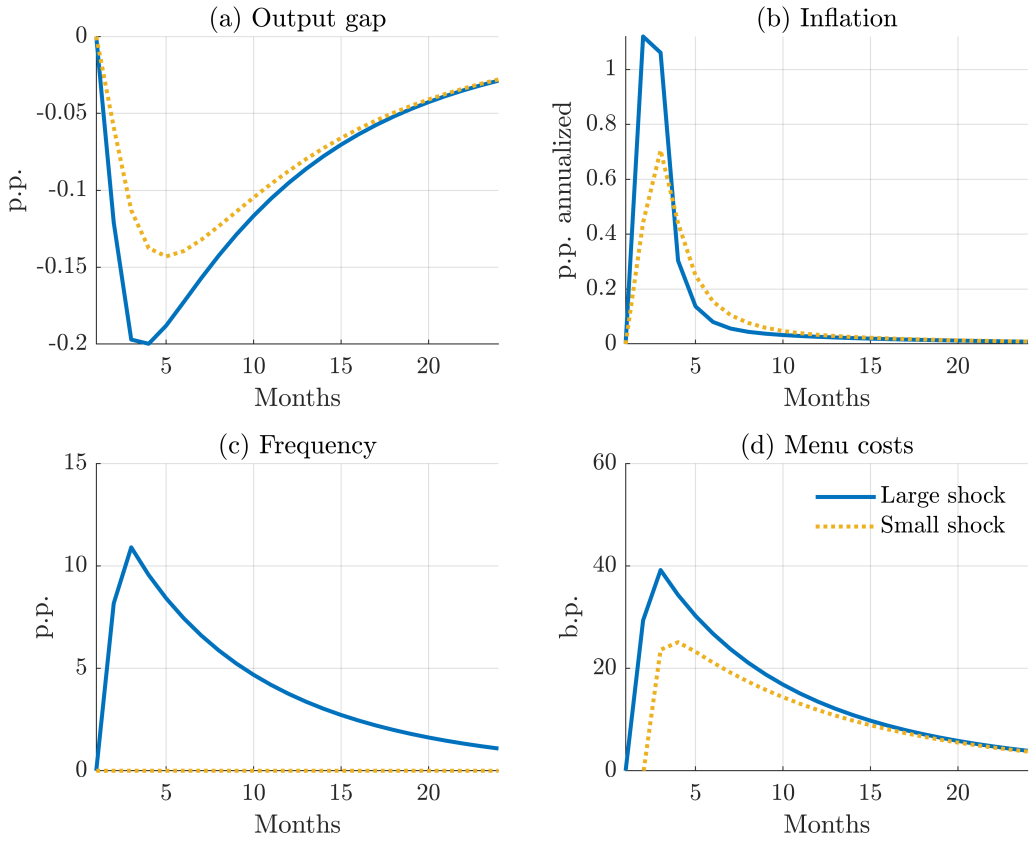


FIGURE A5. Impulse responses to a large and a small dispersion shock in the menu cost model. *Note*: all displayed variables except frequency are linearly-scaled in the small shock according to the ratio between the large and small shocks.

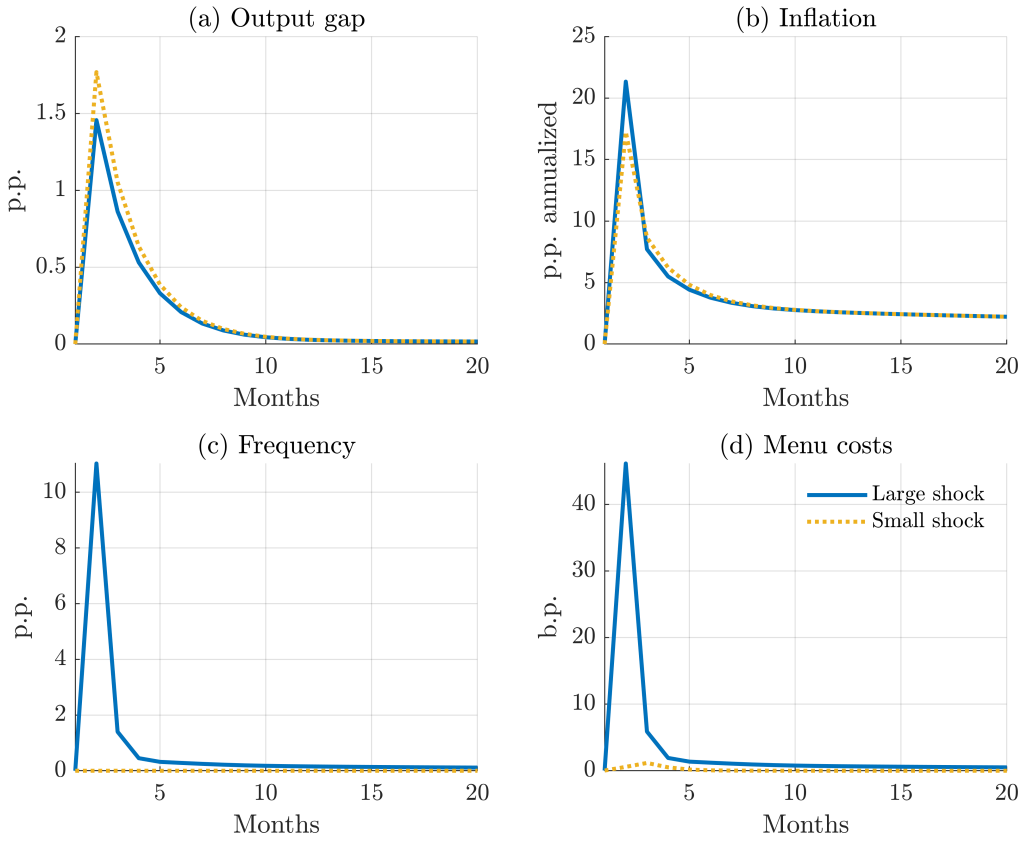


FIGURE A6. Impulse responses to a large and a small TFP shock in the menu cost model.
Note: all displayed variables except frequency are linearly-scaled in the small shock according to the ratio between the large and small shocks.

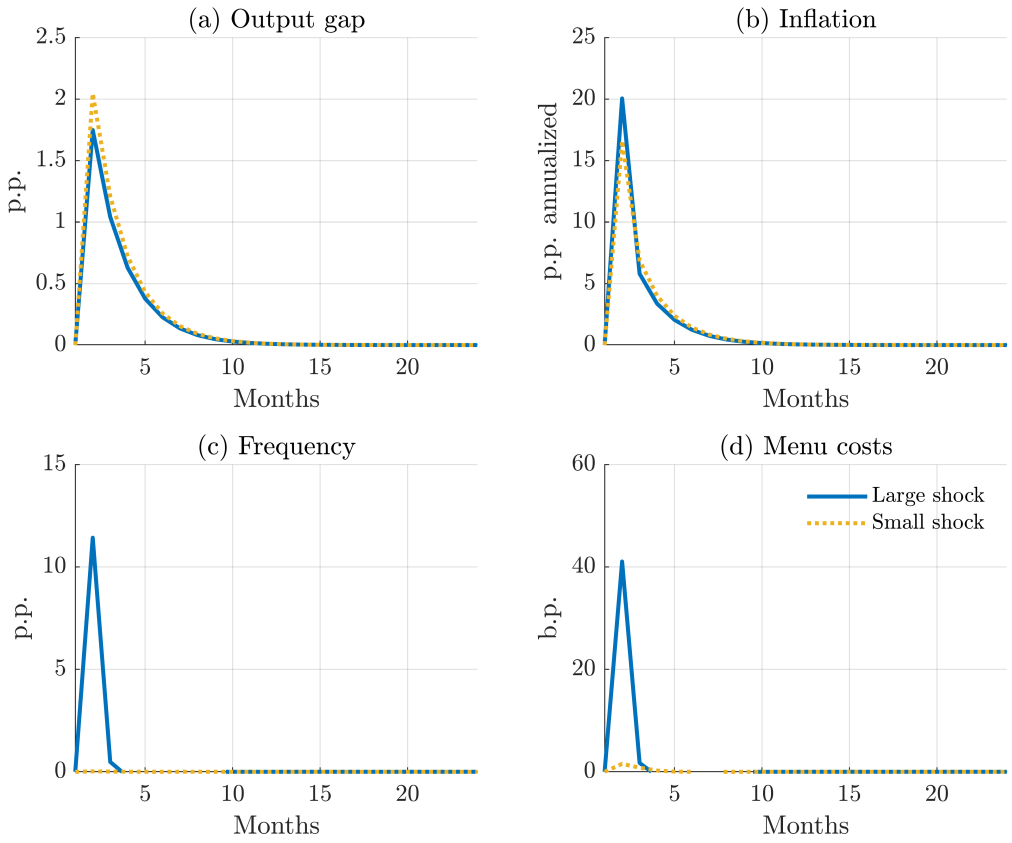


FIGURE A7. Impulse responses to a large and a small monetary policy shock in the menu cost model. *Note*: all displayed variables except frequency are linearly-scaled in the small shock according to the ratio between the large and small shocks.

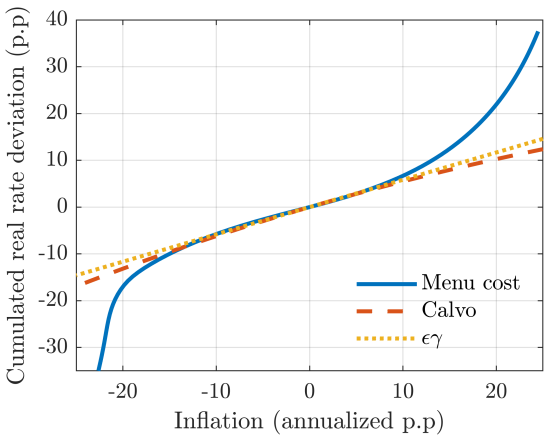


FIGURE A8. Target rule. *Note*: The real rate deviation is from its efficient level, which is equal to the steady state value for cost push shocks. This figure is the mirror image of Figure 5 in the main text.

Appendix E. Computational algorithm

This appendix explains the computational method. We use a three-step approach we use to convert the original infinite-dimensional Ramsey problem into a finite-dimensional one. First, we approximate the distribution and value functions by piece-wise linear functions over a set of nodes. Second, we use endogenous nodes, such that both boundaries of the (s_t, S_t) band and the optimal reset price are "on the grid". Third, given this approximation, we evaluate integrals analytically. Step one makes the problem finite dimensional. Steps two and three ensure that the approximation is accurate, smooth and computationally efficient.We explain those steps in detail below.

Once we have converted the planner's infinite-dimensional problem into a finite-dimension problem in this way, we derive the planner's first order conditions. For this we use symbolic differentiation, and in particular Dynare's `Ramsey` command. The resulting set of first order conditions is then solved in the sequence space under perfect foresight. Here we employ a standard Newton method using Dynare's `perfect foresight solver` command.

To determine the appropriate initial and terminal conditions, and an initial guess for the transition paths, we need to find the non-stochastic steady state of the model. We determine the steady state of the private equilibrium conditional on a particular value of the policy instrument π using a standard Newton based solution method. We then use this function and exploit the linearity of the first order conditions wrt. the Lagrange multipliers to convert the high-dimensional problem of solving for the steady state into a one-dimensional problem, which is solved with a Newton solver. This last step is performed by Dynare's `steady` command. That is, we have to manually convert the problem into a finite-dimension problem and find the steady state conditional on a policy; the rest of the procedure uses Dynare.

The rest of the appendix explains those steps that are not straightforward applications of existing methods. It is organized as follows. First we explain how to make the planner's problem finite dimensional. For this purpose, we first define some useful auxiliary functions in Section E.1. Then we transform the equilibrium conditions to apply an endogenous grid and approximate the value and distribution functions by a piece-wise linear function in Section E.2. Finally, we evaluate the integrals analytically in Section E.3. The result is a discrete set of equations that can conveniently be represented in matrix form, which we summarized in Section E.4. Second, we explain how we determine the steady state in Section E.5.

E.1. Preliminaries

To begin with, let us normalize the variable x_t as

(A7)
$$x_t = \begin{cases} \frac{x_t}{s_t} & \text{if } x_t < 0 \\ \frac{x_t}{S_t} & \text{else} \end{cases}$$

Under this normalization, the optimal price is at $x_t = 0$, the upper boundary of the (S, s) band at $x_t = 1$ and the lower boundary of the (S, s) band at $x_t = -1$. This will later allow us to have all critical points (s_t, S_t, p_t^*) on the grid. The law of motion of x_t conditional on not updating can be derived from $x_t = x_{t-1} - \sigma\varepsilon_t - \pi_t^*$:

(A8)
$$x_t = \begin{cases} \frac{x_t}{S_t} = \frac{x_{t-1}-\sigma_t\varepsilon_t-\pi_t^*}{S_t} = \begin{cases} \frac{x_{t-1}-\sigma_t\varepsilon_t-\pi_t^*}{S_{t-1}}\frac{S_{t-1}}{S_t} = x_{t-1}\frac{S_{t-1}}{S_t} - \frac{\sigma_t\varepsilon_t+\pi_t^*}{S_t} & \text{if } x_t > 0, \text{if } x_{t-1} > 0 \\ \frac{x_{t-1}-\sigma_t\varepsilon_t-\pi_t^*}{s_{t-1}}\frac{s_{t-1}}{S_t} = x_{t-1}\frac{s_{t-1}}{S_t} - \frac{\sigma_t\varepsilon_t+\pi_t^*}{S_t} & \text{if } x_t > 0, \text{if } x_{t-1} < 0 \end{cases} \\ \frac{x_t}{s_t} = \frac{x_{t-1}-\sigma_t\varepsilon_t-\pi_t^*}{s_t} = \begin{cases} \frac{x_{t-1}-\sigma_t\varepsilon_t-\pi_t^*}{S_{t-1}}\frac{S_{t-1}}{s_t} = x_{t-1}\frac{S_{t-1}}{s_t} - \frac{\sigma_t\varepsilon_t+\pi_t^*}{s_t} & \text{if } x_t < 0, \text{if } x_{t-1} > 0 \\ \frac{x_{t-1}-\sigma_t\varepsilon_t-\pi_t^*}{s_{t-1}}\frac{s_{t-1}}{s_t} = x_{t-1}\frac{s_{t-1}}{s_t} - \frac{\sigma_t\varepsilon_t+\pi_t^*}{s_t} & \text{if } x_t < 0, \text{if } x_{t-1} < 0 \end{cases} \end{cases}$$

We now define functions to be used in the next sections to redefine the value and distribution functions. For compactness, let us adopt the notation where $\hat{s}_t(x_t)$ picks the respective extremes (S, s) depending on the value of x_t following (A7). For brevity, at times we will drop the dependence on x_t and just write $\hat{s}_t$.

Solving (A8) for x_t, x_{t-1} and ε respectively, we obtain the following relations:

(A9)
$$x_t = x_{t-1}\frac{\hat{s}_{t-1}}{\hat{s}_t} - \frac{\sigma_t\varepsilon_t + \pi_t^*}{\hat{s}_t}$$

(A10)
$$x_{t-1} = x_t\frac{\hat{s}_t}{\hat{s}_{t-1}} + \frac{\sigma_t\varepsilon_t + \pi_t^*}{\hat{s}_{t-1}}$$

(A11)
$$\varepsilon_t = \frac{\hat{s}_{t-1}x_{t-1} - \hat{s}_t x_t - \pi_t^*}{\sigma_t} \equiv h(x_{t-1}, x_t)$$

where we have defined $h(x_{t-1}, x_t)$ for later use.

E.2. Approximating the distribution and value functions by piecewise linear functions on an endogenous grid

Now we redefine the value and distribution functions over the variable x and approximate them by piece-wise linear functions. The original infinite dimensional problem of the planner are laid out in Section **??**. In the following, we consider each of the equations containing the distribution and value functions one by one.

E.2.1. Distribution

The distribution function is given by

$$g_t(x) = (1-\lambda_t(x)) \int g_{t-1}(x+\sigma_t\varepsilon_t+\pi_t^*)d\xi(\varepsilon)+\delta(x) \int \lambda_t(\tilde{x}) \left(\int g_{t-1}(\tilde{x} + \sigma_t\varepsilon + \pi_t^*)d\xi(\varepsilon) \right) d\tilde{x}$$

with

$$\int_{s_t}^{S_t} g_t(x)dx = 1 \tag{A12}$$

where $\delta(x)$ is the Dirac Delta function that captures the mass point of those firms who update their prices.

We split the distribution into the continuous distribution of agents who do not update their prices plus a mass point of updaters at $x = 0$ (this is already reflected in Section **??**):

$$\begin{aligned} g_t^c(x) &= (1 - \lambda_t(x)) \int g_{t-1}^c(x + \sigma_t\varepsilon + \pi_t^*)d\xi(\varepsilon), \\ g_t^0 &= \int \lambda_t(\tilde{x}) \int g_{t-1}^c(\tilde{x} + \sigma_t\varepsilon - \pi_t^*)d\xi(\varepsilon)d\tilde{x}. \end{aligned}$$

Furthermore, we use equation (A12) to express the latter expression as:

$$g_t^0 = 1 - \int_{s_t}^{S_t} g_t^c(x)dx.$$

Now rewrite it using the newly defined re-normalized x where $x = \mathsf{x}\hat{s}_t$ as in equation (A7): define $g_t(\mathsf{x}\hat{s}_t) \equiv \mathrm{g}_t(\mathsf{x})$ and $g_t^c(\mathsf{x}\hat{s}_t) \equiv \mathrm{g}_t^c(\mathsf{x})$ and, with a slight abuse of notation, $-_t(\mathsf{x}\hat{s}_t) \equiv \lambda_t(\mathsf{x})$ and write

$$\mathrm{g}_t^c(\mathsf{x}) = (1 - \lambda_t(\mathsf{x})) \int \mathrm{g}_{t-1} \left(\frac{\mathsf{x}\hat{s}_t + \sigma_t\varepsilon + \pi_t^*}{\hat{s}_{t-1}} \right) d\xi(\varepsilon), \tag{A13}$$

$$\mathrm{g}_t^0 = 1 - \int_{-1}^{1} \mathrm{g}_t^c(\mathsf{x})\, \hat{s}_t(\mathsf{x})d\mathsf{x}. \tag{A14}$$

Note that for the latter expression for g_t^0 we have applied a change of variable to the integral. In particular, we have used the following substitution:

$$\begin{aligned} \int_{s_t}^{S_t} g_t^c(x)dx &= \int_{s_t}^{S_t} g_t^c(\mathsf{x}\hat{s}_t(\mathsf{x}))d\mathsf{x}\hat{s}_t(\mathsf{x}) \\ &= \int_{s_t}^{S_t} \mathrm{g}_t^c(\mathsf{x})d\mathsf{x}\hat{s}_t(\mathsf{x}) = \int_{s_t/\hat{s}_t(\mathsf{x})}^{S_t/\hat{s}_t(\mathsf{x})} \hat{s}_t(\mathsf{x})\mathrm{g}_t^c(\mathsf{x})d\mathsf{x} = \int_{-1}^{1} \hat{s}_t(\mathsf{x})\mathrm{g}_t^c(\mathsf{x})d\mathsf{x}. \end{aligned}$$

Next we will also change the variable in the integral in the equation for $\mathrm{g}_t^c(\mathsf{x})$ (A13). This change of variable is a bit more involved, so we derive it in detail here. First, we

re-express (A13) as

$$g_t^c(x) = (1 - -_t(x)) \int g_{t-1}\left(\frac{x\hat{s}_t + \sigma_t\varepsilon + \pi_t^*}{\hat{s}_{t-1}}\right)\phi(\varepsilon)d\varepsilon.$$

where $\phi(\cdot)$ is the standard normal pdf.

Second, we define the value of the shock ε necessary to get from a price gap of $x_{t-1} = 0$ to a price gap of x_t as

$$\begin{aligned}\varepsilon_t^* &\equiv \varepsilon_t \in \mathbb{R}|0 = x_t\hat{s}(x_t) + \sigma_t\varepsilon_t + \pi_t^* \\ &= h(0, x_t)\end{aligned}$$

and then we split the integral in two parts at ε_t^*

$$\begin{aligned}g_t^c(x) &= (1 - -_t(x)) \int^{\varepsilon_t^*} g_{t-1}\left(\frac{x\hat{s}_t + \sigma_t\varepsilon + \pi_t^*}{\hat{s}_{t-1}}\right)\phi(\varepsilon)d\varepsilon \\ &+ (1 - -_t(x)) \int_{\varepsilon_t^*} g_{t-1}\left(\frac{x\hat{s}_t + \sigma_t\varepsilon + \pi_t^*}{\hat{s}_{t-1}}\right)\phi(\varepsilon)d\varepsilon,\end{aligned}$$

Since, for a realization ε of the shock at t,

$$\hat{s}(x_{t-1})x_{t-1} = x_t\hat{s}(x_t) + \sigma_t\varepsilon + \pi_t^*, \tag{A15}$$

we have

$$d\varepsilon = \left(\frac{\hat{s}(x_{t-1})}{\sigma_t} + \frac{x_{t-1}}{\sigma_t}\frac{d\hat{s}(x_{t-1})}{dx_{t-1}}\right)dx_{t-1}.$$

In each of the two intervals over which the two integrals are defined, the mapping (A15) is continuous and $\frac{d\hat{s}(x_{t-1})}{dx_{t-1}} = 0$. Thus we can implement a change of variable from ε to x_{t-1} in both integrals:

$$\begin{aligned}g_t^c(x) &= (1 - -_t(x)) \int^{\varepsilon_t^*} \frac{s_{t-1}}{\sigma_t} g_{t-1}(x_{t-1})\phi\left(\frac{s_{t-1}x_{t-1} - \hat{s}_t x - \pi_t^*}{\sigma_t}\right)dx_{t-1} \\ &+ (1 - -_t(x)) \int_{\varepsilon_t^*} g_{t-1}(x_{t-1})\phi\left(\frac{S_{t-1}x_{t-1} - \hat{s}_t x - \pi_t^*}{\sigma_t}\right)\frac{S_{t-1}}{\sigma_t}dx_{t-1}.\end{aligned}$$

Finally, pasting the two integrals together again, re-denoting x_{t-1} by x' and using $h(x', x)$

$$g_t^c(x) = (1 - -_t(x)) \int \frac{\hat{s}_{t-1}(x')}{\sigma_t} g_{t-1}(x')\phi\left(h(x', x)\right)dx'$$

This concludes the change of variable.

The end of period distribution has mass on the (s, S) band, i.e. in the range $x \in$

$[-1, 1]$. We can thus restrict the boundaries of the integral accordingly:

$$\mathrm{g}_t^c(\mathrm{x}) = (1 - \lambda_t(\mathrm{x})) \int_{-1}^{1} \frac{\hat{s}_{t-1}(\mathrm{x}')}{\sigma_t} \mathrm{g}_{t-1}(\mathrm{x}') \phi\left(h(\mathrm{x}', \mathrm{x})\right) \, d\mathrm{x}'.$$

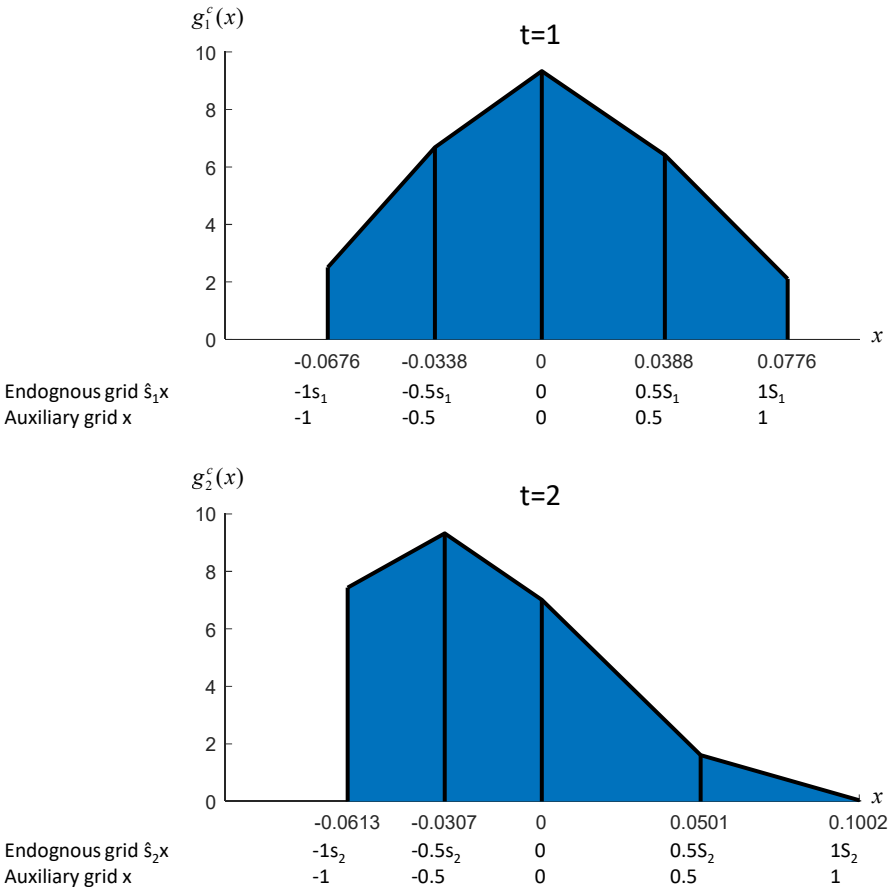


FIGURE A9. This figure schematically explains the linear interpolation with an endogenous grid. It shows the piece-wise linearly approximated distribution $\mathrm{g}_t^c(x)$ at two points in time, $t = 1$ and $t = 2$. The thresholds of the (S, s) band are not symmetric around 0 and differ across time. The endogenous grid x has I grid points, which are automatically adjusted so that half of the grid points cover the negative part of the (s, S) band and half of them cover the positive part. In this illustrative example $I = 5$ (we use a larger I when solving the model). The adjustment is obtained by multiplying the auxiliary grid $\mathrm{x} = [-1, -0.5, 0, 0.5, 1]$ by $\hat{s}_t(\mathrm{x})$: $x = \mathrm{x}\hat{s}_t$

So far we have rewritten the law of motion of the firm distribution g_t. We now introduce the approximation we rely on for g_t. We approximate g^c by a piece-wise linear function with equally spaced nodes $\mathrm{x}_1, \ldots, \mathrm{x}_I = -1, \ldots, 0, \ldots, 1$ with $\mathrm{g}_t^c(\mathrm{x}|\mathrm{x}_i < \mathrm{x} < \mathrm{x}_{i+1}) \approx \mathrm{g}_t^c(\mathrm{x}_i) + \frac{\mathrm{x}-\mathrm{x}_i}{\mathrm{x}_{i+1}-\mathrm{x}_i} \frac{g_{t-1}^c(\mathrm{x}_{i+1}) - g_{t-1}^c(\mathrm{x}_i)}{\mathrm{x}_{i+1}-\mathrm{x}_i}$.

Note that the auxiliary grid for x is exogenous. However, this exogenous auxiliary grid defines an *endogenous grid* for $x = \hat{s}_t \mathrm{x}$, which, at each t, exactly spans the the (s, S) band and has a node at 0. Figure A9 illustrates the use of linear interpolation with an endogenous grid as we apply it here.

From now on, g_t^c denotes the piece-wise linear approximated function and $g_t^c(x_i < x < x_{i+1})$ denotes a linear piece of it. Thus, the functions are approximated as

$$g_t^c(x) = (1 - \lambda_t(x))\left[\sum_{i=1}^{I-1} \int_{x_i}^{x_{i+1}} \frac{\hat{s}_{t-1}(x')}{\sigma_t} g_{t-1}^c(x_i < x' < x_{i+1}) \phi\left(h(x', x)\right)\, dx' + \frac{1}{\sigma_t} g_{t-1}^0 \phi\left(h(0, x)\right)\right],$$

$$g_t^0 = 1 - \sum_{i=1}^{I-1} \int_{x_i}^{x_{i+1}} g_t^c(x_i < x < x_{i+1}) \hat{s}_t(x) dx.$$

Notice that, in these expressions, the integrands are continuous in the interval $x_i < x < x_{i+1}$ since x and x' are of constant sign.

Also note that the distribution function is 0 outside the (S,s) band. Our piecewise linear g_t^c in fact is only defined over the range where the distribution has positive mass, that is for $x \in [-1, 1]$. This is computationally efficient.

Withing this range $(1 - \lambda_t(x)) = 1$ so we can drop it from the expression above.

$$g_t^c(x) = \left[\sum_{i=1}^{I-1} \int_{x_i}^{x_{i+1}} \frac{\hat{s}_{t-1}(x')}{\sigma_t} g_{t-1}^c(x_i < x' < x_{i+1}) \phi\left(h(x', x)\right)\, dx' + \frac{1}{\sigma_t} g_{t-1}^0 \phi\left(h(0, x)\right)\right]$$

E.2.2. Other Aggregation Equations

The equilibrium conditions contain two further aggregation equations that contain the function $g(\cdot)$, for which we use the piece-wise linear approximation of $g^c(\cdot)$. Recall the aggregate price index and the labor market clearing condition

$$\begin{aligned} e^{p_t^*(\epsilon-1)} &= \int e^{x(1-\epsilon)} g_t(x)dx, \\ N_t &= \frac{C_t}{A_t} e^{p_t^*(-\epsilon)} \int e^{x(-\epsilon)} g_t(x)d(x) + \eta \int \lambda_t(x + p_t^* - \sigma_t \varepsilon_t - \pi_t^*) g_{t-1}(x)d(x) \end{aligned}$$

which we approximate as follows, after the change of variable to x,

$$e^{p_t^*(\epsilon-1)} = \sum_{i=1}^{I-1} \int_{x_i}^{x_{i+1}} e^{x(1-\epsilon)} g_t^c(x_{i-1} < x < x_{i+1}) \hat{s}_t(x)dx + g_t^0,$$

$$N_t = \frac{C_t}{A_t} e^{p^*(-\epsilon)} \sum_{i=1}^{I-1} \int_{x_i}^{x_{i+1}} \left(e^{x(-\epsilon)} g_t^c(x_{i-1} < x < x_{i+1}) \hat{s}_t(x)dx + g_{t-1}^0 \right) + \eta g_{t-1}^0.$$

E.2.3. Value Function

Recall the value function is

$$\begin{aligned} V_t(x) =& \Pi_t(x) + \Lambda_{t,t+1} \int \left(1 - \lambda_{t+1}(x - \sigma_{t+1}\varepsilon - \pi_{t+1}^*)\right) V_{t+1}(x - \sigma_{t+1}\varepsilon - \pi_{t+1}^*) d\xi(\varepsilon) \\ &+ \Lambda_{t,t+1} \left(V_{t+1}(0) - \eta w_{t+1}\right) \int \lambda_{t+1}(x - \sigma_{t+1}\varepsilon - \pi_{t+1}^*) d\xi(\varepsilon). \end{aligned}$$

We now express it in terms of x with $V_t(x) \equiv V_t(x\hat{s}_t)$:

$$\begin{aligned} V_t(x) = \Pi_t(x) &+ \Lambda_{t,t+1} \int \left(1 - \lambda_{t+1}\left(\frac{x\hat{s}_t + \sigma_t\varepsilon + \pi_t^*}{\hat{s}_{t-1}}\right)\right) V_{t+1}\left(\frac{x\hat{s}_t + \sigma_t\varepsilon + \pi_t^*}{\hat{s}_{t-1}}\right) d\xi(\varepsilon) \\ &+ \Lambda_{t,t+1} \left(V_{t+1}(0) - \eta w_{t+1}\right) \int \lambda_{t+1}\left(\frac{x\hat{s}_t + \sigma_t\varepsilon + \pi_t^*}{\hat{s}_{t-1}}\right) d\xi(\varepsilon). \end{aligned}$$

Note that by definition $V_t(0) - \eta \frac{w_{t+1}}{A_{t+1}} = V_t(-1) = V_t(1)$ and $V_t'(0) = 0$. The first two equalities are straightforward; the next subsection discusses the latter.

After the change of variable to x', which is analogous to the change of variable applied to g_t^c previously, we can rewrite $V_t(x)$ as

$$\begin{aligned} V_t(x) =& \Pi_t(x) + \frac{\Lambda_{t,t+1}}{\sigma_{t+1}} \int \hat{s}_{t+1}(x') \left(1 - \lambda_{t+1}(x')\right) V_{t+1}(x') \phi\left(h(x, x')\right) dx' \\ &+ \Lambda_{t,t+1} \left(V_{t+1}(0) - \eta w_{t+1}\right) \int \hat{s}_{t+1}(x') \lambda_{t+1}(x') \phi\left(h(x, x')\right) \frac{1}{\sigma_{t+1}} dx' \end{aligned}$$

Since the price updating probability $\lambda_{t+1}(x) = 1$ for any x outside the (S, s) band, we can restrict the first integral to the range $[-1, 1]$. The last term in the second line (which captures the probability of updating a price tomorrow, given the current state) can be replaced by 1 minus the probability of not updating the price tomorrow. The latter is

given by an integral over the range $[-1, 1]$. So we write:

$$\begin{aligned}V_t(x) =&\Pi_t(x) + \frac{\Lambda_{t,t+1}}{\sigma_{t+1}} \int_{-1}^{1} \hat{s}_{t+1}(x') \left(1 - \lambda_{t+1}(x')\right) V_{t+1}(x') \phi\left(h(x, x')\right) dx' \\ &+ \Lambda_{t,t+1} \left(V_{t+1}(0) - \eta w_{t+1}\right) \left(1 - \frac{1}{\sigma_{t+1}} \int_{-1}^{1} \hat{s}_{t+1}(x') \left(1 - \lambda_{t+1}(x')\right) \phi\left(h(x, x')\right) dx'\right).\end{aligned}$$

In the inaction region, the price updating probability $\Lambda_{t,t+1}(x) = 0$, so:

$$\begin{aligned}V_t(x) =&\Pi_t(x) + \frac{\Lambda_{t,t+1}}{\sigma_{t+1}} \int_{-1}^{1} \hat{s}_{t+1}(x') V_{t+1}(x') \phi\left(h(x, x')\right) dx' \\ &+ \Lambda_{t,t+1} \left(V_{t+1}(0) - \eta w_{t+1}\right) \left(1 - \frac{1}{\sigma_{t+1}} \int_{-1}^{1} \hat{s}_{t+1}(x') \phi\left(h(x, x')\right) dx'\right).\end{aligned}$$

So far we have normalized the support of the value function. Additionally, it is convenient to normalize further the value function itself. We normalize the value function by its maximal value $V_t(0)$, and denote the normalized value function by $v_t(x)$: $v_t(x) \equiv V_t(x) - V_t(0)$. The expression above can be re-written as:

$$\begin{aligned}&v_t(x) \equiv V_t(x) - V_t(0) = \Pi_t(x) - \Pi_t(0) \\ &+ \frac{\Lambda_{t,t+1}}{\sigma_{t+1}} \left(\int_{-1}^{1} \hat{s}_{t+1}(x') \left[V_{t+1}(x') \phi\left(\frac{x - x' - \pi^*_{t+1}}{\sigma_{t+1}} \right) - V_{t+1}(x') \phi\left(\frac{0 - x' - \pi^*_{t+1}}{\sigma_{t+1}} \right) \right] dx' \right) \\ &+ \frac{\Lambda_{t,t+1}}{\sigma_{t+1}} \left(- \int_{-1}^{1} \hat{s}_{t+1}(x') \left[\phi\left(\frac{x - x' - \pi^*_{t+1}}{\sigma_{t+1}} \right) - \phi\left(\frac{0 - x' - \pi^*_{t+1}}{\sigma_{t+1}} \right) \right] dx' \right) \left(V_{t+1}(0) - \eta w_{t+1}\right) \\ &= \Pi_t(x) - \Pi_t(0) \\ &+ \frac{\Lambda_{t,t+1}}{\sigma_{t+1}} \left(\int_{-1}^{1} \hat{s}_{t+1}(x') \left[v_{t+1}(x') \left(\phi\left(\frac{x - x' - \pi^*_{t+1}}{\sigma_{t+1}} \right) - \phi\left(\frac{0 - x' - \pi^*_{t+1}}{\sigma_{t+1}} \right) \right) \right] dx' \right) \\ &+ \frac{\Lambda_{t,t+1}}{\sigma_{t+1}} \left(- \int_{-1}^{1} \hat{s}_{t+1}(x') \left[\phi\left(\frac{x - x' - \pi^*_{t+1}}{\sigma_{t+1}} \right) - \phi\left(\frac{0 - x' - \pi^*_{t+1}}{\sigma_{t+1}} \right) \right] dx' \right) (-\eta w_{t+1})\end{aligned}$$

Following our approach for $g^c(\cdot)$, we approximate $v(\cdot)$ by a piece-wise linear function with nodes $x_1, \ldots, x_I = -1, \ldots, 0, \ldots, 1$ with $v_t(x | x_i < x < x_{i+1}) \approx v_t(x_i) + \frac{x - x_i}{x_{i+1} - x_i} \frac{v_t(x_{i+1}) - v_t(x_i)}{x_{i+1} - x_i}$.

From now on, v_t denotes the piece-wise linear approximated function and $v_t(x_i < x < x_{i+1})$ denotes a linear piece of it. Thus, this function $v_t(x)$ is approximated as

$$\begin{aligned}v_t(x) =&\Pi_t(x) - \Pi_t(0) \\ &+ \frac{\Lambda_{t,t+1}}{\sigma_{t+1}} \sum_{i=1}^{I-1} \int_{x_i}^{x_{i+1}} \hat{s}_{t+1}(x') v_{t+1}(x_i < x' < x_{i+1}) (\phi\left(h(x, x')\right) - \phi\left(h(0, x')\right)) dx' \\ &+ \frac{\Lambda_{t,t+1}}{\sigma_{t+1}} (-\eta w_{t+1}) \int_{-1}^{1} \hat{s}_{t+1}(x') (\phi\left(h(x, x')\right) - \phi\left(h(0, x')\right)) dx'.\end{aligned}$$

E.2.4. Optimality condition for reset price

We proceed in the same way for the derivative of the value function. We start with

$$0 = V_t'(0) = \Pi_t'(0) + \frac{\Lambda_{t,t+1}}{\sigma_{t+1}} \int_{s_{t+1}}^{S_{t+1}} V_{t+1}(x') \left. \frac{\partial \phi\left(\frac{x-x'-\pi^*_{t+1}}{\sigma_{t+1}}\right)}{\partial x} \right|_{x=0} dx' + \frac{\Lambda_{t,t+1}}{\sigma_{t+1}} \left(\phi\left(\frac{-S_{t+1}-\pi^*_{t+1}}{\sigma_{t+1}}\right) - \phi\left(\frac{-s_{t+1}-\pi^*_{t+1}}{\sigma_{t+1}}\right)\right)(V_{t+1}(0) - \eta w_{t+1})$$

where

$$\left. \frac{\partial \phi\left(\frac{x-x'-\pi^*_{t+1}}{\sigma_{t+1}}\right)}{\partial x} \right|_{x=0} = \frac{1}{\sqrt{2\pi}\sigma_{t+1}} \frac{-\pi^*_{t+1}-x'}{\sigma_{t+1}} e^{-\frac{1}{2}\left(\frac{-\pi^*_{t+1}-x'}{\sigma_{t+1}}\right)^2},$$
$$= \frac{\phi\left(\frac{-\pi^*_{t+1}-x'}{\sigma_{t+1}}\right)}{\sigma_{t+1}} \frac{-\pi^*_{t+1}-x'}{\sigma_{t+1}}$$

After change of variable to x, this expression becomes

$$0 = \Pi_t'(0) + \frac{\Lambda_{t,t+1}}{\sigma_{t+1}} \int_{-1}^{1} \hat{s}_{t+1}(x') V_{t+1}(x') h(0,x') \frac{\phi\left(h(0,x')\right)}{\sigma_{t+1}} dx' + \frac{\Lambda_{t,t+1}}{\sigma_{t+1}} \left(\phi\left(\frac{-S_{t+1}-\pi^*_{t+1}}{\sigma_{t+1}}\right) - \phi\left(\frac{-s_{t+1}-\pi^*_{t+1}}{\sigma_{t+1}}\right)\right)(V_{t+1}(0) - \eta w_{t+1}).$$

Now we re-express this in terms of $v(x)$ using $V_t(x) = v_t(x) + V_t(0)$ first, and the rearranging

$$\begin{aligned}
0 &= \Pi_t'(x) + \Lambda_{t,t+1} \int_{-1}^{1} \hat{s}_{t+1}(x') \left(v_{t+1}(x') + V_{t+1}(0)\right) h(0,x') \frac{\phi\left(h(0,x')\right)}{\sigma_{t+1}} dx' \\
&\quad + \frac{\Lambda_{t,t+1}}{\sigma_{t+1}} \left(\phi\left(\frac{-S_{t+1}-\pi^*_{t+1}}{\sigma_{t+1}}\right) - \phi\left(\frac{-s_{t+1}-\pi^*_{t+1}}{\sigma_{t+1}}\right)\right)(V_{t+1}(0) - \eta w_{t+1}) \\
&= \Pi_t'(x) + \Lambda_{t,t+1} \int_{-1}^{1} \hat{s}_{t+1}(x') v_{t+1}(x') h(0,x') \frac{\phi\left(h(0,x')\right)}{\sigma_{t+1}} dx' \\
&\quad + \Lambda_{t,t+1} \int_{-1}^{1} \hat{s}_{t+1}(x') h(0,x') \frac{\phi\left(h(0,x')\right)}{\sigma_{t+1}} dx' V_{t+1}(0) \\
&\quad + \frac{\Lambda_{t,t+1}}{\sigma_{t+1}} \left(\phi\left(\frac{-S_{t+1}-\pi^*_{t+1}}{\sigma_{t+1}}\right) - \phi\left(\frac{-s_{t+1}-\pi^*_{t+1}}{\sigma_{t+1}}\right)\right)(V_{t+1}(0) - \eta w_{t+1}) \\
&= \Pi_t'(x) + \Lambda_{t,t+1} \int_{-1}^{1} \hat{s}_{t+1}(x') v_{t+1}(x') h(0,x') \frac{\phi\left(h(0,x')\right)}{\sigma_{t+1}} dx' \\
&\quad - \frac{\Lambda_{t,t+1}}{\sigma_{t+1}} \left(\phi\left(\frac{-S_{t+1}-\pi^*_{t+1}}{\sigma_{t+1}}\right) - \phi\left(\frac{-s_{t+1}-\pi^*_{t+1}}{\sigma_{t+1}}\right)\right) V_{t+1}(0)
\end{aligned}$$

$$
\begin{aligned}
&+\frac{\Lambda_{t,t+1}}{\sigma_{t+1}}\left(\phi\left(\frac{-S_{t+1}-\pi^*_{t+1}}{\sigma_{t+1}}\right)-\phi\left(\frac{-s_{t+1}-\pi^*_{t+1}}{\sigma_{t+1}}\right)\right)(V_{t+1}(0)-\eta w_{t+1})\\
=\quad &\Pi'_t(0)+\Lambda_{t,t+1}\int_{-1}^{1}\hat{s}_{t+1}(x')v_{t+1}(x')h(0,x')\frac{\phi\left(h(0,x')\right)}{\sigma_{t+1}}dx'\\
&+\frac{\Lambda_{t,t+1}}{\sigma_{t+1}}\left(\phi\left(\frac{-S_{t+1}-\pi^*_{t+1}}{\sigma_{t+1}}\right)-\phi\left(\frac{-s_{t+1}-\pi^*_{t+1}}{\sigma_{t+1}}\right)\right)(-\eta w_{t+1})
\end{aligned}
$$

and apply the piece-wise linear approximation of $v(x)$:

$$
\begin{aligned}
0=\Pi'_t(0)+\Lambda_{t,t+1}\sum_{i=1}^{I-1}\int_{-1}^{1}\hat{s}_{t+1}(x')v_{t+1}(x_i<x'<x_{i+1})h(0,x')\frac{\phi\left(h(0,x')\right)}{\sigma_{t+1}}dx'\\
+\frac{\Lambda_{t,t+1}}{\sigma_{t+1}}\left(\phi\left(\frac{-S_{t+1}-\pi^*_{t+1}}{\sigma_{t+1}}\right)-\phi\left(\frac{-s_{t+1}-\pi^*_{t+1}}{\sigma_{t+1}}\right)\right)(-\eta w_{t+1}).
\end{aligned}
$$

E.3. Solving for Integrals

Let us collect the approximated equations we defined so far.

(A16)

$$
\begin{aligned}
v_t(x)=&\Pi_t(x)-\Pi_t(0)\\
&+\frac{\Lambda_{t,t+1}}{\sigma_{t+1}}\sum_{i=1}^{I-1}\int_{x_i}^{x_{i+1}}\hat{s}_{t+1}(x')v_{t+1}(x_i<x'<x_{i+1})(\phi\left(h(x,x')\right)-\phi\left(h(0,x')\right))dx'\\
&+\frac{\Lambda_{t,t+1}}{\sigma_{t+1}}(-\eta w_{t+1})\int_{-1}^{1}\hat{s}_{t+1}(x')(\phi\left(h(x,x')\right)-\phi\left(h(0,x')\right))dx',
\end{aligned}
$$

(A17)

$$
\begin{aligned}
0=&\Pi'_t(0)+\Lambda_{t+1}\int_{-1}^{1}\hat{s}_{t+1}v_{t+1}(x')h(0,x')\frac{\phi\left(h(0,x')\right)}{\sigma_{t+1}}dx'\\
&+\frac{\Lambda_{t,t+1}}{\sigma_{t+1}}\left(\phi\left(\frac{-S_{t+1}-\pi^*_{t+1}}{\sigma_{t+1}}\right)-\phi\left(\frac{-s_{t+1}-\pi^*_{t+1}}{\sigma_{t+1}}\right)\right)(-\eta w_{t+1}),
\end{aligned}
$$

(A18)
$$
g^c_t(x)=\sum_{i=1}^{I-1}\int_{x_i}^{x_{i+1}}\frac{\hat{s}_{t-1}(x')}{\sigma_t}g^c_{t-1}(x_i<x'<x_{i+1})\phi\left(h(x',x)\right)\,dx'+\frac{1}{\sigma_t}g^0_{t-1}\phi\left(h(0,x)\right),
$$

(A19)
$$
g^0_t=1-\sum_{i=1}^{I-1}\int_{x_i}^{x_{i+1}}g^c_t(x_i<x'<x_{i+1})\hat{s}_t(x)dx,
$$

(A20)
$$
e^{p^*_t(\epsilon-1)}=\sum_{i=1}^{I-1}\int_{x_i}^{x_{i+1}}e^{(x)(1-\epsilon)}g^c_t(x_i<x'<x_{i+1})\hat{s}_t(x)dx+g^0_t,
$$

$$N_t = \frac{C_t}{A_t} e^{p_t^*(-\epsilon)} \left(\sum_{i=1}^{I-1} \int_{x_i}^{x_{i+1}} e^{x(-\epsilon)} g_t^c(x_{i-1} < x < x_{i+1}) \hat{s}_t(x) dx + g_{t-1}^0 \right) + \eta g_{t-1}^0. \tag{A21}$$

The integrals in all of these expressions can be computed analytically, since the integrands consist of affine functions multiplied by expressions that have closed form anti-derivatives. Figure A10 illustrates this graphically for the integral in the equation for $g_t^c(x)$ (A18).

We now determine the solution of those integrals, equation by equation. Given the coefficients of the affine functions, which depend on the values of $v_{t+1}(g_{t-1})$ at the grid points x_i, we can then write the solutions as a function that is linear in the elements of the vector $v_{t+1}(x_i)$ $(g_{t-1}(x_i))$. We now explain this for the simple case of the integral in equation A19. The other equations require some more tedious algebra, which we conveniently executed using symbolic math and which we omit here for brevity, but are conceptually equivalent.

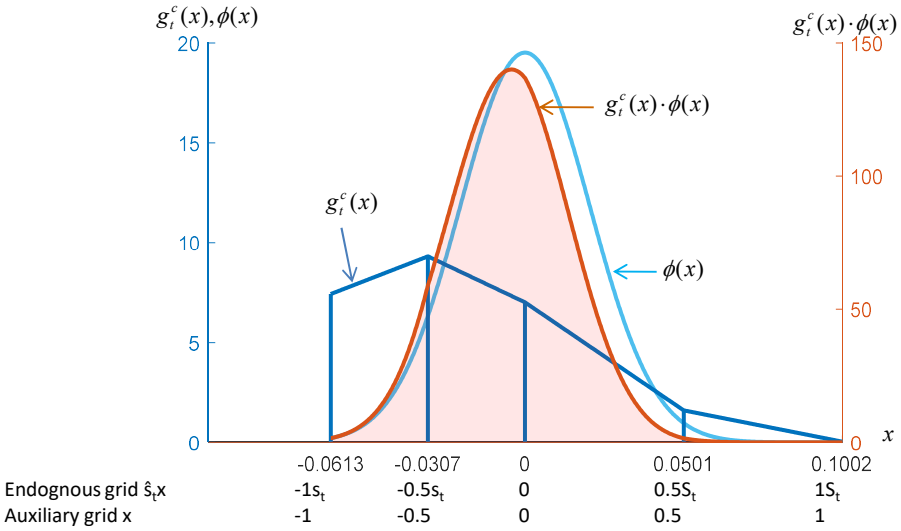


FIGURE A10. This figure schematically explains the analytical evaluation of integrals, given the linear approximation of the distribution and value functions. It shows the piece-wise linearly approximated distribution $g_t^c(x)$ in blue, the normal pdf $\phi(x)$ in light blue and the product of the two $g_t^c(x)\phi(x)$ in orange, where $x = x\hat{s}_t$. The orange area thus corresponds to the term $\sum_{i=1}^{I-1} \int_{x_i}^{x_{i+1}} \frac{\hat{s}_{t-1}(x')}{\sigma} g_{t-1}^c(x_i < x' < x_{i+1}) \phi\left(h(x', x)\right) dx'$ in equation (A18).

.

E.3.1. Mass Point

The integral over an affine function $f(x)$ from x_1 to x_2 is given by

$$\int_{x_1}^{x_2} f(x)\, dx = \frac{(f(x_1) + f(x_2))}{2} (x_2 - x_1)$$

thus

$$\sum_{i=1}^{I-1} \int_{x_i}^{x_{i+1}} f(x)\, dx = \sum_{i=1}^{I-1} \frac{(f(x_i) + f(x_{i+1}))}{2} (x_{i+1} - x_i).$$

Collecting the common terms on the right-hand side we get

$$\sum_{i=1}^{I-1} \int_{x_i}^{x_{i+1}} f(x)\, dx = \frac{\Delta x}{2} \left(f(x_1) + 2 \sum_{i=2}^{I-1} f(x_i) + f(x_I) \right).$$

Applying this formula to equation (A19), which defines the mass point at $x = 0$, and re-arranging terms we get

$$\mathrm{g}_t^0 = 1 - \mathbf{e}_t^T \mathbf{g}_t^{\boldsymbol{c}} \tag{A22}$$

where $\mathbf{e}_t^T = [0.5,\ 1, \ldots, 1,\ 0.5]\Delta x$. Note that this formula corresponds to the trapezoid rule. The blue area in Figure A9 illustrates the application of the trapezoid rule.

E.3.2. Aggregate Price Index

By the same logic, the aggregate price index in (A20) is computed as

$$e^{p_t^*(\epsilon-1)} = \sum_{i=1}^{I} (\mathrm{g}_t^c(\mathrm{x}_i) \mathbb{1}_{i \neq 1} d_{t,i,i-1,1-\varepsilon} + \mathrm{g}_t^c(\mathrm{x}_i) \mathbb{1}_{i \neq I} d_{t,i,i+1,1-\varepsilon}) + \mathrm{g}_t^0 \tag{A23}$$

where

$$d_{t,i,j,\varepsilon} = \frac{\left(e^{(\epsilon)\mathrm{x}_i \hat{s}_{t,i}} \left((\epsilon) \left(\mathrm{x}_i \hat{s}_{t,i} - \mathrm{x}_j \hat{s}_{t,j} \right) - 1 \right) + e^{(\epsilon)\mathrm{x}_j \hat{s}_{t,j}} \right)}{(\epsilon)^2 \left(\mathrm{x}_i \hat{s}t, i - \mathrm{x}_j \hat{s}_{t,j} \right)}$$

and where $\hat{s}_{t,i} \equiv \hat{s}_t(x_i)$ and where $\mathbb{1}_{i \neq 1}$ and $\mathbb{1}_{i \neq I}$ are indicator functions equal to 1 when i is different from 1 or I, that is whenever $\mathrm{g}_t^c(\mathrm{x}_i)$ is evaluated at the boundaries of the (S, s) band. It plays a similar role as the values 0.5 at the two extremes of the vector $\mathbf{e}_t^T$ above.

Hence, we can re-write equation (A23) in matrix form as

$$e^{p_t^*(\epsilon-1)} = \mathbf{d}_{t,1-\varepsilon}^T \mathbf{g}_t^{\boldsymbol{c}} + \mathrm{g}_t^0 \tag{A24}$$

where $\mathbf{g}_t^{\boldsymbol{c}}$ is the vector collecting the values of the the distribution function g_t^c at the grid points and where the vector $\mathbf{d}_{t,1-\varepsilon}$ is

$$\mathbf{d}_{t,1-\varepsilon} = \left[\mathbb{1}_{i \neq 1} d_{t,i,i-1,1-\varepsilon} + \mathbb{1}_{i \neq I} d_{t,i,i+1,1-\varepsilon} \right]_{i=1}^{I}.$$

Here we have adopted the notation that $[x_i]_{i=1}^I$ denotes a $I \times 1$ vector with elements x_i.

E.3.3. Labor Market

Following the previous subsection, the labor market condition (A21) is computed as

$$N_t = \frac{C_t}{A_t} e^{p_t^*(-\epsilon)} \left(\sum_{i=1}^{I} (g_t^c(x_i) \mathbb{1}_{i \neq 1} d_{t,i,i-1,-\varepsilon} + g_t^c(x_i) \mathbb{1}_{i \neq I} d_{t,i,i+1,-\varepsilon}) + g_{t-1}^0 \right) + \eta g_{t-1}^0$$

which we re-write in matrix form as

$$N_t = \frac{C_t}{A_t} e^{p_t^*(-\epsilon)} \left(\mathbf{d}_{t,-\varepsilon}^T \mathbf{g}_t^{\boldsymbol{c}} + g_{t-1}^0 \right) + \eta g_{t-1}^0. \tag{A25}$$

E.3.4. Distribution

Once we have evaluated the integrals, the distribution function in (A18) can be written as:

$$g_t^c(x_j) = \sum_{i=1}^{I} \frac{1}{2\sqrt{2\pi}} g_{t-1}^c(x_i) \left[\mathbb{1}_{i \neq 1} f_{t,i,i-1,j} + \mathbb{1}_{i \neq I} f_{t,i,i+1,j} \right] + \frac{1}{\sigma_t} g_{t-1}^0 \phi \left(\frac{-\hat{s}_{t,j} x_j - \pi_t^*}{\sigma_t} \right) \tag{A26}$$

where from now on, π without time subindex, denotes the scalar π, $f_{t,i,\bar{i},j}$ and $\mathcal{P}_{t,i,j}$ are defined as

$$f_{t,i,\bar{i},j} = \frac{\sqrt{2\pi} \left(\mathcal{P}_{t,\bar{i},j} \right) \left(\operatorname{erf}\left(\frac{\mathcal{P}_{t,\bar{i},j}}{\sqrt{2}\sigma_t} \right) - \operatorname{erf}\left(\frac{\mathcal{P}_{t,i,j}}{\sqrt{2}\sigma_t} \right) \right) + 2\sigma_t \left(\exp\left(-\frac{\mathcal{P}_{t,\bar{i},j}^2}{2\sigma_t^2} \right) - \exp\left(-\frac{\mathcal{P}_{t,i,j}^2}{2\sigma_t^2} \right) \right)}{\left| x_i \hat{s}_{t-1,i} - x_{\bar{i}} \hat{s}_{t-1,\bar{i}} \right|},$$

$$\mathcal{P}_{t,i,j} = -x_i \hat{s}_{t-1,i} + x_j \hat{s}_{t,j} + \pi_t^*.$$

For compactness, define

$$\mathbf{g}_t^{\boldsymbol{c}} \equiv \left[g_t^c(x_j) \right]_{j=1}^{I}$$

$$\mathbf{F}_t \equiv \left[\frac{1}{2\sqrt{2\pi}} \left(\mathbb{1}_{i \neq 1} f_{t,i,i-1,j} + \mathbb{1}_{i \neq I} f_{t,i,i+1,j} \right) \right]_{j=1,i=1}^{I,I}$$

$$\mathbf{f}_t \equiv \left[\frac{1}{\sigma_t} \phi \left(\frac{-\hat{s}_{t,j} x_j - \pi_t^*}{\sigma_t} \right) \right]_{j=1}^{I}$$

where $\mathbf{g}_t^{\boldsymbol{c}}$ and $\mathbf{f}_t$ are vectors with the probability mass function g_t^c and the scaled and shifted normal distribution at the grid points, respectively, $\mathbf{F}_t$ is a matrix that captures the idiosyncratic transitions due to firm-level quality shocks and where we have adopted the notation that $\left[x_{i,j} \right]_{j=1,i=1}^{J,I}$ denotes a $J \times I$ matrix with elements $x_{j,i}$. Thus, equation A26 can be represented in matrix form as

(A27) $$\mathbf{g}_{\boldsymbol{t}}^{\boldsymbol{c}} = \mathbf{F}_t \mathbf{g}_{\boldsymbol{t-1}}^{\boldsymbol{c}} + \mathbf{f}_t g_{t-1}^0.$$

E.3.5. Value function

Once we have evaluated the integrals, and denoting the standard normal cdf by $\Phi(\cdot)$ and the central grid point by i_0 (i.e. for $x_{i_0} = 0$), the value function A16 can be written as

(A28)
$$\begin{aligned} v_t(x_j) = {} & \Pi_{j,t} - \Pi_{j,t}(0) \\ & + \Lambda_{t,t+1} \sum_{i=1}^{I} \frac{1}{2\sqrt{2\pi}} v_{t+1}(x_i) \left(\mathbb{1}_{i \neq 1}(a_{t,i,i-1,j} - a_{t,i_0,i_0-1,j}) + \mathbb{1}_{i \neq I}(a_{t,i,i+1,j} - a_{t,i_0,i_0+1,j}) \right) \\ & + \Lambda_{t,t+1} (-\eta w_{t+1}) \left(\Phi\left(\frac{\mathcal{P}_{t+1,j,I}}{\sigma_{t+1}} \right) - \Phi\left(\frac{\mathcal{P}_{t+1,j,1}}{\sigma_{t+1}} \right) - \Phi\left(\frac{\mathcal{P}_{t+1,i_0,I}}{\sigma_{t+1}} \right) + \Phi\left(\frac{\mathcal{P}_{t+1,i_0,1}}{\sigma_{t+1}} \right) \right) \end{aligned}$$

where

(A29)
$$a_{t,i,\bar{i},j} = \frac{\sqrt{2\pi}\left(\mathcal{P}_{t+1,j,\bar{i}}\right)\left(\operatorname{erf}\left(\frac{\mathcal{P}_{t+1,j,\bar{i}}}{\sqrt{2}\sigma_{t+1}} \right) - \operatorname{erf}\left(\frac{\mathcal{P}_{t+1,j,i}}{\sqrt{2}\sigma_{t+1}} \right) \right) + 2\sigma_{t+1}\left(\exp\left(-\frac{\left(\mathcal{P}_{t+1,j,\bar{i}}\right)^2}{2\sigma_{t+1}^2} \right) - \exp\left(-\frac{\left(\mathcal{P}_{t+1,j,i}\right)^2}{2\sigma_{t+1}^2} \right) \right)}{\left| x_i \hat{s}_{t+1,i} - x_{\bar{i}} \hat{s}_{t+1,\bar{i}} \right|}.$$

For compactness, let us define

$$\begin{aligned} \mathbf{v}_t &\equiv \left[v_t(x_j) \right]_{j=1}^{I}, \\ \Delta_t &\equiv \left[\Pi_{j,t} - \Pi_{j,t}(0) \right]_{j=1}^{I}, \\ \mathbf{A}_t &\equiv \left[\Lambda_{t,t+1} \frac{1}{2\sqrt{2\pi}} \left(\mathbb{1}_{i \neq 1}(a_{t,i,i-1,j} - a_{t,i_0,i_0-1,j}) + \mathbb{1}_{i \neq I}(a_{t,i,i+1,j} - a_{t,i_0,i_0+1,j}) \right) \right]_{j=1,i=1}^{I,I}, \\ \mathbf{b}_{t+1} &\equiv \left[\Lambda_{t,t+1} \left(\Phi\left(\frac{\mathcal{P}_{t+1,j,I}}{\sigma_{t+1}} \right) - \Phi\left(\frac{\mathcal{P}_{t+1,j,1}}{\sigma_{t+1}} \right) - \Phi\left(\frac{\mathcal{P}_{t+1,i_0,I}}{\sigma_{t+1}} \right) + \Phi\left(\frac{\mathcal{P}_{t+1,i_0,1}}{\sigma_{t+1}} \right) \right) \right]_{j=1}^{I} \end{aligned}$$

where $\mathbf{v}_t$ and $\mathbf{b}_{t+1}$ are vectors that evaluate the value function v_t and the adjustment probability at different grid points, Δ_t is the vector of profit differences, while $\mathbf{A}_t$ is a matrix that represents the idiosyncratic transition due to firm-level quality shocks and price updating. Thus, equation (A28) can be represented in matrix form as

(A30) $$\mathbf{v}_t = \Delta_t + [\mathbf{A}_t \mathbf{v}_{t+1} - \mathbf{b}_{t+1} \eta w_{t+1}].$$

E.3.6. Optimality condition for reset price

After evaluating the integral, we can write the optimality condition in (A17) as

$$\begin{aligned} 0 = {} & \Pi_t'(0) + \Lambda_{t,t+1} \sum_{i=1}^{I} \mathsf{v}_{t+1}(\mathsf{x}_i) \frac{1}{2} \left(\mathbb{1}_{i \neq 1} c_{t,i,i-1,i_0} + \mathbb{1}_{i \neq I} c_{t,i,i+1,i_0} \right) \\ & + \frac{\Lambda_{t,t+1}}{\sigma_{t+1}} \left(\phi \left(\frac{-S_{t+1} - \pi^*_{t+1}}{\sigma_{t+1}} \right) - \phi \left(\frac{-s_{t+1} - \pi^*_{t+1}}{\sigma_{t+1}} \right) \right) (-\eta w_{t+1}) \end{aligned} \tag{A31}$$

where

$$c_{t,i,\bar{i},j} = \frac{\operatorname{erf}\left(\frac{\mathcal{P}_{t+1,j,i}}{\sqrt{2}\sigma} \right) - \operatorname{erf}\left(\frac{\mathcal{P}_{t+1,j,\bar{i}}}{\sqrt{2}\sigma} \right)}{x_i \hat{s}_{t+1,i} - x_{\bar{i}} \hat{s}_{t+1,\bar{i}}} - \frac{\sqrt{\frac{2}{\pi}} \exp\left(-\frac{\left(\mathcal{P}_{t+1,j,i} \right)^2}{2\sigma^2} \right)}{\sigma}. \tag{A32}$$

We can write this equation using matrix notation:

$$\begin{aligned} 0 = {} & \Pi_t'(0) + \mathbf{c}_{t+1}^T \mathbf{v}_{t+1} \\ & + \frac{\Lambda_{t,t+1}}{\sigma_{t+1}} \left(\phi \left(\frac{-S_{t+1} - \pi^*_{t+1}}{\sigma_{t+1}} \right) - \phi \left(\frac{-s_{t+1} - \pi^*_{t+1}}{\sigma_{t+1}} \right) \right) (-\eta w_{t+1}) \end{aligned} \tag{A33}$$

where

$$\mathbf{c}_{t+1} = \left[\Lambda_{t,t+1} \frac{1}{2} \left(\mathbb{1}_{i \neq 1} c_{t,i,i-1,i_0} + \mathbb{1}_{i \neq I} c_{t,i,i+1,i_0} \right) \right]_{i=1}^{I}. \tag{A34}$$

E.4. Final equation system

Collecting the thus derived equations, and combining them with the remainder of the private equilibrium conditions (which contain no infinite dimensional objects) and the objective, we can approximate the infinite dimensional planner's problem by the following finite dimensional planner's problem

$$\max_{\left\{ \mathbf{g}_t^{\boldsymbol{c}}, \mathrm{g}_t^0, \mathbf{v}_t, C_t, w_t, p_t^*, s_t, S_t, \pi_t^* \right\}_{t=0}^{\infty}} \mathbb{E}_0 \sum_{t=0}^{\infty} \beta^t \left(\frac{C_t^{1-\gamma}}{1-\gamma} - \upsilon \left(\frac{C_t}{A_t} e^{p_t^*(-\epsilon)} \left(\mathbf{d}_{t,-\varepsilon}^T \mathbf{g}_t^{\boldsymbol{c}} + \mathrm{g}_{t-1}^0 \right) + \eta \mathrm{g}_{t-1}^0 \right) \right)$$

subject to

$$\begin{aligned} w_t &= \upsilon C_t^{\gamma}, \\ \mathbf{v}_t &= {}''_t + \mathbf{A}_t \mathbf{v}_{t+1} - \mathbf{b}_{t+1} \eta w_{t+1}, \\ \mathbf{v}_{t,1} &= -\eta w_t, \\ \mathbf{v}_{t,I} &= -\eta w_t, \\ 0 &= \Pi_t'(0) + \mathbf{c}_{t+1}^T \mathbf{v}_{t+1} + \frac{\Lambda_{t,t+1}}{\sigma_{t+1}} \left(\phi \left(\frac{-S_{t+1} - \pi^*_{t+1}}{\sigma_{t+1}} \right) - \phi \left(\frac{-s_{t+1} - \pi^*_{t+1}}{\sigma_{t+1}} \right) \right) (-\eta w_{t+1}), \\ \mathbf{g}_t^{\boldsymbol{c}} &= \mathbf{F}_t \mathbf{g}_{\boldsymbol{t-1}}^{\boldsymbol{c}} + \mathbf{f}_t \mathrm{g}_{t-1}^0, \end{aligned}$$

$$
\begin{aligned}
g_t^0 &= 1 - \mathbf{e}_t^T \mathbf{g}_t^{\boldsymbol{c}}, \\
e^{p_t^*(\epsilon-1)} &= \mathbf{d}_{t,1-\varepsilon}^T \mathbf{g}_t^{\boldsymbol{c}} + g_t^0.
\end{aligned}
$$

Here the choice variables $\mathbf{v}_t$ and $\mathbf{g}_t^{\boldsymbol{c}}$ are vectors of length I. The rest of the choice variables are scalars. Note that the choice variables p_t^*, s_t, S_t, π_t^* implicitly appear in the problem (inside the vectors and matrices $\mathbf{A}_t$, $\mathbf{b}_t$, etc.)

As already explained at the beginning of this Appendix, we solve for the FOCs of this system by symbolic differentiation. The resulting system of FOCs is then solved in the sequence space. We next explain how we find the steady state, which serves as initial and terminal condition for dynamic simulations.

E.5. Steady state

To solve for the steady state of the private equilibrium conditions, given a policy $\bar{\pi}$, the algorithm is as follows. We rely on steady-state relationships $w = \upsilon C^{\gamma}$, and $R = (1+\pi)/\beta$ and $\pi = \pi^*$. We start with a guess for the real wage w, the optimal rest price p^*, and the boundaries of the (S, s) band s and S then:

a. Compute consumption $C = \left(\frac{w}{\upsilon}\right)^{1/\gamma}$.

b. Using $\pi = \pi^* = \bar{\pi}$, C and the 4 initial guesses, solve for that stationary value function using the Bellman equation and the stationary distribution using the law of motion of the distribution. Both have closed form solutions given the guesses.

$$
\begin{aligned}
\mathbf{v} &= (\mathbf{I} - \mathbf{A})^{-1} (\mathbb{''} - \mathbf{b}\eta w), \\
\mathbf{g}^c &= \left(\mathbf{I} - \mathbf{F} + \mathbf{f}\mathbf{e}^T\right)^{-1} \mathbf{f}, \\
g^0 &= 1 - \mathbf{e}^T \mathbf{g}^c
\end{aligned}
$$

c. Compute the residuals of the 4 remaining equations

$$
\begin{aligned}
\mathbf{v}_{t,1} &= -\eta w_t, \\
\mathbf{v}_{t,I} &= -\eta w_t, \\
0 &= \Pi_t'(0) + \mathbf{c}_{t+1}^T \mathbf{v}_{t+1} + \frac{\Lambda_{t,t+1}}{\sigma_{t+1}} \left(\phi \left(\frac{-S_{t+1} - \pi_{t+1}^*}{\sigma_{t+1}} \right) - \phi \left(\frac{-s_{t+1} - \pi_{t+1}^*}{\sigma_{t+1}} \right) \right) (-\eta w_{t+1}), \\
e^{p_t^*(\epsilon-1)} &= \mathbf{h}_{t,1-\varepsilon}^T \mathbf{g}_t^{\boldsymbol{c}} + g_t^0.
\end{aligned}
$$

d. Use a Newton method to update the 4 guesses (w, p^*, s, S) and return to step 1, until convergence of the residuals.

Appendix F. The CalvoPlus model

The setup follows very closely Section 2, so we introduce minimal modifications to notation. The menu cost now is a random variable $\tilde{\eta}$ such that

$$\tilde{\eta} = \begin{cases} \eta & \text{with prob } \alpha \\ 0 & \text{with prob } 1-\alpha \end{cases}$$

so the probability that a price p is adjusted is

$$\Omega_t(p) = Pr[\tilde{\eta} = 0] + Pr[\tilde{\eta} = \eta]\lambda_t(p) = (1-\alpha) + \alpha\lambda_t(p).$$

The function $\lambda_t(p)$ is identical to the one in Section 2, but its interpretation is slightly different: it is the probability of a price change conditional on the menu cost being η. We reproduce it here for convenience:

$$\lambda_t(p) = 1[L(p) > 0]$$

where the difference in value between adjusting and not adjusting the price must be higher than the menu cost – which is expressed in terms of labor cost:

$$L(p) = \max_{p'} V_t(p') - \eta w_t - V(p).$$

With that, the firm's value function now is

$$\begin{aligned} V_t(p) \;=\; & \Pi(p, w_t, A_t) \\ & + \alpha \mathbb{E}_t\left[(1-\lambda_{t+1}(p - \sigma_{t+1}\varepsilon_{t+1} - \pi_{t+1}))\Lambda_{t,t+1}V_{t+1}(p - \sigma_{t+1}\varepsilon_{t+1} - \pi_{t+1})\right] \\ & + \alpha \mathbb{E}_t\left[\lambda_{t+1}(p - \sigma_{t+1}\varepsilon_{t+1} - \pi_{t+1})\,\Lambda_{t,t+1}\left(\max_{p'} V_{t+1}(p') - \eta w_{t+1}\right)\right] \\ & + (1-\alpha)\,\mathbb{E}_t\left[\Lambda_{t,t+1}\left(\max_{p'} V_{t+1}(p')\right)\right] \end{aligned}$$

which accounts for the fact that with probability $1-\alpha$ the price can be adjusted for free. As the menu cost is expressed in labor units, the labor market clearing condition in equation (**??**) in Section 2 must be modified to

$$N_t = \frac{C_t}{A_t}\int e^{p(-\epsilon)} g_t(p)\,dp + \alpha\eta \int \lambda_t(p - \sigma_t\varepsilon_t - \pi_t)\, g_{t-1}(p)\,dp$$

such that a share α of firms for which it is worthwhile to incur the menu cost η actually pay it. Note that now the frequency of price changes is given by

$$f_t = \int \Phi_t(p)\, g_{t-1}(p)\,dp = (1-\alpha) + \alpha \int \lambda_t(p - \sigma_t\varepsilon_t - \pi_t)\, g_{t-1}(p)\,dp.$$

The next equation to modify is the law of motion of the price density function:

$$\begin{aligned} g_t(p) &= \alpha(1-\lambda_t(p))\int g_{t-1}(p+\sigma_t\varepsilon_t+\pi_t)\,d\xi(\varepsilon) \\ &\quad +\delta\left(p-p_t^*\right)\int\left[(1-\alpha)+\alpha\lambda_t(\widetilde{p})\right]\left(\int g_{t-1}(\widetilde{p}+\sigma_t\varepsilon_t+\pi_t)\,d\xi(\varepsilon)\right)d\widetilde{p}. \end{aligned}$$

Summing up, the objective of the Ramsey problem in Section **??** now is

$$\max_{\substack{\{g_t^c(\cdot),g_t^0,V_t(\cdot),C_t,\\ w_t,p_t^*,s_t,S_t,\pi_t^*\}_{t=0}^{\infty}}} \mathbb{E}_0\sum_{t=0}^{\infty}\beta^t\left(\frac{C_t^{1-\gamma}}{1-\gamma}-\upsilon\frac{C_t}{A_t}\left(\int e^{\left(x+p_t^*\right)(-\epsilon_t)}g_t^c(p)\,dx+g_t^0e^{\left(p_t^*\right)(-\epsilon)}\right)-\upsilon\eta[g_t^0-(1-\alpha)]\right)$$

subject to

$$\begin{aligned} w_t &= \nu C_t^{\gamma}, \\ V_t(x) &= \Pi\left(x,p_t^*,w_t,A_t\right)+\alpha\frac{\Lambda_{t,t+1}}{\sigma_{t+1}}\int_{s_t}^{S_t}\left[V_{t+1}\left(x'\right)\phi\left(\frac{\left(x-x'\right)-\pi_{t+1}^*}{\sigma_{t+1}}\right)\right]dx'+ \\ &\quad +\alpha\Lambda_{t,t+1}\left(1-\frac{1}{\sigma_{t+1}}\int_{s_t}^{S_t}\phi\left(\frac{\left(x-x'\right)-\pi_{t+1}^*}{\sigma_{t+1}}\right)dx'\right)\left[V_{t+1}(0)-\eta w_{t+1}\right] \\ &\quad +(1-\alpha)V(0), \\ V_t(s_t) &= V_t(0)-\eta w_t, \\ V_t(S_t) &= V_t(0)-\eta w_t, \\ V_t'(0) &= 0, \\ g_t^c(x) &= \frac{\alpha}{\sigma_t}\int_{s_{t-1}}^{S_{t-1}}g_{t-1}^c(x_{-1})\,\phi\left(\frac{(x_{-1}-x)-\pi_t^*}{\sigma_t}\right)dx_{-1}+\alpha g_{t-1}^0\phi\left(\frac{-x-\pi_t^*}{\sigma_t}\right), \\ g_t^0 &= 1-\int_{s_t}^{S_t}g_t^c(x)\,dx, \\ 1 &= \int e^{\left(x+p_t^*\right)(1-\epsilon)}g_t^c(x)\,dx+g_t^0e^{p_t^*(1-\epsilon)}. \end{aligned}$$

Appendix G. Implications for the 2022-2023 US inflation surge

Scenario description. We use our model to assess its optimal policy prescriptions in a stylized scenario akin to the 2022-2023 post-Covid US inflation surge. Besides the large increase in repricing frequency, a further notable feature of the inflationary episode was the significant *increase* in the dispersion of price changes (Montag and Villar 2023). This is relevant because large aggregate shocks with uniform impact on firms' optimal reset prices, including demand, supply, and cost-push shocks in our framework, would *decrease* the price-change dispersion. The reason is that the new price changes, resulting from price gaps pushed over one of the inaction thresholds by the shock, are necessarily closer to the mean of price changes than the canceled price adjustments, which are around the other inaction threshold. The contradictory

evidence, therefore, suggests that concurrent forces raised the dispersion of reset prices, like an increase in the volatility of idiosyncratic demand or supply shocks.[26] In this section, we construct a scenario as a combination of a cost-push shock, a dispersion shock, and a monetary policy that follows an inertial Taylor rule. The scenario broadly captures key features of the 2022-2023 US inflation surge. Then we use our model to characterize the counterfactual optimal Ramsey commitment policy.

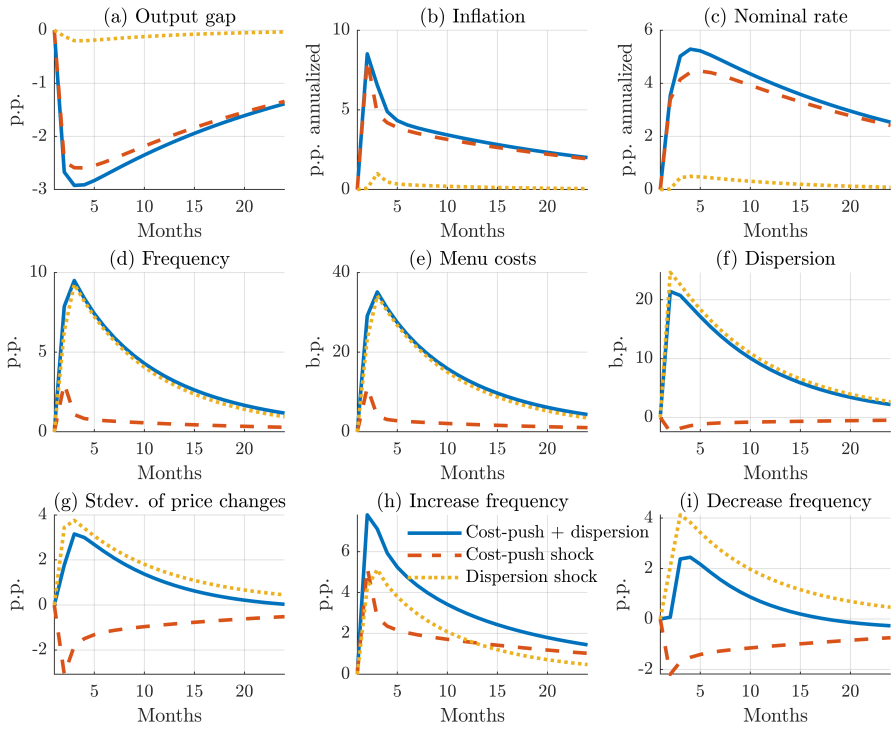


FIGURE A11. Inflation surge caused by a cost-push and dispersion shocks.
Note: The figure shows a scenario (blue solid line) as a response to a combination of a large cost push τ_t and a dispersion σ_t shock, which captures some key features of the 2022-2023 inflation surge. The figure also shows the individual responses to the cost-push shock (red dashed line) and the dispersion shock (yellow dotted line) components.

Figure A11 shows the impulse responses to a combination of a cost-push and a dispersion shock, alongside the impulse responses to the two shock components. The two shock broadly capture both the large increase in the frequency of price changes (which increases by 9.5 p.p. in the model versus 11 p.p. in the data), and the increase in the standard deviation of the price changes (which increases by around 3 p.p. in the model versus 1.5 percentage points during the 2022-2023 inflation surge (Montag and Villar 2023)).

The scenario captures broad features of the 2022-2023 US inflation surge. The shocks raise the inflation rate from the steady-state 2 percent to around 10.5 percent.[27] Around

[26] Similar idiosyncratic volatility shock and its interaction with aggregate shocks is analyzed in Vavra (2014). Berger and Vavra (2019) explore the possibility of increased dispersion caused by heterogeneous response to aggregate shocks.

[27] We have reduced the interest-rate smoothing parameter of the inertial Taylor rule from 0.75 quarterly

half of the inflation surge is temporary and recedes quickly, while the remaining half is persistent and declines slowly. The nominal interest rate increases quickly by slightly over 5 percent, broadly in line with the magnitude of the Fed's 2022 policy tightening. The output gap declines by 3 percentage points.[28] The figure also shows that the scenario captures the sizable and persistent increase in the frequency of price changes.

The figure also confirms that the standard deviation of price changes prove the necessity of a dispersion shock accompanying the aggregate shock and helps identify its magnitude. The standard deviation of price changes declines as a response to the cost-push shock, while it increases significantly after the dispersion shock. Their combination in the baseline leads to an overall increase as in the data. Notably, the exercise also captures the around 2 percentage-point *increase* in the frequency of price decreases, even though it is not a moment we explicitly target. An aggregate shock alone would have reduced the frequency of price decreases, while a sole dispersion shock would have increased it by more than 4 percentage points. All in all, the large increase in the overall frequency is driven mostly by the increase in price increases reaching around 14% from around 6%, similar to the data (Montag and Villar 2023).

How would optimal Ramsey policy have reacted to such a combination of shocks? The answer is not obvious, as the dispersion shock generates variation in optimal relative prices and, consequently, a welfare-enhancing increase in the frequency of price changes that monetary policy might not want to counteract. Figure A12 shows the counterfactual optimal policy response. It shows that the optimal policy would prescribe a substantially tighter policy in the initial periods than the Taylor rule. The optimal policy would have led to an increase in inflation by only around 4 percentage points at the cost of a somewhat lower output gap. This is substantially lower than the 8.5 percentage points increase in inflation under the Taylor rule. The policy would have reduced the frequency of price changes only marginally: it would have stayed persistently high. The low optimal inflation, furthermore, would be accompanied by a substantial shift from price increases towards price decreases, which are not costlier than price increases in our framework.[29]

rate to 0.33 quarterly rate to capture the unusually fast pace of interest-rate increase observed in 2022.

[28]The decline in output is contrary to the evidence. A more realistic scenario should also include a positive demand shock raising output, caused, for example, by heightened consumption demand from excess savings built up during the Covid-19 lock-downs and from fiscal transfers. Excluding such a demand shock is a conservative choice: a scenario with demand shock would prescribe an even more aggressive optimal policy tightening than our baseline. The reason is that monetary policy would optimally fully offset an efficient demand shock, while it leans only partially against the inefficient cost-push shock in our scenario.

[29]There is no reason for downward nominal rigidity in our framework, up to first order. Price increases are more frequent than price decreases even under zero inflation only due to the asymmetry of the profit function, a higher-order feature. It raises the incentives of firms to adjust their relative prices if it is below the optimal reset price than when it is above it.

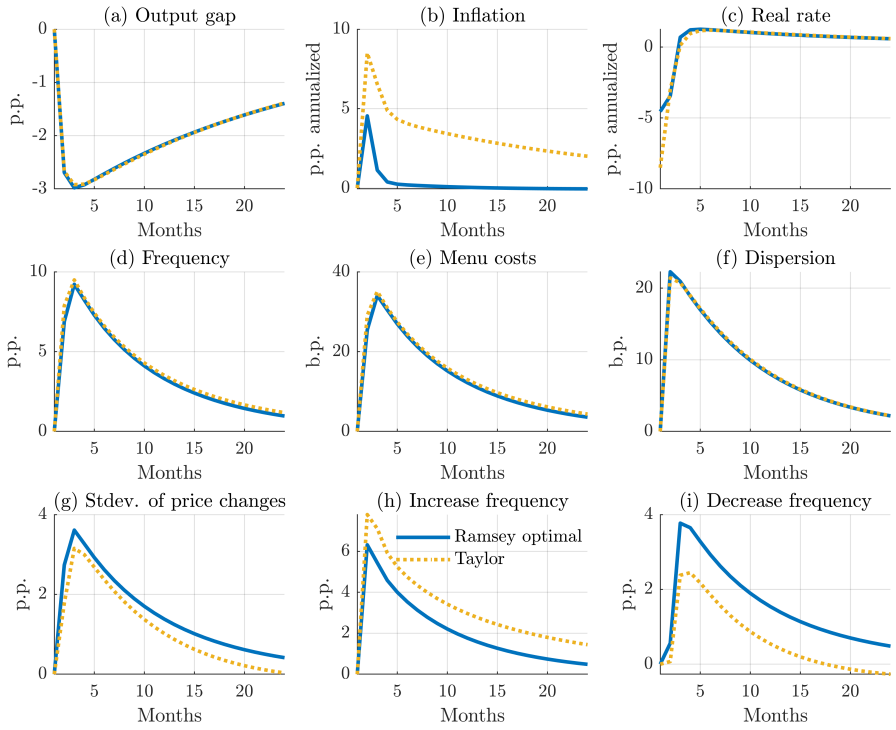


FIGURE A12. Optimal monetary policy response to a joint cost-push and dispersion shock.

Note: The figure shows the optimal Ramsey commitment response (blue solid line) to a combination of a large cost push τ_t and a dispersion σ_t shocks. It contrasts it to the policy following an inertial Taylor rule (yellow dotted line).